Brigham Young University
BYU ScholarsArchive

All Theses and Dissertations

2012-07-12

Homogeneous Viologens for Use as Catalysts in Direct Carbohydrate Fuel Cells

Dane C. Hansen
Brigham Young University - Provo

Follow this and additional works at: https://scholarsarchive.byu.edu/etd

 Part of the Chemical Engineering Commons

BYU ScholarsArchive Citation

Hansen, Dane C., "Homogeneous Viologens for Use as Catalysts in Direct Carbohydrate Fuel Cells" (2012). *All Theses and Dissertations*. 3647.
https://scholarsarchive.byu.edu/etd/3647

This Dissertation is brought to you for free and open access by BYU ScholarsArchive. It has been accepted for inclusion in All Theses and Dissertations by an authorized administrator of BYU ScholarsArchive. For more information, please contact scholarsarchive@byu.edu, ellen_amatangelo@byu.edu.

Homogeneous Viologens for Use as Catalysts in Direct Carbohydrate Fuel Cells

Dane Cameron Hansen

A dissertation submitted to the faculty of
Brigham Young University
in partial fulfillment of the requirements for the degree of

Doctor of Philosophy

Dean R. Wheeler, Chair
Gerald D. Watt
William G. Pitt
W. Vincent Wilding
Randy S. Lewis

Department of Chemical Engineering

Brigham Young University

August 2012

Copyright © 2012 Dane Cameron Hansen

All Rights Reserved

ABSTRACT

Homogeneous Viologens for Use as Catalysts
in Direct Carbohydrate Fuel Cells

Dane Cameron Hansen
Department of Chemical Engineering, BYU
Doctor of Philosophy

Deriving electrical energy from glucose and other carbohydrates under mild conditions is an important research objective because these biomolecules are abundant, renewable, and can provide 12 to 24 electrons per molecule, yielding substantial electrical power. It was previously observed that disubstituted viologens, salts of N,N'-disubstituted 4,4'-bipyridine, are able to oxidize glucose under alkaline conditions. Building on that initial result, the objective of this work was to understand and quantify the effectiveness and utility of viologens as catalysts for use in direct carbohydrate fuel cells.

The extent that viologens oxidize carbohydrates, the conditions under which that oxidation occurs, and the mechanism for the oxidation were examined using oxygen-uptake and other methods. Viologens were found to catalytically oxidize carbohydrates extensively in alkaline solution. Viologens were also found to react with the enediol form of the carbohydrate, initiating carbohydrate oxidation with subsequent reduction of the viologen. If the viologen/carbohydrate ratio is low, electron transfer from the carbohydrate to the viologen becomes limiting and the carbohydrates undergoing oxidation rearrange into unreactive intermediates such as carboxylic acids and alcohols. At high catalyst ratios, excess viologen more rapidly oxidizes the carbohydrate and minimizes formation of unreactive intermediates. We also found that viologen polymers were more efficient than an equivalent concentration of monomers, suggesting that the higher localized concentration in polymeric viologen acts to efficiently oxidize carbohydrates and simulates high viologen/carbohydrate ratios.

Monoalkyl viologens, aminoviologens, indigo carmine, and methylene blue were investigated by the method of cyclic voltammetry to inform their use as catalysts in the oxidation of carbohydrates. Redox potentials, diffusion coefficients, and heterogeneous electron-transfer rate constants were determined. Stability in alkaline solution and aqueous solubility were also examined in a semi-quantitative fashion. A comparison between the catalysts was made and viologens were found to be superior based on the examined parameters.

The catalytic oxidation of carbohydrates by viologen was also examined using a fuel cell-like device. For the conditions in which a test cell was operated, oxidation efficiencies of up to 33% were observed, compared to previously reported values from about 2.5% to 80%. Anode polarization curves were obtained and used to determine the behavior of the viologen-controlled anode as a function of pH, viologen and carbohydrate concentration, and carbohydrate identity. pH was found to have a stronger effect on the performance at the anode for carbohydrates with a higher number of carbons than those with a lower number.

Keywords: viologen, catalysis, carbohydrate oxidation, mechanism, fuel cell, voltammetry

ACKNOWLEDGMENTS

To my wife, the love of my life. To my children, my joy (most of the time). To my parents; I'm grateful for your love and support all of these years.

Thank you Dr. Wheeler, for guiding me. Thank you Dr. Watt, for your generosity.

I'm grateful for the many friends I've made as a student. Life is much better when you have friends; to teach and to learn from.

TABLE OF CONTENTS

LIST OF TABLES

LIST OF FIGURES

1 INTRODUCTION

1.1 Motivation

Concern over fossil fuel depletion, anthropogenic climate change, and complex geopolitical energy distribution problems has led to the important objective of utilizing biorenewable energy sources to supplement the use of fossil fuels. Carbohydrates are abundant, high-energy biomolecules whose stored chemical energy is released through complex enzymatic cycles to meet the energy requirements of diverse living organisms on earth [1]. The convenience, availability, and high energy content of glucose, carbohydrates in general, and certain related molecules suggest they can be used to directly produce electricity [2-5].

Although the possibility of directly producing electricity has been investigated for the last half century [6], little progress using carbohydrates as a useful source for electrical power has been made. Two major types of fuel cells are currently being evaluated for the production of electricity from carbohydrates: biologically derived (enzymatic and microbial) and abiotic using inorganic catalysts such as noble metals and activated carbon. Prior to this work, an avenue that had received relatively little attention was the use of electro-active organic dye molecules as catalysts.

The initial observation that methyl viologen is reduced by glucose under basic conditions was reported by Yu and Wolin [7], who used the resulting reduced methyl viologen as a protein reductant. Gerald Watt at BYU subsequently recognized that this reaction could potentially also

be used to produce useful electricity from carbohydrates [8]. Methyl viologen is a disubstituted viologen, which is a salt of N,N'-disubstituted-4,4'-bipyridine. Disubstituted viologens have been heavily studied for a number of applications [9], but never directly for use as a catalyst for the oxidation of carbohydrates to produce electrical energy. Though some information applicable to this use is available [9], other questions needed to be answered before viologen could be used effectively as a catalyst for the oxidation of carbohydrates.

1.2 Scope of work

The primary goal of this work was to answer questions about the effectiveness and utility of viologen as a catalyst for use in direct carbohydrate fuel cells (DCFCs). Chapter 2 provides background information so that the answers to those questions may be appreciated. Included in Chapter 2 are brief summaries of fuel cell basics, the basics of electrochemical experimental techniques and test apparatuses, viologen and DCFCs in the literature, and a discussion of carbohydrates as a fuel source.

With limited information on the oxidation of carbohydrates by viologen available in the literature, and to gain some understanding of the reaction, a number of basic questions needed to be answered. The work reported in Chapter 3, based on Refs. [8] and [10], was completed to answer the following questions. Other than glucose, are other carbohydrates and chemical species oxidized by viologen? Do other types of viologen, besides methyl viologen, also catalytically oxidize glucose and other molecules? At what efficiency are the electrons available in the oxidized species obtained? Which factors in the oxidation are most important in affecting that efficiency? Is there a specific part of the carbohydrate molecule that is oxidized preferentially by the viologen? What can be learned about the oxidation by examining the

products of the oxidation? What is the behavior of the oxidation as the oxidation proceeds in time, and what can be learned from that behavior?

The research presented in Chapter 3 was carried out using a variety of tools, some standard, and one created specifically to test the large number of variables required. Reduced viologen is readily oxidized by oxygen and two methods made use of oxygen consumption to answer the questions posed above. One method was useful for testing the large number of variables and the other was useful for real time measurements. Products of the reaction were identified using NMR and mass spectrometry.

From the data gathered for Chapter 3, a hypothesis on the mechanism by which the viologen catalyzes the oxidation of carbohydrates was formulated. Briefly, the hypothesis was that the viologen oxidizes the enediol form of the carbohydrate and that the viologen/carbohydrate ratio affects the efficiency with which the carbohydrate is oxidized due to the formation of inactive intermediates at relatively low ratios. It was also hypothesized that viologen polymers would be more efficient than an equivalent concentration of monomers due to higher localized concentration simulating high viologen/carbohydrate ratios. This work was completed using the same suite of experiments used to get the data presented in Chapter 3. This work is reported in Chapter 4 and is based on an article published in the journal *Renewable Energy* in 2011 [10].

During the course of experimentation, it was found that a class of viologens, monosubstituted viologens or salts of N-substitited-4,4'-bipyridine, also appeared to be catalytically active in the oxidation of carbohydrates. Monosubstituted viologens have received significantly less attention in the literature than disubstituted viologens such as methyl viologen. Based on the monosubstituted-viologen results as reported in Chapter 3, experiments were

completed to answer the following research questions. What are the redox potentials of representative monosubstituted viologens? Redox potential is an important factor in the efficiency at which the energy contained in the fuel molecule is obtained. What is the effect of substituent length on redox potential of the monosubstituted viologen? Substituent length has important implications for the immobilization of viologen at an electrode, which is the focus of current and future work by our group in the creation of a practical fuel cell. What are the heterogeneous electron-transfer rate constants for representative monosubstituted viologens? These rate constants affect the current produced by the cell and the ratio of viologen present in the oxidized and reduced forms. This ratio has important implications for the mechanism by which the carbohydrate is oxidized by the viologen, as discussed in Chapter 4 of this document. These same questions were asked for two other potential organic catalysts, indigo carmine and methylene blue, and a comparison between all the potential catalysts is made based on the examined parameters. This work was completed using a standard electrochemical method known as cyclic voltammetry. This work is reported in Chapter 5 and is based on a publication under review for publication in the *Journal of the Electrochemical Society* (*JES*) [11].

After the publication by our group of Ref. [8], in 2009, another research group based at the University of Hawaii, published a paper [12], also in 2009, and also reporting estimates of the efficiency at which viologen catalyzes the oxidation of carbohydrates. There is a wide variation between the efficiency values reported in the two groups' publications. Accurate efficiencies are important because the energy density, and thus utility, of the carbohydrate fuel relies directly on the extent to which the fuel can be oxidized. A hypothesis was generated that the variation was based, in part, on the different test conditions prevailing in the two publications. The hypothesis was tested using a specially constructed fuel cell-like device

connected to a potentiostat. Additionally, to gain a better understanding of how a viologen-controlled anode performs under various conditions, the same cell was used to determine what effect pH, viologen and carbohydrate concentration, and carbohydrate identity have on the performance at the viologen-controlled anode. This work is presented in Chapter 6 and is based on a publication under review for publication in *JES* [13].

Summary, conclusions, and recommendations for future work are presented in Chapter 7.

2 BACKGROUND

2.1 Introduction

To understand the research presented in this dissertation it is helpful to have some understanding of fuel cell basics, electrochemical experimental techniques, and test apparatuses. Also included here are brief summaries of viologen and direct carbohydrate fuel cells (DCFCs) in the literature, and a discussion of carbohydrates as a fuel.

2.2 Fuel cell

Fuel cells, like all electrochemical cells, are constructed [14] with an anode and a cathode, spatially separated and in electrical contact with an electrolyte. In an operating fuel cell, the fuel is electro-oxidized at the anode, which liberates electrons. The liberated electrons then flow through an external circuit, where they are used to do useful work, and delivered to the cathode. At the cathode, the electrons reduce the terminal electron acceptor, which is usually oxygen. The driving force for the flow of electrons is the difference in the electrochemical potential of the anode and cathode redox pairs.

2.2.1 Direct carbohydrate fuel cell reactions

A representation of the reactions occurring in a generic alkaline DCFC with glucose as fuel is shown in Equations 2.1 through 2.3 [8].

Anode: $C_6H_{12}O_6 + 36\ OH^- = 6\ CO_3^{2-} + 24\ H_2O + 24\ e^-$ (2.1)

Cathode: $6\ O_2 + 12\ H_2O + 24\ e^- = 24\ OH^-$ (2.2)

Overall: $C_6H_{12}O_6 + 12\ OH^- + 6\ O_2 = 6\ CO_3^{2-} + 12\ H_2O$ (2.3)

An idealized schematic of the overall redox process is shown in Figure 2.1. The anode reaction is given by Equation 2.1, the reaction occurring at the cathode by Equation 2.2, and an overall reaction by Equation 2.3. At the anode, glucose and OH^- react to produce 24 e^-. The electrons travel from the anode through an external circuit and are delivered to the cathode where they are used by oxygen and water to form OH^-. The OH^- then travels through the electrolyte to the anode where it will be used in the oxidation of the carbohydrates. Equations 2.1 and 2.2 combine to yield Equation 2.3, which is the overall equation representing the reaction in the alkaline DCFC where glucose is oxidized to carbonate and water [6].

2.2.2 Anode

In an operating fuel cell, the anode is where the fuel is oxidized. In an alkaline DCFC, to produce useful currents, a catalyst is required to increase the rate of the oxidation of the carbohydrate fuel [6]. In alkaline conditions, precious and transition metals have been used as catalysts but, to our knowledge, are only marginally effective. As presented here, viologens appear to be more effective as catalysts.

2.2.3 Cathode

To increase the rate of reduction of oxygen at the cathode in basic conditions, a catalyst is also required, which is commonly a non-precious metal. This is advantageous compared to the reduction of oxygen in acidic conditions, under which other types of fuel cells operate, where

precious-metal catalysts are widely employed [15, 16]. Cathode material that functions in alkaline condition, like Electric Fuel's E-5 cobalt-based catalyzed-carbon cathode [17], is commercially available. The E-5 cathode is the cathode material that was used to obtain the results reported in Chapter 6.

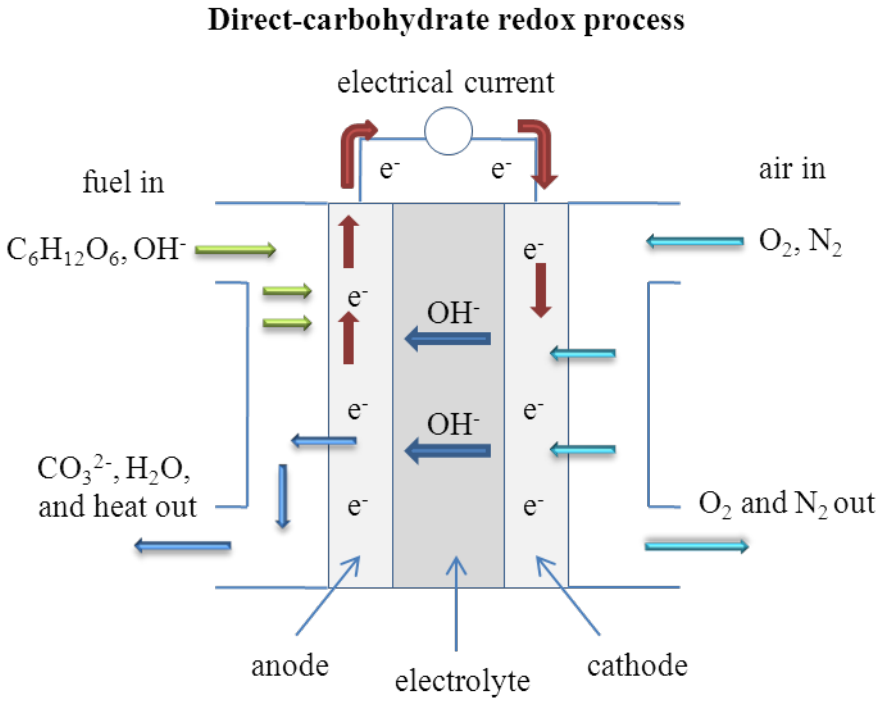

Figure 2.1 The overall redox process occurring in an idealized alkaline direct carbohydrate fuel cell.

2.2.4 Separator and electrolyte

In an electrochemical cell the separator region blocks the free flow of electrons and shuttles the current, in the form of ions, from one electrode to the other. In some cases the separator is a porous film filled with electrolyte. In other cases a polymer electrolyte membrane (PEM) serves as both separator and electrolyte [18] (the acronym PEM is also used as shorthand for proton exchange membrane, and the terms are sometimes used interchangeably). An

electrolyte is a substance containing free ions, which allows the substance to be electrically conductive.

PEMs additionally help reduce reactant crossover [19]. If the reactants cross over they can possibly react on the improper electrode, causing a mixed potential. This mixed potential reduces the useful potential produced by the cell and lowers fuel efficiency.

Even with a PEM, crossover can be a source of mixed potential, as with direct methanol fuel cells (DMFCs) [20]. One major source of crossover in operating fuel cells, including cells with a PEM as separator/electrolyte, is caused by a phenomenon known as electro-osmotic drag. Electro-osmotic drag occurs when an ion, migrating in an electric field, effectively drags one or more other molecules with it by diffusive interactions [21]. The molecules thus dragged may be the fuel, as when methanol is dragged from the anode side to the cathode side of the membrane by migrating protons. Under acidic conditions the cathodes of DMFCs rely on platinum, the same catalyst at the anode, and when the methanol reaches the cathode it is oxidized, wasting fuel and causing the mixed potential. Under alkaline conditions, the anions flow the opposite direction than protons in acidic fuel cells, which is an advantage for alkaline fuel cell environments because the electro-osmotic drag opposes crossover of liquid fuels.

Water may also be affected by electro-osmotic drag, as when it is dragged across the PEM by protons in a hydrogen fuel cell [22] operating in acidic conditions. The PEM typically used in low-temperature hydrogen fuel cells is Nafion. To be conductive, Nafion must be solvated, typically by water for hydrogen fuel cell applications. Without humidification of the hydrogen stream, the only source of water at the anode is by diffusion from the cathode side, which is counteracted by the electro-osmotic drag. Water management is thus an important consideration in some hydrogen-powered cells [23].

2.2.5 Available polymer electrolyte membranes

Polymer electrolyte membranes are semi-permeable membranes designed to have high ionic conductivity while blocking the flow of gases like oxygen and hydrogen, and to serve as the separator region. PEMs have been developed that can conduct cations or anions.

Nafion membranes have high chemical and electrochemical stability, are selective, have relatively high cation conductivity [15, 24], and are the membranes of choice for low temperature hydrogen and methanol fuel cells operating in acidic conditions [15, 18, 25]. Nafion has a tetrafluoroethylene (Teflon) backbone, which is partly responsible for the high thermal, mechanical, and chemical stability of the material [26]. Extending off this backbone are perfluorovinyl ether groups which terminate with sulfonate groups. The cations are conducted along the sulfonate groups. Nafion conductivity varies by membrane thickness and test conditions, but is on the order of 0.1 to 0.2 S cm^{-1} [27], where S (siemens) is Ω^{-1}.

Though Nafion is a cation conductor, it has been tested for use in alkaline fuel cells [28, 29], and recently the Nafion precursor polymer has been modified to conduct anions [30]. For the alkaline DMFC in Ref. [29] Na^+ was used to conduct the current. At the anode of the cell, the methanol and OH^- react to CO_2 and water, liberating 6 e^-. The Na^+ ions and some of the water travel through the membrane, where they combine with electrons and O_2 to form NaOH at the cathode. To maintain the sodium balance, the Na^+ is recycled in some unstated fashion. In Ref. [28], the Nafion was coated with anion exchange membrane material, and was used to conduct protons for the hydrogen-powered cell. High pH was maintained at both the anode and the cathode, with water being split into OH^- and H^+ at the anode, the H^+ carrying the current through the Nafion, and then combining with OH^- at the cathode to create water. Such methods may be attempted for use in a future viologen-catalyzed DCFC. However, this may lead to

problems because viologen molecules are cations with approximately 150 to 200 g mol^{-1} mass, and if they are in solution, as they were for the experiments presented in this dissertation, they can potentially enter and block the pores through which the cations conduct.

No anion exchange membranes (AEMs) have yet emerged that can match the desirable properties of Nafion and the area is an area of active, and promising [31], study [32-34]. Current limitations in the technology are related to the possibility of obtaining a membrane having: high ionic conductivity, chemical stability in strong alkaline media, low permeability to fuel crossover, low swelling, and good mechanical properties [33]. The development of suitable AEMs is of great interest due to the following superior qualities gained operating under alkaline conditions compared to acidic conditions: faster electrokinetics, lower fuel crossover, reduced CO poisoning, and use of non-precious metal catalysts, such as silver, nickel, and perovskite [34, 35].

A wide variety of materials have been used to make AEMs [34], several examples being polysiloxane [36], polysulphone [37], poly(arylene ether sulfone) [38], and poly(vinyl alcohol)/poly-(acrylamide-co-diallyldimethylammonium chloride) [34]. Reported conductivities range from 10^{-4} S cm^{-1} [36] up to 10^{-2} S cm^{-1} [33, 34, 38].

At the outset of this work, available commercial AEMs were typically based on cross-linked polystyrene and were not very stable in alkaline or electrochemical environments and had relatively low ionic conductivity [32]. AEMs were obtained by our group (Membranes International, AMI-7001S), tested, and found to have poor stability under our operating conditions. As mentioned above, efforts were not undertaken to use or modify Nafion for use in the cell. Therefore, the tests reported in Chapter 6 that were done with a fuel cell-like device do not make use of an ionomer membrane as separator/electrolyte.

2.2.6 Glucose-fuel-cell technology

There are many papers that describe glucose as a potential fuel for fuel cells, and the area has been the subject of some lengthy reviews [6, 39, 40]. The earliest article was published in 1964 [41], with enzymes as catalysts. Other researchers have since created cells utilizing bacteria and various metals as catalysts. Bacterial cells, as well as enzymatic cells, typically operate in a phosphate buffer at physiological pH [42], while metal catalyzed cells have been shown to operate in alkaline [43] and acidic conditions [44]. In acidic conditions, the reactions are similar to those represented by Equations 2.1 through 2.3, the difference being that H^+ is liberated at the anode and combined with O_2 at the cathode to make water [45]. Specific examples reported below are representative of power densities and efficiencies achieved.

State-of-the-art bacterial cells [3] have achieved up to 100% coulombic efficiency (coulombic efficiency is defined as the percentage of available electrons that are freed for useful work). However, these cells rely on bacterial metabolism, which is thus far kinetically slow, greatly limiting the current density produced by the cell. Of note, these cells generally require viologen or another mediator to shuttle the electrons between the bacteria and the electrode [46, 47]. For their microbe-catalyzed cell, Chaudhuri and Lovely [3] report a maximum power density of approximately 3.3 $\mu W\ cm^{-2}$ at a current of 7.4 $\mu A\ cm^{-2}$ and 0.445 V.

Bacteria-free enzymatic cells are generally based on glucose oxidase [41, 48, 49], an enzyme that converts glucose to gluconic acid. This conversion only liberates two of the available 24 electrons for useful work. Soukharev et al. [50] report that power densities of up to 0.35 $mW\ cm^{-2}$ at 0.88 V cell voltage are achievable. It is claimed in the publication that the power density reported in Ref. [50] is superior to that which is achieved with platinum as catalyst. Kavanagh et al. [51] recently reported an enzyme-catalyzed cell having a maximum

power density of 52 μW cm^{-2} at 0. 21 V. Enzymes require complex immobilization schemes [50, 51] to be used in cells.

Researchers have made use of both precious metals [43, 52] and transition metals [2, 53-55] as catalysts in DCFCs. With platinum as catalyst, Bubis et al. [56] report a peak power density of 0.36 mW cm^{-2} at a current density of 1.44 mA cm^{-2} with 0.22 M glucose in 0.35 M KOH. A maximum power density of 0.22 mW cm^{-2} and an open circuit voltage of 0.65 V was reported by Jin and Taniguchi [57] using 10 mM glucose in 0.3 M KOH in a glucose-air AFC with a silver-modified gold film as anode. Metal-catalyst anodes suffer from poisoning by intermediate oxidation products, the amelioration of which is an area of active research [58]. As is evident from the examples cited above, metal-catalyzed DCFCs also suffer from slow electro-oxidation kinetics at low temperature.

One of the main focuses of both the enzymatic and metal-catalyzed fuel cells appears to be for use to power implanted medical devices [6]. For such devices, the end product of choice is the two-electron oxidation of glucose to gluconic acid, which is a non-toxic metabolite [59]. As such, it is generally reported that the oxidation of glucose by metal catalysts leads to gluconic acid as the end product [12, 60]. However, depending on the conditions [6, 61], it has been reported that an estimated 20 electrons have been liberated from glucose using a platinized platinum electrode. In contrast, coulombic efficiencies as low as 5% have been reported for metal-catalyzed cells, even assuming a maximum two-electron oxidation of glucose [62].

Regardless of continuing interest in the technology, carbohydrates are not being effectively used as an alternative fuel source. This is despite attempts to employ DCFCs using a wide range of potential catalysts. Even with some promising results, efforts to use metals (precious or otherwise), bacteria, and enzymes as catalysts have yet to result in the practical use

of carbohydrates as an energy source for fuel cells. If the potential of carbohydrates as an energy source for portable devices [58, 62] and stationary power supplies is to be realized, higher power densities, higher coulombic efficiencies, and more stable, lower maintenance catalysts are required.

2.3 Viologen

Viologens can be categorized in two types: disubstituted and monosubstituted. The disubstituted type are N,N'-disubstituted-4,4'-bipyridine salts [9], e.g. methyl viologen. The monosubstituted type are N-substitited-4,4'-bipyridine salts, e.g. monomethyl viologen. Structures of representative viologens studied here are seen in Figure 2.2.

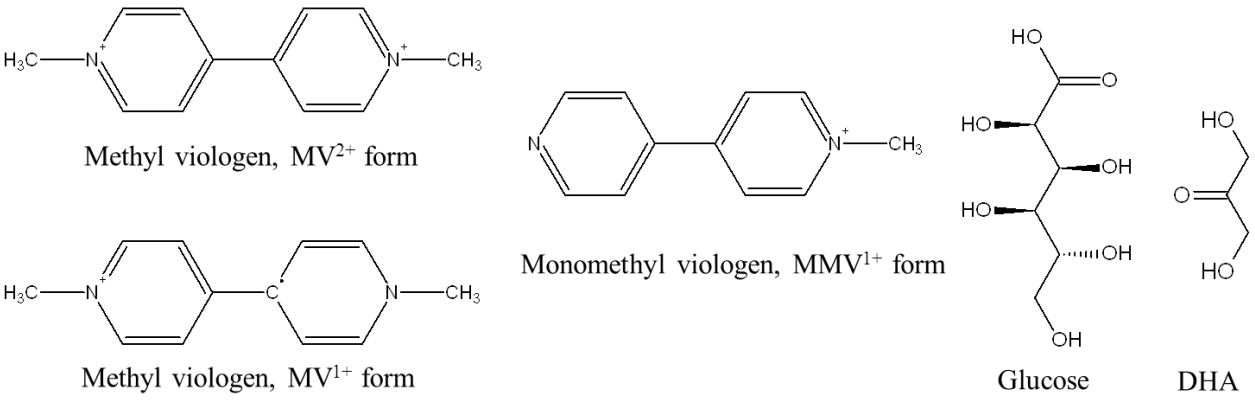

Figure 2.2 Representative structures for molecules discussed here.

Viologens were discovered over 75 years ago [63] and named viologen for the intense blue color of the cation radical. Endowed with many "very interesting" properties [9], disubstituted viologens have been studied extensively [64-74]. A decade ago a book [9] was written that discusses the many uses of disubstituted viologens and details other information;

including synthesis, spectroscopic and structural information, charge-transfer properties and dimerization [66]. Methyl viologen is used as an herbicide and other types of disubstituted viologen have been studied for use in electrochromic displays, photochemical hydrogen production, and as an electron mediator [9]. Little information about monosubstituted viologens was available in the literature before the beginning of this work, and a portion of the work presented in this dissertation is on the study of homogeneous monosubstituted viologens.

2.3.1 Viologen electrochemistry

Disubstituted viologens are able to undergo two potentially reversible redox steps and monosubstituted viologens are able to undergo one. Throughout this dissertation, MV is used as the general term for methyl viologen and MV^{2+} and MV^{1+} are used to represent the electro-active oxidized and reduced forms, respectively. The mechanism for the reduction of disubstituted viologens is understood to follow two successive steps, as seen in Equations 2.4 and 2.5, with methyl viologen being used for a generic disubstituted viologen. Monosubstituted viologens only undergo one reversible reduction. With monomethyl viologen (MMV) as a generic monosubstituted viologen, the reduction reaction is presented in Equation 2.6.

$$MV^{2+} + e^{-} = MV^{1+} \tag{2.4}$$

$$MV^{1+} + e^{-} = MV^{o} \tag{2.5}$$

$$MMV^{1+} + e^{-} = MMV^{o} \tag{2.6}$$

The open-circuit potential of a redox couple, denoted by ΔE, is given by Equation 2.7, where the equilibrium potential is related to the Gibbs energy [14].

$$\Delta G = -n F \Delta E \quad (2.7)$$

where n is the number of electrons exchanged during an oxidation or reduction step and F is the Faraday constant. In a viologen-catalyzed cell, the redox couple which generates useful energy is the oxidation of MV^{1+} and the reduction of oxygen. Disubstituted viologens were considered good candidates for such cells, because they form a stable, reversible radical at reasonably negative redox potentials [9]. The redox potential of the organic catalyst is important because, as is seem in Equation 2.7, the free energy of the electrons to do work depends on the difference in potential between the anode redox couple, and the terminal electron acceptor at the cathode (usually oxygen). Analysis is complicated by the fact that viologen does not have an ionizable proton so its redox potential is hardly affected by pH, while the redox potential of oxygen is affected by pH. Regardless of pH effects, the redox potential of the viologen is still more negative, and therefore the ΔG between MV^{1+} and oxygen larger is than other redox dyes that have also been tested as catalysts for DCFCs [12, 75].

2.3.2 Anode reactions in a viologen-catalyzed DCFC

In a viologen-catalyzed DCFC, the reactions occurring at the cathode, and the overall reaction are the same as seen in a generic alkaline DCFC, represented by Equations 2.2 and 2.3, respectively. The oxidation of the carbohydrate fuel at the anode is Equation 2.1 broken into two parts, as given by Equations 2.8 and 2.9. The oxidation of MV^{1+} at the cathode is the rate-limiting step.

$$C_6H_{12}O_6 + 36\ OH^- + 24\ MV^{2+} = 6\ CO_3^{2-} + 24\ H_2O + 24\ MV^{1+} \quad (2.8)$$

$$24\ MV^{1+} = 24\ MV^{2+} + 24\ e^- \quad (2.9)$$

At the anode, glucose and OH^- react to produce 24 e^- (Eq. 2.8). This reaction is facilitated by MV and causes the MV to be reduced. The MV is then oxidized by the anode current collector (Eq. 2.9), which in turn is connected to the external circuit.

2.3.3 Viologen immobilization

The focus of this work has been on the characterization of homogenous viologens as catalysts. Viologens are highly soluble in water and toxic, so for use in a practical fuel cell the viologen will have to be immobilized. The methods for immobilizing viologen that have been reported fall into one of two broad categories. Either the viologen monomers are attached to a carbon or metal electrode, or the monomers are polymerized, as described in the following two subsections. Whichever way the viologen is immobilized, the end goal of the DCFC project at BYU is to create a catalytically-active anode that is durable, nontoxic, and operates at high currents.

Viologen immobilization at electrode surface: There are a wide variety of electrode surfaces onto which viologen has been immobilized. Immobilization can be as simple as adsorbing the viologen onto a metal [76, 77] or onto Nafion [78-80]. In an effort to create biosensors, several researchers have immobilized viologen on glassy carbon electrodes [81-84]. Viologens have also been incorporated into a zeolite-modified carbon-paste electrode [85, 86] and also attached to polymeric microspheres [87] and titanium dioxide [88].

Immobilization can require the modification of the viologen with a functional group before the viologen can be adequately attached to the surface [89, 90]. One common

derivatization technique is to attach a thiol group so the viologen will form a self-assembled monolayer (SAM) on gold [91-97]. These viologen SAMs are known to be stable, electro-active and to manifest well-behaved electrochemical responses [98].

Polyviologens: While some researchers have created stand-alone viologen polymers [99-106], many of the polymerization techniques have been used to attach the viologen to an electrode. Bauerle and Gaudl [107] write that electropolymerization (which occurs when the monomer is electrochemically oxidized at a polymerization potential giving rise to free radicals which are adsorbed onto the electrode surface and subsequently undergo reactions leading to a polymer network [108]) "is frequently used to modify an electrode surface with an electrically conducting film." They and others [109, 110] have used the electropolymerization technique. Two research groups [111, 112] have made polypyrrole films containing viologen. Other researchers have made films of the polythiophene derivative with viologen pendant [113], of a Langmuir-Blogett film [114] and with surface-grafted moieties [115, 116]. Researchers have also made a membrane with viologen moiety as anion-exchange groups [117] and investigated viologen for use in a solid polymer electrolyte [118].

Effect on Parameters of Immobilization Method: The method of viologen immobilization affects the value of parameters such as electrode surface coverage, which in turn affect cell performance. Though the specifics of a method do affect the parameters, in the literature reviewed above there is no generalization that can be made about the broad immobilization categories. Depending on the immobilization technique, surface coverage varies from 10^{-10} mol cm^{-2} to 10^{-8} mol cm^{-2}. The surface coverage does not seem to control the limiting current density for the various methods, though, with currents densities ranging from nA cm^{-2} to mA cm^{-2}. The limiting current density produced by these immobilized viologen may be misleading, however,

as the conditions under which the immobilized viologens were tested are different than the conditions under which they will be used in this work; none of these immobilized viologens were tested for the purpose of oxidizing carbohydrates, nor were any of the viologens tested in alkaline conditions. It is known that the redox potentials of the immobilized viologen depend on the solvent, substituent radicals, anion, and temperature used in the immobilization [77].

Purpose of homogeneous viologen testing: Testing such a wide variety of immobilization techniques is a non-trivial task. With even basic questions about the catalytic ability of viologen unanswered it was thought prudent at the outset of this project to use readily available and relatively easily testable homogeneous viologens to answer those questions. Clear answers could be obtained about the suitability of the catalyst and the kinetics and mechanism of the catalysis without having to contend with complications arising from the immobilization at the same time. A parallel effort has been underway by other members of our research group for the last two years to perform immobilization methods.

2.3.4 Viologen stability

It has been claimed [119] that the viologen cation radical has a lifetime of over one year at room temperature, and that "life problems have not been encountered after well over 10^5 write-erase cycles." This suggests that viologen could be used for energy storage so the cell maintains a charge even after the cell is turned off, and that the dication/cation transition is reversible.

2.4 The carbohydrate fuel

Glucose, in the form of cellulose, and in free and complexed carbohydrates, is the most abundant biomolecule formed on earth [1]. With a mandate to increase biodiesel production in Europe and the United States [120], an overproduction of glycerol has lowered its commodity

price and increased disposal costs for biodiesel manufacturers. Two potential carbohydrate fuels, glyceraldehyde and dihydroxy acetone (DHA) can be made from glycerol under mild refining conditions [121]. These two fuels may be used for electrical energy production at room temperature and mildly alkaline (pH 12) conditions. These two fuels are sufficiently safe that the FDA has approved them (at food grade purity) for human consumption.

As can be seen by the images of glucose and DHA in Figure 2.2, carbohydrates are partially oxidized hydrocarbons. Therefore, the complete oxidation of carbohydrates releases less energy than for the analogous hydrocarbon. Nevertheless, carbohydrates contain a substantial amount of energy, which can be compared to the energy that is released upon the oxidation of two other fuels that have been considered for other types of fuel cells, methanol and ethanol. When glucose is oxidized all the way to CO_2 and water, ΔG = -4420 Wh/kg glucose, which is on the order of the ΔG for the oxidation of methanol and ethanol to CO_2 and water, at -5530 Wh/kg and -7450 Wh/kg, respectively.

Carbohydrates are inherently resistant to complete O_2-oxidation and efficient and inexpensive catalytic systems have not been developed to fully catalyze this reaction. The difficulty in utilizing carbohydrates as a fuel is that, like methanol and ethanol (also considered as fuels in fuel cells), they are complex molecules that require many elementary steps before they can be oxidized to CO_2 and water. This is part of the reason that the only type of fuel cell that can oxidize carbohydrates completely is the microbial cell, which can make use of complex metabolic networks.

2.5 Coulombic efficiency and voltage efficiency

Many of the scientific questions answered in this dissertation are about the overall efficiency, η, with which the energy contained in the carbohydrate fuel may be obtained by a fuel cell as the carbohydrate is oxidized during cell operation. The efficiency with which the Gibbs energy (Eq. 2.7) of the system may be harvested is the quotient of the actual energy obtained during fuel cell operation and the ideal value for that system (ΔG_{ideal} = -4420 Wh/kg glucose if glucose is oxidized to CO_2 and water), as shown in Equation 2.10.

$$\eta = \frac{\Delta G}{\Delta G_{ideal}} = \frac{-n\,F\,\Delta E}{-n_{ideal}\,F\,\Delta E_{ideal}} = \eta_{coul}\,\eta_{volt} \qquad (2.10)$$

This overall efficiency ($\eta = \Delta G/\Delta G_{ideal}$) is the product of the efficiency with which the available electrons are obtained ($\eta_{coul} = n/n_{ideal}$) and the efficiency with which the chemical potential of those electrons is obtained, which we will call the voltage efficiency ($\eta_{volt} = \Delta E/\Delta E_{ideal}$). The determination of the coulombic efficiency under various reaction conditions is part of the subject matter covered in Chapters 3, 4, and 6.

The voltage efficiency in a viologen-catalyzed DCFC is affected by a number of variables. Some of the chemical potential of the electrons in the carbohydrate fuel is used to reduce the viologen (the amount of which is the difference in redox potential between the carbohydrate fuel and the viologen). Therefore, the redox potential of the viologen, and not of the carbohydrate being oxidized, determines the open circuit voltage (ΔE_{OCV}) of the cell. The open circuit voltage represents the maximum chemical potential of the electrons obtained by the cell, and is part of the subject matter covered in Chapter 5. In a viologen catalyzed cell, once the

viologen is reduced, the ΔE, and thus η_{volt}, obtained by the cell during operation, depends in part on the behavior of the viologen-controlled anode as current is drawn, which is part of the subject matter covered in Chapter 6.

2.6 Experimental

This section is a summary of information that can be found in Refs. [122-124] and other books on the fundamentals of electrochemistry.

2.6.1 Electrochemical test apparatuses and methods

Electrochemical test apparatuses include the two-electrode cell and the three-electrode cell. The three-electrode cell is made up of a working electrode, a reference electrode, and a counter electrode. In this case, the current flows between the working electrode and the counter electrode, and the reference electrode is used to sense the electrolyte potential near the working electrode. In the two electrode cell, the reference and counter electrodes are combined into one electrode. In this case, the current is passed between the working electrode and the counter electrode, and the potential at the working electrode is not sensed independent of the potential at the counter electrode, as it is in the three-electrode cell.

Two- and three-electrode cells can be used for many different types of experiments, including the potentiostatic, galvanostatic, and voltammetric experiments used to obtain data for this dissertation. Those three types of experiments are typically done with an instrument called a potentiostat, which uses an external power source to impose a particular current on the cell or a potential on the working electrode. A potentiostatic experiment is undertaken when the potential between the working electrode and the electrode acting as the reference electrode is held constant and the resulting current is detected. Galvanostatic experiments are undertaken when a current is

imposed on the cell and the resulting potential between the working electrode and the electrode acting as the reference is sensed. Both two- and three-electrode cells can be used galvanostatically and potentiostatically. The results of potentiostatic two-electrode experiments and galvanostatic three-electrode experiments are reported Chapter 6.

In voltammetric experiments neither the potential nor the current are static. The potential is controlled in dynamic fashion, typically by a potentiostat. In cyclic voltammetry, as used to obtain the results presented in Chapter 5, the potential is ramped or swept linearly in the form of a triangle wave, repeated for multiple cycles. The resulting current profile is recorded. The potentiostat controls the potential at the working electrode, and thereby the energy state of the electrons in the electrode, relative to the reference electrode. This method is typically done in the three-electrode setup, so that inefficiencies and reactions at the counter electrode do not affect the electric potential conditions at the working electrode.

2.6.2 Working, reference, and counter electrodes

The working electrode is where the electrochemical reaction of interest takes place. The working electrode can be the anode or the cathode. In some experiments, such as cyclic voltammetry, the working electrode serves as both a cathode and an anode at different times during the test as the potential of the working electrode is scanned back and forth from more negative to more positive. The anode is where the oxidation takes place and the cathode is where the reduction takes place, which means that electrons are flowing into the solution from the electrode at the cathode and out of the solution into the electrode at the anode.

The electrochemical redox processes happening at the working electrode and the counter electrode happen simultaneously, so if oxidation is happening at the working electrode, reduction must be happening at the counter electrode and vice versa. In order that the current at the

working electrode is not impeded by the counter electrode being the source of the limiting current, the counter electrode usually has high surface area. The potentiostat will impose whatever potential is necessary, within the working limits of the instrument, to generate the requested current. This means that the potential at the counter electrode is not controlled relative to the reference electrode and can be a more negative or positive value than the working electrode. The redox process happening at the counter electrode is usually not important, unless the product of the reaction can interfere with the working-electrode reaction (such as the oxidation of water, which produces oxygen, when the working-electrode reaction produces an oxygen-sensitive reduced species).

Electrode potentials are always relative values and the reference electrode serves the purpose of establishing the location of the potential of the working electrode relative to a well-known, stable, and reproducible equilibrium electrode potential. The equilibrium potential of the reference electrode depends on the environment of the reference electrode. For instance, in the silver/silver chloride (AgCl) reference electrode the concentration of the Cl^- anion, which is the ion that participates in the AgCl redox reaction, affects the potential of the reference electrode. The change in reference potential with the change in concentration is governed by the Nernst equation [14], which relates the equilibrium potential to the concentrations of the reactants and products. In the aqueous AgCl reference electrode, typically KCl is used as the source of Cl^- ions. Standard concentrations are also typically used. For instance, for the AgCl reference electrode, saturated KCl, 3.5 M KCl, 3.0 M KCl, or 0.1 M KCl are typically used.

2.6.3 Advice for beginning experimentalists

New methods: When trying a new experimental method in which no one in the research group has any practical experience, the following method may work to aid understanding. This

method is especially important when a new experimental setup for the experimental method must be simultaneously constructed. First, find books that cover the fundamentals and the practical aspects of the subject. The authors of journal articles typically assume the basics are already known, so it is sometimes difficult to piece together from the article everything that is needed. Next, study the books. After the books are read, go to the lab, construct the setup, and run experiments using the method. When the experimental setup is being perfected and you are getting experience with the practical aspects of the method, sometimes trial and error is the best way forward. Additionally, when first using the new setup, if the option is available, gain experience with the method and setup by repeating a simple experiment (for instance, testing aqueous ferrocene solution in a cyclic voltammetry setup). In this case, repeating something found in a journal article may be helpful. After you have obtained some experience with the method, read the books again. You might not understand everything you read the first time through the book, even though most, if not all, the pertinent information was contained in the book. After gaining some experience with the method, you may find the books to much more understandable. Additionally, although constructing a new experimental setup while simultaneously learning a new method can be challenging, this will allow you to gain intimate knowledge of the equipment so that it is not a "black box" to you. When problems arise, you will be in a position to understand and fix what is wrong.

Cleanliness: In electrochemical experiments involving a working electrode, the condition of the surface of the working electrode is important. Books, such as Ref. [122], usually have information on proper cleaning techniques, but articles are also helpful in this regard because the authors typically describe, at least briefly, the method they used to clean their apparatuses. The methods I used to make sure my electrodes were clean are described in Chapter 5.

It is also important and to maintain a vigilant attitude during the course of experimentation. For example, when I first did my cyclic voltammetry experiments, again, as described in Chapter 5, I was very careful to exclude oxygen from my system because I knew that reduced viologen is sensitive to oxygen. As time went by, I became less careful and did not use the flow rate of nitrogen that was required to ensure all the oxygen was purged from my system. I wasted a lot of time trying to figure out why my later experiments didn't look like my earlier experiments.

2.7 Summary

Carbohydrates are abundant, high-energy molecules that can potentially be used to power fuel cells. Carbohydrate fuel cells are an area of active investigation. In principle, fuel-cell units have a much higher energy density than batteries and also the ability to be rapidly "recharged" by mechanical means. Due to the potential lack of precious-metal catalyst, the cells based on this work may be cheap, or cheaper, to make than with previous technologies. The cells can potentially be portable and simple with no need for high-pressure containers or pretreatment equipment. Most of the cells being developed by other groups have only been shown to be functional with glucose, whereas MV has been shown, as reported in Chapter 3, to be highly versatile in regards to utilizable fuels. MV is reduced by all tested monosaccharides, and even some non-carbohydrate fuels.

3 INITIAL INVESTIGATION INTO THE UTILITY OF VIOLOGENS FOR USE AS CATALYSTS IN DIRECT CARBOHYDRATE FUEL CELLS

3.1 Introduction

With limited information on the catalytic oxidation of carbohydrates by viologen available in the literature, and to evaluate the utility of viologens for that purpose, the following basic questions needed to be answered.

Other than glucose, are other carbohydrates and chemical species oxidized by viologen? At the outset of this work, the mechanism by which the viologen oxidizes glucose was unknown, and it was thought that observing which species are oxidized by viologen, and which are not, would give us information on which functional group(s) are required for the oxidation to take place. Additionally, glucose is not the only potential fuel that researchers have investigated for fuel cell use. It is useful to know if viologens oxidize fuels such as methanol and ethanol, as well as other carbohydrates.

Do other types of viologen, besides methyl viologen, also catalytically oxidize glucose and other molecules? To create a practical fuel cell, it is likely that the viologen catalyst must be immobilized on a surface so that it does not leave the cell with the fuel stream. It is useful to know before any attempted immobilization how widespread the catalytic activity is among viologens so that knowledge can be used in the immobilization efforts. Additionally, values important to the catalysis, such as redox potentials, are known to vary from viologen to viologen

[9], depending on the substituents at the nitrogen, so it is again important to know how widespread the catalytic activity is.

At what efficiency is the fuel oxidized? Accurate efficiencies are important because the energy density, and thus utility, of the carbohydrate fuel relies directly on the extent to which the fuel can be oxidized.

Which factors in the oxidation are most important in affecting that efficiency? Due to the importance of efficiency in the utility of a carbohydrate fuel cell, it is useful to know which factors affect that efficiency.

What can be learned about the oxidation by examining the products of the oxidation? With the mechanism of the oxidation unknown, it was thought that the products of the oxidation could provide answers about the mechanism. With these answers, a hypothesis for the mechanism could be generated and then tested (Chapter 4).

Reduced methyl viologen, MV^{1+}, is readily oxidized by O_2, and two O_2-uptake methods, the so-called sealed-vial and pressure-cell methods, were used to evaluate catalytic oxidation of a wide variety of species by the viologens, the extent of that oxidation, and what factors most affect that oxidation. These same methods were also used to determine the activity of viologens other than MV. Products of the reactions were determined using NMR and mass spectrometry (MS).

The work presented in this chapter was undertaken in collaboration with Gerald Watt of the Department of Chemistry and Biochemistry at BYU, and Joseph Nichols and Adam Read of the Department of Chemical Engineering at BYU. The work has been published in two separate journals [8, 125]. Ref. [8] was a study of the catalysis of carbohydrates by disubstituted viologens from pH 9 to pH 12. In order to expand those initial studies we examined

carbohydrate oxidation in 1 M to 3 M KOH. These results established that dialkyl viologens are initially catalytically active but are inherently unstable in strong base and undergo hydrolysis to release one alkyl group, forming the analogous monoalkyl viologen in high yield. These monoalkyl viologens were also tested and appear to be catalytically active towards carbohydrates as well [125].

3.2 Experimental

3.2.1 Materials

The carbohydrates and other compounds listed in Table 3.1, the potassium and sodium bicarbonate and phosphate buffer components, methyl, ethyl and benzyl viologens, 4,4'-bipyridine, and methyl iodide were obtained from Sigma and used without purification. Specifically labeled glucose $^{13}C_1$ and $^{13}C_6$ glucose (99-atom percent, Sigma, St. Louis, MO) and labeled ^{13}C glyceraldehyde (98-atom percent, Omicron Biochemicals, Inc. South Bend, IN) were used to identify carbohydrate oxidation products. Milli Q water was used to make all solutions. Saturated KOH solutions (~19.6 M), in which K_2CO_3 is not soluble, were used to prepare carbonate-free 1.0-3.0 M KOH solutions for the monosubstituted viologen-catalyzed carbohydrate oxidation reactions.

3.2.2 Synthesis of viologens

Monomethyl viologen (MMV) was synthesized as follows. First, 0.2 grams of 4,4'-bipyridine was dissolved into 20 mL of acetone in a round bottom flask. Next, 0.25 mL of iodomethane was added to the round bottom flask. The solution was then stirred continuously under nitrogen for 8 hours at 60 ^{o}C. The precipitate was filtered on filter paper, and then washed

with acetone and dried. The MMV iodide salt precipitated as high purity product, though a small amount of MV (at least 4% of the precipitate) was also formed. 1,1'-ethylene-2,2'-bipyridinium dichloride and 1,2,3,6-tetramethyl-ethylene-2,2'-bipyridinium dichloride were synthesized as reported [1].

3.2.3 Methods

Sealed-vial method: The purpose of this method is to relatively quickly screen the effect of many reaction variables. This method involves placing a small amount of reactants in a serum-capped pressure-tight 10 mL glass vial and, after the reaction, measuring oxygen uptake to estimate the coulombic efficiency. With this method, 5-20 individual reactions were conducted simultaneously by placing 1.0 mL of buffer, the desired amounts of viologen and carbohydrate and a "flea stir bar" in a vial at 23 ^{o}C under 1.0 atm of air and immediately sealing the vial with an aluminum capped septum. The vial was vented with a needle, resealed with rubber cement, placed in a controlled temperature oven and rapidly stirred as the O_2-consuming reaction proceeded. When the reaction was completed, the vials were cooled to room temperature, weighed, submerged in distilled water and the serum cap punctured with a 23 gauge needle to fill with water the vacuum created from the O_2-consumption. The vials were dried and reweighed. The increase in mass (H_2O, 0.9970 g/mL) gave the volume of O_2 taken up by the reaction.

Pressure cell: A variation of the sealed-vial experiments is the pressure-cell experiment, in which the sealed vial is connected to a pressure transducer. These experiments produce pressure vs. time plots, which show how the oxygen consumption reaction proceeds in time. The pressure-cell experiments provide a check on the sealed-vial coulombic efficiencies because they are set up and measured in a similar way. A Micro Lab pressure sensor (Bozeman, MT) was

connected to pressure-tight vessels of 2.0-10.0 mL nominal volume. 1.0-2.0 mL of buffer (0.20 to 0.50 M) was placed in the pressure cell under 1.0 atm of air and the desired viologen was added to 0.50-30.0 mM. An aluminum capped rubber septum sealed the cell and a glass tight syringe containing 10-100 uL of carbohydrate solution (0.10-0.50 M) was put through the septum. When the cell and syringe assembly were equilibrated at 25-70 ^{o}C, the carbohydrate was added. The pressure change was monitored as a function of time (0.50-12 hrs) and pressure-time files were collected using a PC. From the change in pressure during the viologen-catalyzed carbohydrate oxidation, the amount of O_2 consumed by the reaction was determined. Pressure changes for control reactions of buffer plus carbohydrate or buffer plus viologen were determined and subtracted from the carbohydrate-viologen reactions. Generally, these corrections for non-specific carbohydrate oxidation were less than 5% of the overall catalyzed reaction.

Analytical investigation of products: The products of carbohydrate oxidation were identified by ^{13}C-NMR (Bruker Ultrashield 300 for the disubstituted viologen tests and Inova 300 for the monosubstituted viologen tests), using natural abundance glucose and specifically labeled $^{13}C_1$ and $^{13}C_6$ glucose. Viologen species were identified by both NMR (Inova) and mass spectrometry (MS, Agilent Technologies LC/MS TOF). H_2O_2 was measured using peroxide test strips from EMD Chemicals Inc., Gibbstown NJ sensitive to 0.5 mg/L. The presence of reducing carbohydrates was determined by Benedict's solution with a sensitivity of 1.0 μmol under the conditions of the experiment.

Microcoulometry: Microcoulometry was conducted anaerobically [126] in a coulometry cell containing viologen and buffer that was set at -400 mV relative to the saturated calomel electrode. As the viologen catalyst oxidizes the carbohydrate and forms reduced viologen, the

latter is oxidized at the silver electrode and the resulting oxidation current is integrated over time to obtain the total coulombs transferred during carbohydrate oxidation. The cathode for this cell is made of a coiled silver wire place in the test solution. The cathode reaction is the oxidation of the silver to form AgCl.

3.3 Results

3.3.1 Sealed-vial results

The sealed-vial method was used to obtain coulombic efficiencies (where $\eta_{coul} = n/n_{ideal}$, as described in Chapter 2) for 28 potential fuels, as catalyzed by one or more of four disubstituted viologens and one monosubstituted viologen (Table 3.1). A coulombic efficiency of 100% (6 O_2/glucose) corresponds to 24 electrons with subsequent formation of carbonate (Equations 2.2, 2.3, 2.8, 2.9). The disubstituted viologen reactions were carried out at 50 ^oC at a viologen/sugar ratio of 1.0 at pH 11.0 in 0.50 M sodium phosphate buffer. Monosubstituted viologen reactions were carried out at a viologen/sugar ratio of 1.0 in 1 M KOH and 23 ^oC (the elevated temperatures used for the disubstituted viologen tests were not necessary in 1 M KOH). IPV is isopropyl viologen; I and II are, respectively, 1,1'-ethylene-2,2'-bipyridine dichloride and 1,2,3,6-tetramethyl-ethylene-2,2'-bipyridine dichloride. Reactions identical to those with MV were conducted with ethyl viologen and nearly identical results were obtained (not shown). The data reported in sealed-vial tests was taken from tests that were run until the intense blue/purple of reduced viologen was no longer seen—5 or more hours—which suggests that the viologen was in the same oxidation state as when the test started.

Table 3.1 Coulombic efficiencies (%) for the oxidation of the named species by the named viologen. No tests were done in table locations filled with '-.'

Molecule (no. of C atoms)	MV	IPV	I	II	MMV
glucose (6)	20-40	48	14	48	35
fructose (6)	42	-	-	-	-
galactose (6)	35	-	-	-	-
ribose (5)	47	50	57	50	-
xylose (5)	45	52	25	52	-
erythrose (4)	48	-	-	-	-
glyceraldehyde (3)	40	32	40	42	35
dihydroxy acetone (DHA) (3)	35	-	-	-	41
monohydroxy acetone (MHA) (3)	35	-	-	-	-
acetone (3)	1	-	-	-	-
maltose (12)	19	21	9	20	-
lactose (12)	22	19	6	20	-
sucrose (12)	0	-	-	-	-
cellobiose (12)	25	20	-	-	-
glucosamine (6)	43	-	-	-	-
glycerol (3)	2	-	-	-	-
formaldehyde (1)	1	-	-	-	-
formate (1)	0	-	-	-	-
gluconic acid (6)	2	-	-	-	-
methanol	1	1	-	-	-
methyl-a-D-glucopyranoside (7)	0	-	-	-	-
sorbitol (6)	2	-	-	-	-
glyceric acid (3)	0	-	-	-	-
acetic acid (3)	0	-	-	-	-
methyl isobutyl ketone (5)	0	-	-	-	-
ethanol (2)	0	-	-	-	-
hydrazine	0	-	-	-	-
ethyl acetate (4)	0	-	-	-	-

The results are seen in Table 3.1, which shows that all tested viologens appear to be able to oxidize a variety of molecules. The species in Table 3.1 that react most readily with the viologens all share a common characteristic; they are all carbohydrates (or carbohydrate derivatives) with a free anomeric carbon. This important observation is expanded in Chapter 4, where it is shown conclusively that the active intermediate is the enediol form of the oxidized

molecule. An enediol is a functional group made of two hydroxyl groups on neighboring carbons connected with a double bond (Figure 3.1). Other functional groups, including simple alcohols, polyols, carboxylic acids, ketones, and aldehydes were found to be inactive towards the viologen, or to have very low activity.

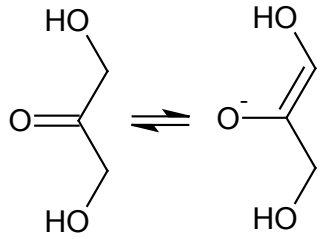

Figure 3.1 Dihydroxy acetone (DHA) and enediol form.

Table 3.1 shows coulombic efficiencies that are significantly higher than the two-electron oxidation of carbohydrates that would lead to the carboxylic acid form of the carbohydrate, as is often reported for glucose fuel cells. However, the high reported coulombic efficiencies are consistent with precedent (Chapter 2).

Four 12-carbon carbohydrates were tested, with results shown in Table 3.1. Three of the carbohydrates, the disaccharides maltose, lactose, and cellobiose, have coulombic efficiencies roughly half those of the 6-carbon monosaccharaides. This is due to the sugar units being linked to each other in such a way that only one of the units is capable of forming the enediol. In sucrose, also a disaccharide, the monomers are linked so that neither unit can form the enediol, and therefore no oxidation is seen.

It is also evident from Table 3.1 that, under the same conditions, the tested monosaccharaides capable of forming the enediol (the top eight entries in the table) are oxidized to roughly the same extent, whether they have 3, 4, 5, or 6 carbons. This means that, under the

conditions of the test, hexoses are seen giving up approximately 10 of their 24 available electrons, while trioses are seen giving up only 5 of their 12 electrons.

Because we see that all carbohydrates with a free anomeric carbon are oxidized by the viologen, Table 3.1 also suggests that a fuel stream containing a mixture of sugars may be used by a fuel cell catalyzed by viologen. The main carbohydrate products of the hydrolysis of lignocellulose are the sugars glucose, xylose, arabinose, and cellobiose [127], which are all oxidized by the viologen. The hydrolysis process is under investigation for the production of "cellulosic ethanol." The hydrolysis mixture also contains byproducts such as furfural, acetic acid, and formic acid, which inhibit the production of ethanol [128]. It is unknown at this time whether these byproducts would interfere with the oxidation of the carbohydrates by the viologen.

3.3.2 Sealed-vial, viologen/carbohydrate ratio effect

Figure 3.2 shows a series of reactions at 50 ^{o}C at pH 11.0 in 0.25 M sodium phosphate buffer and one atmosphere of air as a function of MV/glucose ratio. The ratios shown were achieved with two series run different ways. One series was done by holding the glucose concentration in the vial constant while the concentration of viologen was varied, and the other was done by holding the viologen concentration constant while the glucose concentration was varied. For the former series, the glucose concentration was 0.010 M and the MV concentration was varied to produce ratios ranging from 0.045 to 15.0. For the latter series, the MV concentration was held constant at 0.025 M and the glucose concentration was varied to attain the indicated ratios.

Figure 3.2 shows that the extent of glucose oxidation depends on the MV/glucose ratio and is seen to be between 20-40% at ratios of 0.10 to 2.0. However, above this ratio, the

coulombic efficiency slowly increases until at 12, approximately 80% efficiency is reached. At a ratio of 2.0 and approximately 35% efficiency, the MV catalyst cycles about 4 times but at a ratio of 0.10, at 22% efficiency, the catalyst makes about 53 cycles. Under conditions of Figure 3.2, no H_2O_2 was observed and O_2 was reduced to H_2O. At each MV/glucose ratio examined, the pH decreased less than 0.20, demonstrating that the reaction was not pH limited.

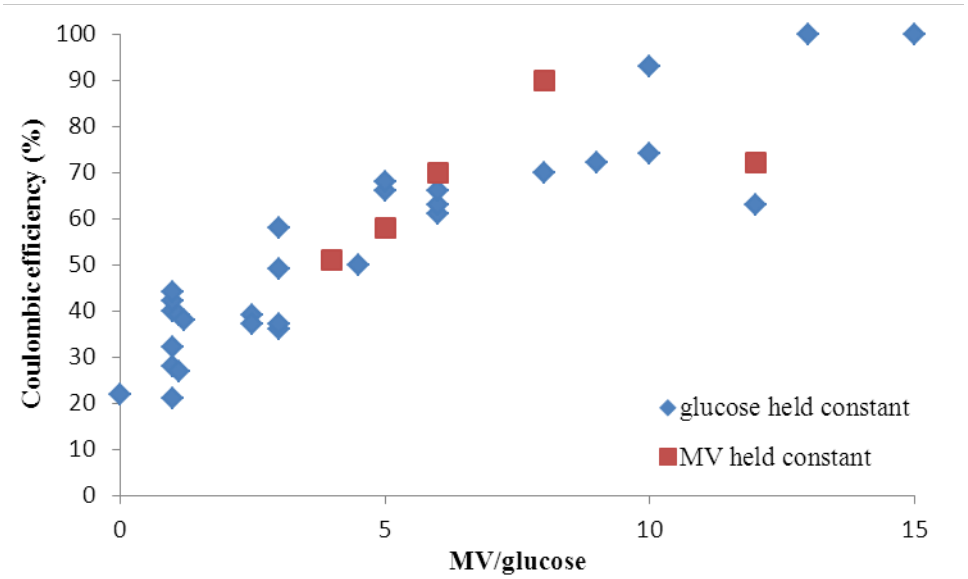

Figure 3.2 The efficiency of glucose oxidation by O_2 using MV as catalyst. The results shown are based on single experiments.

The results in Figure 3.2 show some variation, as seen by the measurements near a 1:1 ratio, which was studied extensively. A number of factors may contribute to this irreproducibility. The presence of metal ions functioning as catalysts can alter the extent of reaction and precautions were taken to minimize this effect. Perhaps the more important problem is that the stable free radical, MV^{1+}, is first formed that initially reduces $O_2 \rightarrow O_2^- \rightarrow H_2O_2 \rightarrow H_2O$. The presence of free radicals and formation of reactive O_2 species likely contribute to uncontrollable reaction pathways that lead to irreproducibility. Glucose

inactivation by polymerization was previously reported in alkaline glucose fuel cells [62] that could also influence reproducibility. This polymerization is discussed below, when the products of the oxidation are examined. Additionally, though the sealed-vial method has the advantage of high throughput, the way in which the coulombic efficiency was measured may not allow for the most precise measurements.

Similar to the glucose oxidation shown in Figure 3.2, glyceraldehyde oxidation is also dependent on the MV/glyceraldehyde ratio. At MV/glyceraldehyde ratios of 0.1 to 1.0 the efficiency is initially constant at approximately 40% but as the ratio increases to 10, approximately 80% oxidation of glyceraldehyde occurs. The reaction of glyceraldehyde is more efficient at low MV/glyceraldehyde ratios and the efficiency increases slightly faster with MV/glyceraldehyde ratio than that with glucose, indicating the greater reactivity of glyceraldehyde.

Table 3.2 shows a similar type of data as is seen in Figure 3.2, but for MV and monomethyl viologen (MMV) with sugars other than glucose. The reactions were conducted in air at either pH 11 in 0.5 M phosphate buffer, or in 1.0 M KOH. The uncertainty was obtained from 6-8 separate sets of measurements under the same conditions, with the spread in the data being a simple expression of the total scatter seen in the data.

Table 3.2 Effect of pH and viologen/carbohydrate ratio on the coulombic efficiency (% ± S.D.) of viologen-catalyzed carbohydrate oxidation by O_2.

			Efficiency (%) at indicted viologen/carb. ratio				
Viologen	Carbohydrate	pH	0.5	1	2	5	8
MV	glyceraldehyde	11	33±3	40±3	43±2	68±5	81±4
MMV	glyceraldehyde	11	28±3	35±3	40±5	60±4	72±4
MMV	glyceraldehyde	14	33±3	39±4	44±2	58±3	78±3
MMV	DHA	14	41±4	41±2	48±2	60±2	84±5

Rows 1 and 2 compare the efficiency of carbohydrate oxidation by O_2 using MV and MMV at pH 11 as a function of viologen/glyceraldehyde ratio. Glyceraldehyde oxidation reached approximately 80% efficiency for both at MV (MMV)/glyceraldehyde ratios above 8. MMV was also found to be slightly less efficient than MV in oxidizing glucose and other carbohydrates in a similar ratio dependent manner. In part, this is because the rates of MMV reaction are slower (see Figure 3.5 below). Although less extensively studied, monoethyl and monoisopropyl viologens gave similar results at pH 11 as those shown in Table 3.2 for MMV.

A comparison between MV and MMV in 1.0 M KOH was also carried out with both glyceraldehyde and DHA, but the reaction with MV is only valid for a short time because the MV hydrolyzes to MMV. Nevertheless, results suggest that at both pH 11 and in 1.0 M KOH, MV more completely oxidizes carbohydrates by a factor of 1.2 to 1.5 compared to MMV.

3.3.3 pH dependence

Disubstituted-viologen-catalyzed oxidation of glucose by O_2 only occurs at basic pH and has a pH plateau above 10.5. The same pH profile occurs with either sodium or potassium carbonate or phosphate buffers at concentrations from 0.10 to 0.5 M. The shape of the curve suggests that proton ionization from glucose is occurring with a pKa near 10 because MV does not have ionizable protons. However, the pKa for glucose is approximately 12 but could be shifted downward to approximately 10 if strong MV^{2+} binding facilitates proton ionization.

At pH values above 14, disubstituted viologen degradation becomes important and is manifest as formation of a yellow-brown solution. Degradation can be minimized by lowering the pH of the reaction mixture to less than 12.5 and maintaining the temperature below 60 ^{o}C.

The pH dependence of glyceraldehyde oxidation under the same conditions as glucose discussed above showed maximum activity at pH 9.5 vs a pH of 10.5 for glucose. DHA and

monohydroxy acetone (MHA) were slightly more reactive than glyceraldehyde. Tetroses and pentoses are intermediate in reactivity between glyceraldehyde and glucose.

3.3.4 Pressure-cell results

Glucose: Figure 3.3 shows the pressure decrease when 0.01 M glucose, 0.01 M MV with 0.025 M phosphate buffer at pH 11.0 react with air at 50 ^{o}C in the pressure cell. Under different conditions, such as concentrations of glucose below 0.5 mM, the reaction was very slow, and at temperatures less than 40 ^{o}C, no appreciable reaction occurred.

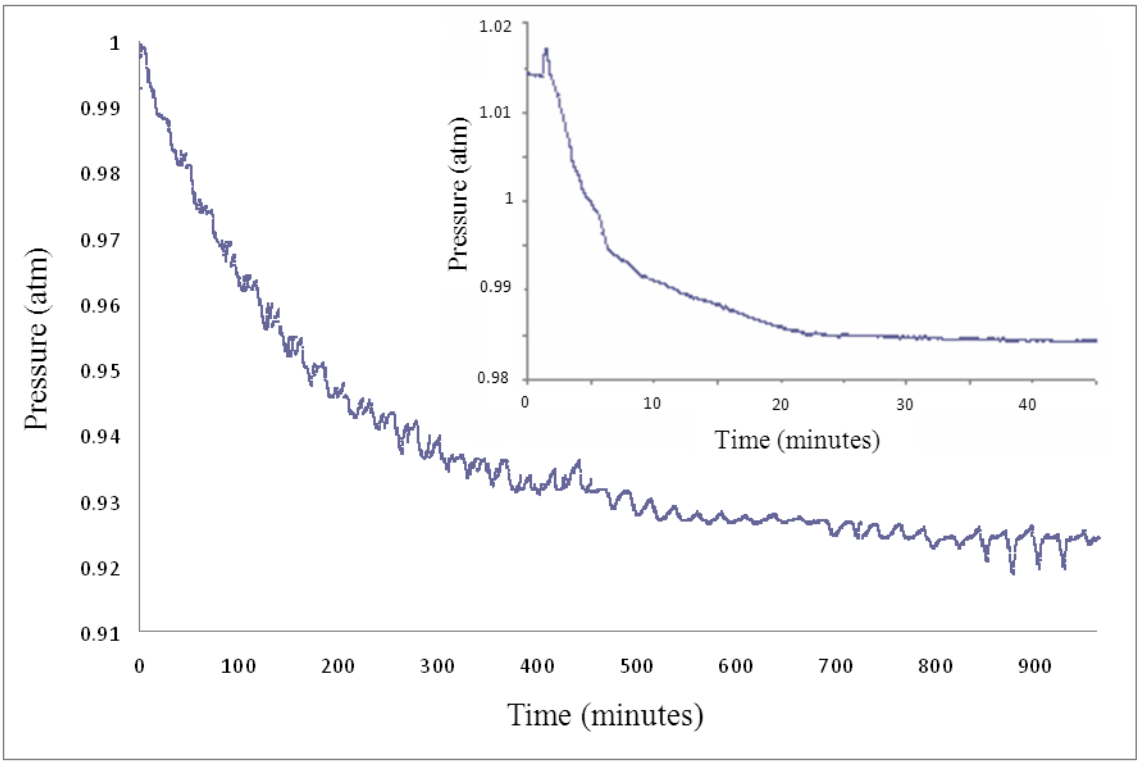

Figure 3.3 Pressure decrease (O_2-uptake) for the reaction of glucose with MV at pH 11 and 50 ^{o}C, Figure 3.3 insert. Pressure decrease (O_2-uptake) for the reaction of glyceraldehyde, MV at pH 11 and 23 ^{o}C.

The pressure change corresponds to 41.5% efficiency (10 electrons/glucose) of glucose oxidation. Figure 3.3 shows two distinct regimes. An exponential pressure decrease (O_2-uptake) for approximately 500 min, after which a slow linear pressure decrease continues for a much longer time. This two-regime behavior is also seen in the fuel cell results reported in Chapter 6, where an initial high current is followed by a steady, much lower current when the cell is run at closed-circuit potential.

Glyceraldehyde: A reaction conducted under identical condition to Figure 3.3 (see insert) produced a pressure-time curve for the MV-catalyzed O_2-oxidation of glyceraldehyde that was complete in only approximately 30 minutes at 23 ^{o}C, in contrast to glucose which requires approximately 6 hours at 50 ^{o}C. The pressure change corresponds to a 32.3% (3.9 electrons/glyceraldehyde) efficiency of glyceraldehyde oxidation. The near exponential pressure decrease changes to a slow linear decrease at approximately 23 minutes.

3.3.5 Product identification from carbohydrate oxidation

Glucose: Figure 3.4a shows the natural abundance ^{13}C NMR spectrum following glucose oxidation at a 12:1 MV/glucose ratio at pH 11, giving approximately 80% (19 electrons/ glucose) efficiency. The inset in Figure 3.4a is a carbon NMR of natural abundance glucose in water. Significant amounts of carbonate (168 ppm) and formate (171 ppm) and lesser amounts of gluconic acid (179 ppm) are seen, establishing that carbon-carbon bonds were broken and extensive oxidation of glucose occurred. Unreacted glucose (resonances between 60-80 ppm) is barely detectible. A control spectrum of glucose plus buffer (minus MV) in air under the same conditions did not produce carbonate and only trace amounts of formate, establishing that MV is required for glucose oxidation. MV^{2+} resonances occur at 48, 126, 146 and 149 ppm.

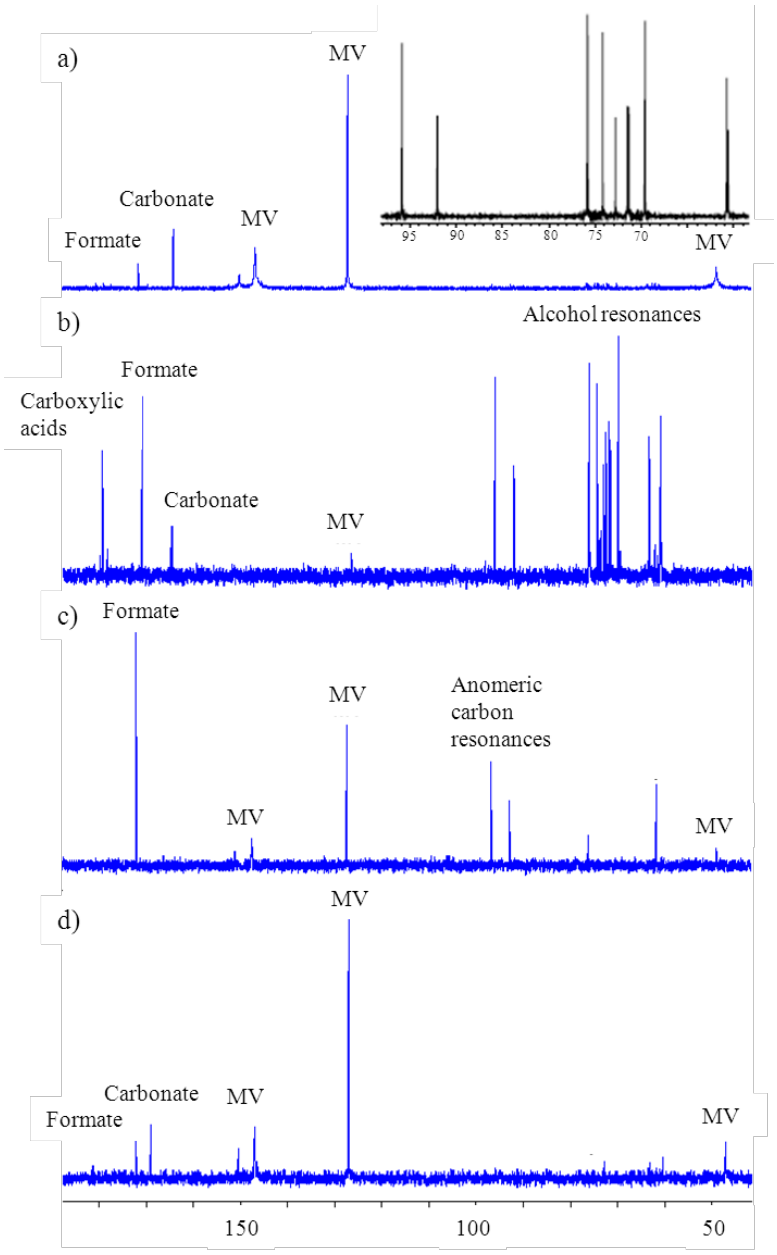

Figure 3.4 ^{13}C-NMR spectra of the products of the oxidation of glucose and glyceraldehyde by viologen.

Figure 3.4b shows a ^{13}C natural abundance spectrum of a reaction conducted at a MV/glucose ratio of 0.1 at pH 11 with an efficiency of 31% (7.4 electrons/glucose). This reaction corresponds to the low ratio end of Figure 3.2. The ^{13}C spectrum shows significant

amounts of formate, carbonate and gluconic acid (as well as glucose and non-glucose resonances, 60 to 96 ppm), establishing that under these conditions MV catalytically cycles numerous times and catalyzes significant carbon-carbon bond breaking.

Figure 3.4c shows the spectrum after $^{13}C_1$-labeled glucose (92.3 and 96.4 ppm) was reacted at a MV/glucose ratio of 1.0 in air at pH 11 giving 30% efficiency (7.2 electrons/glucose). ^{13}C-labeled formate is formed early along with a much smaller resonance likely due to $^{13}C_1$ gluconic acid. When identical reactions were conducted with $^{13}C_6$–labeled glucose, weak resonances of ^{13}C-labeled carbonate and stronger formate resonances were observed but in lesser amounts than the corresponding $^{13}C_1$-labeled reactions.

Control reactions corresponding to Figure 3.4a over 5.5 hours using ^{13}C-labeled glucose compounds minus MV showed only the presence of unreacted glucose and a very weak formate resonance but no ^{13}C-labeled carbonate. These labeling experiments and their controls establish that viologen catalyzes the oxidation of glucose by O_2 in air and that non-specific glucose oxidation is minimal under the conditions of the tests. The results are consistent with oxidation beginning at the more reactive C_1 end of glucose and progressing to the C_6 end but do not exclude the possibility of simultaneous oxidation occurring at both ends.

The presence of what appears to be unreacted glucose in Figure 3.4a-c and only 35% efficiency at low ratios raise an important question of why some glucose is oxidized to formate and carbonate and yet some remains apparently unreactive. This lack of glucose reactivity is a major factor causing low conversion efficiency at low MV/glucose ratios. If reactions producing 35% efficiency at MV/glucose ratios below 2.0 are allowed to react much longer, a greater O_2-uptake is observed, suggesting this unreacted glucose slowly undergoes reaction. This reactivity corresponds to the slow linear O_2-uptake evident in Figure 3.3 after 500 min.

Vials that had been reacted to completion were tested with Benedict's solution and the peaks that appear to be unreacted glucose were found to not be reducing sugars. Non-reducing carbohydrates, such as sucrose, show peaks in the same 90 to 100 ppm range where the anomeric C_1 carbon of glucose is seen. Non-reducing sugars do not form the enediol, and so will not react with viologen appreciably. It is possible that the peaks that are seen are some form of carbohydrate polymer. Whatever compound is the source of the peaks, it is inactive, or has very low activity, toward the viologen catalyst.

Glyceraldehyde: At a 1/1 MV/glyceraldehyde ratio and at approximately 40% efficiency, Figure 3.4d shows the presence of ^{13}C resonances from carbonate and formate, along with smaller resonances due to glyceric acid. At pH 11, ^{13}C resonances from unreacted glyceraldehyde are not observed. From the intensities of formate and carbonate resonances in spectrum Figure 3.4d and from the measurement of O_2-uptake giving 40% efficiency, an accounting of electrons was made consistent with the presence of some unreacted glyceraldehyde. However, reaction with Benedict's solution also showed the absence of reducing carbohydrates. As the MV/glyceraldehyde ratio increases, the efficiency of glyceraldehyde oxidation increases as does the amount of formate and carbonate. These results are similar to those discussed above for glucose and indicate that unreactive glyceraldehyde is present that causes the efficiency to be only 40% at a 1/1 MV/glyceraldehyde ratio but, as with glucose, the efficiency can be increased to approximately 80% at higher MV/glyceraldehyde ratios.

3.3.6 Viologen stability

The stability of MV and MMV was examined by MS and NMR at pH 12 and in 1.0 M KOH by following the loss of the parent peaks and the appearance of MMV. MV is stable and

catalytically functional at pH 12 for at least 40 days, with no degradation seen in NMR. Within 20 minutes in 1 M KOH the dialkyl viologen MS peak begins to disappear and within 48 hours the parent MS peak is no longer visible. Within this time frame monoalkyl peaks dominate all the peaks, with the remainder of the area being made up of small unidentified peaks. In contrast to MV, the independently synthesized MMV remained unchanged after 48 hours in even 1 M KOH.

3.3.7 Electrochemical carbohydrate oxidation

For the O_2-uptake measurements discussed above, the rates of MV or MMV reduction by glyceraldehyde were more rapid than the mass transport of O_2 from air to the solution to oxidize the reduced viologen species even with vigorous stirring. As a consequence the reactions were limited by O_2 transport so the rate of carbohydrate oxidation by MV and MMV could not be determined from the pressure-cell method. To efficiently utilize the energy of carbohydrates in a fuel cell, it is important to understand the relative rates of carbohydrate oxidation by MMV and MV and to separately study this carbohydrate oxidation process from the O_2-utilization reaction.

Figure 3.5 compares the electrochemical oxidation of DHA mediated with MV and MMV under the same conditions in the absence of O_2. 20 μmol each of MMV and MV were added in separate reactions to 2.0 mL of 0.50 M potassium phosphate buffer pH 11 containing 20 μmol of DHA. The viologens oxidized DHA and in turn were oxidized by the silver electrode.

From the brief steady-state rate at the peak current, the rate of glyceraldehyde oxidation by MV was seen to be approximately 3.0 times faster with MV than with MMV. The integrated area of both curves indicate that the extent of oxidation of DHA was typically 1.2 times greater

for MV than that for MMV, a result consistent with the results in Table 3.2. The reactions were conducted under an atmosphere of N_2 to eliminate any O_2, as the O_2 quickly oxidizes any MV^{1+}.

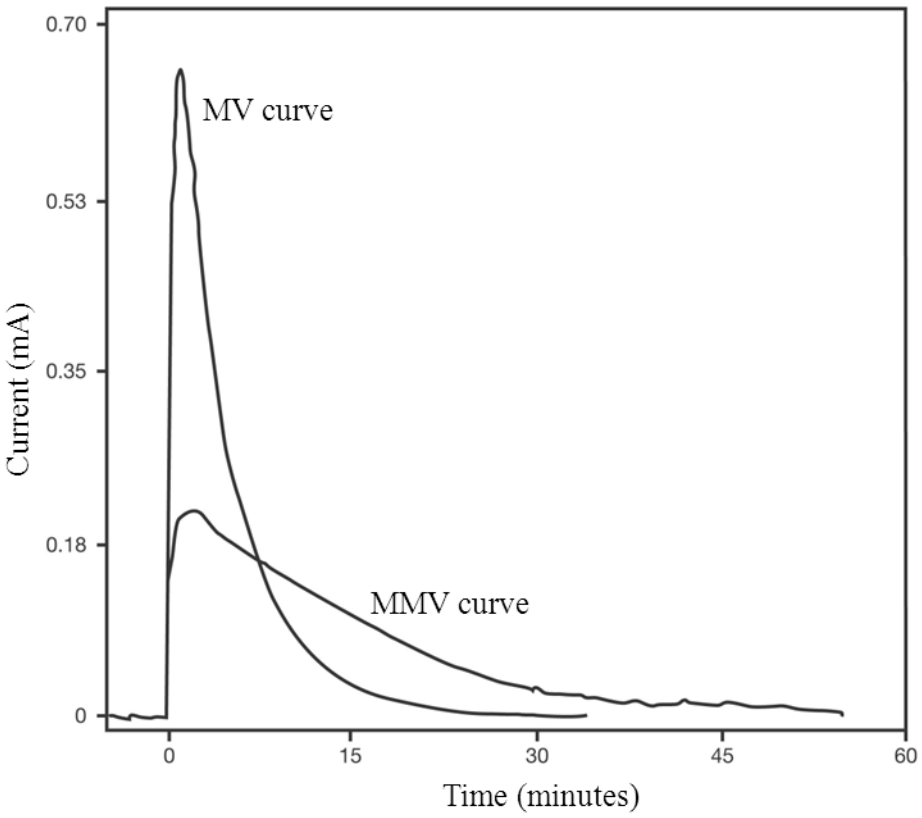

Figure 3.5 Coulometric oxidation of reduced MV and MMV formed from viologen-catalyzed oxidation of DHA at pH 11.

The results seen in Figure 3.5 are similar to results from early experiments using the fuel cell-like device described in Chapter 6. However, fuel cell experiments done at a later time under which extensive measures were taken to purify the MMV of any trace of MV suggest that the relative current produced by MMV is less than seen here. This is discussed in Chapter 6.

3.4 Discussion

Figures 3.2 and 3.3 establish that carbohydrate oxidation by air is catalyzed by the presence of the redox active viologen catalysts shown in Table 3.1 and that the coulombic efficiency of the reaction is highly dependent on the MV/sugar ratio. During this reaction, O_2 is consumed and carbohydrate is oxidized to formate and carbonate, establishing the significant result that carbon-carbon bonds have been broken. Ultimately, at high MV/glucose ratios formate and carbonate appear to dominate as major products.

The absence of H_2O_2 during the reaction establishes that H_2O is the product of O_2 reduction. Only minimal non-specific sugar oxidation occurs under these mildly basic conditions of the MV tests, establishing that viologen is a requirement for sugar oxidation. Careful preparation of solutions using acid washed glassware is essential to minimize metal ion contamination, which accelerates non-specific glucose oxidation.

The reaction is highly pH dependent and only occurs at pH > 10.5 for glucose and other hexoses but at lower pH values for the more reactive glyceraldehyde and DHA (pH > 9.5). The pH reaction profile suggests that the carbohydrate undergoes proton ionization before reaction with MV. Above pH 14, no additional reaction enhancement is observed and disubstituted viologen degradation becomes significant. Running reactions with disubstitited viologen at pH values at or below approximately 12 and temperatures below 60 ^{o}C minimize catalyst alteration.

Figure 3.2 shows that at MV/glucose ratios less than 2.0, MV turns over many times but that the overall oxidation reaction of glucose by O_2 is only approximately 35% complete. The inefficiency is due to the presence of unreacted or inactive modified glucose. As the ratio increases, the extent of glucose oxidation increases but the number of catalytic cycles of MV decreases. The addition of more glucose to these low efficiency reactions results in oxidation of

the added glucose again to approximately 35%, demonstrating that the MV catalyst is still functional but that part of the added glucose undergoes inactivation. At 10-12 MV per glucose approximately 80% glucose oxidation occurs and under these conditions the MV only cycles twice. The reactivity of glyceraldehyde and DHA parallels that of glucose but the reactions occur more rapidly and at lower temperatures.

The results for glucose oxidation are not easily understood in terms of a simple catalytic cycle. Our initial hypothesis was that the inefficiency is a thermodynamic consequence of glucose being converted stepwise to more oxidized products with higher oxidation potentials that are not as easily oxidized by MV as the parent glucose molecule. Higher concentrations of MV would be required to shift the equilibrium in favor of MV reduction by these less reactive glucose oxidation products. While such an explanation is reasonable, it does not account for all of the observations and we sought additional explanations.

Figure 3.2 suggests that proton ionization from the sugar is required for reaction to occur. If strong complex formation occurs between MV^{2+} and the glucose anion, or between MV^{2+} and strongly anionic buffer components (HPO_4^{2-}, PO_4^{3-}, CO_3^{2-}), then these electrostatic interactions could effectively remove MV^{2+} from solution and additional MV^{2+} would be required to drive the reaction toward completion. This explanation is consistent with the results in Figure 3.2 and is also consistent with the observation that the addition of the soft I^- ion to MV^{2+} causes formation of an intensely yellow colored complex, suggesting complex formation [9].

Another explanation is that carbohydrate alteration is occurring by a reaction byproduct generated during the reaction or by polymerization of carbohydrate, perhaps facilitated by the presence of free radicals generated during reaction. Either type of inactivation must alter the anomeric carbon of the carbohydrate, which is still visible in NMR spectra of reactions that have

gone to completion, because reaction with Benedict's solution shows the absence of reducing carbohydrate reactivity in the inactive product. In either case inactive carbohydrate is formed, but how does increasing the MV/carbohydrate ratio prevent or overcome this inactivation and increase the efficiency seen in Figures 3.2?

When the reaction is initiated, we propose that two reactions are possible: 1) carbohydrate oxidation by MV, which can potentially completely oxidize carbohydrate to formate and carbonate and 2) a MV- or hydroxide-promoted polymerization or inactivation reaction that occurs simultaneously with carbohydrate oxidation [129]. As the MV/carbohydrate ratio increases, the rate of carbohydrate oxidation appears to increase faster than inactivation. Acceleration of carbohydrate oxidation decreases the extent of the inactivation reaction, until, at high ratios, the carbohydrate oxidation approaches the prediction of Equation 2.3. This subject is studied in more detail in Chapter 4.

Comparison of monoalkyl and dialkyl viologens: Monoalkyl and dialkyl viologens have different advantages and disadvantages in their role as catalysts for the oxidation of carbohydrates and in potential uses in carbohydrate fuel cells. These differences include the pH regime in which each type is usable, differences in reaction rate, and coulombic efficiency.

Monoalkyl viologens are more stable in strong base. This behavior potentially makes them more versatile for catalytic reactivity because they are able to catalyze carbohydrate oxidation from approximately pH 11 to pH 14 and above. In contrast, dialkyl viologens slowly hydrolyze to release alkyl groups in strong base and are only effective catalysts between pH 9 and 12.

Monoalkyl viologen appears to react with carbohydrates at approximately one-third the rate for dialkyl viologen under identical conditions (Figure 3.5). The slower rate of catalysis by

monoalkyl viologens compared to their dialkyl analogues probably arises from two factors. First, the monoalkyl viologens have only one quaternized positively charged center, whereas the dialkyl viologens have two in their respective oxidized states. The two-fold greater positive charge and the presence of two positive quaternized and reactive centers at each end of the viologen structure likely facilitate interaction and subsequent oxidation of the negatively charged endiol form of the carbohydrate by the dialkyl viologens. The second factor is that the dialkyl viologens are stronger oxidants than the monoalkyl viologens, which implies a greater driving force and an increased rate of oxidation by the dialkyl viologens compared to their monoalkyl derivatives.

These differences in reactivity have consequences for the coulombic efficiency achieved by either type of viologen catalyst. Due to slower reaction rates with monoalkyl viologen, carbohydrate oxidation in a fuel cell could become less efficient, leading to unreactive intermediates and a lower overall coulombic efficiency (Chapter 4). The oxidation of the carbohydrate by dialkyl viologens is faster, so more of the carbohydrate follows the formate/carbonate oxidation pathway and coulombic efficiencies are higher.

A disadvantage of using either the monoalkyl and dialkyl viologens as homogeneous catalysts is that their catalytic efficiency varies with viologen/carbohydrate ratio [8, 10]. At low ratios, both have higher coulombic efficiencies than are typically reported for metal-catalyzed DCFCs (Table 3.2), but this efficiency at low ratios is relatively low compared the efficiency seen at high ratios. The reason for this ratio-sensitive efficiency is elucidated in Chapter 4. To provide high utilization of carbohydrate energy, operation of a fuel cell would require high ratios of either monoalkyl or dialkyl viologens. Because monoalkyl viologens more slowly transfer

electrons from carbohydrates to the electrode, a higher ratio is required to compensate for this slowness.

3.5 Conclusion

In summary, our results demonstrate that carbohydrates are readily oxidized by O_2 in the presence of various viologen catalysts at pH values of 9 to 14. The extent of carbohydrate oxidation depends on the viologen/carbohydrate ratio with low ratios (less than 2.0) producing oxidation efficiencies of 30-50% and higher ratios yielding efficiencies approaching 80%. A wide variety of carbohydrates undergo this reaction as long as the anomeric carbon is free, meaning that the enediol intermediate may be formed.

The results reported here are relevant to using various forms of viologens for fuel cell applications. Monoalkyl viologens are functional as carbohydrate oxidation catalysts from approximately pH 11 to over pH 14, whereas dialkyl viologens only function stably between pH 9-12. Within their stability ranges MMV and MV function for several hundred turn-over events without undergoing any chemical modifications or loss in catalytic activity.

4 MECHANISTIC INSIGHTS FOR THE VIOLOGEN-CATALYZED OXIDATION OF CARBOHYDRATES

4.1 Introduction

The results reported in Chapter 3 indicate that the coulombic efficiency of viologen-catalyzed carbohydrate oxidation increases at high catalyst ratios. Several possible reactivity patterns were proposed to explain the low carbohydrate reactivity at low ratios. Prominent among these was the possibility that the anomeric carbon of carbohydrates was altered by reaction intermediates or that the carbohydrates had undergone polymerization forming multimeric carbohydrates that were inactive. We have now examined a number of those initially proposed explanations and report that the inefficiency noted earlier is due to the formation of inactive intermediates, which prevent efficient oxidation of the parent carbohydrate.

The same methods described in Chapter 3 were employed to obtain the results presented in this chapter, and the particular experiments described and the hypotheses tested here are in part a product of the conclusions based on the data presented in Chapter 3. Though the subject matter of this chapter and Chapter 3 is related, they are presented here as separate chapters because they cover slightly different topics and were presented in separate publications.

As in Chapter 3, the sealed-vial and pressure-cell methods were used to estimate the coulombic efficiencies with which test molecules were oxidized by test viologens. These methods were used to examine hypotheses by testing model compounds and for testing the effectiveness of viologens polymers in the oxidation of carbohydrates. Analysis of model-

compound and carbohydrate oxidation products was used to generate and confirm the mechanism proposed for the oxidation. The microcoulometry experiments were used to obtain rates of oxidation for different carbohydrates, and to compare anaerobic coulombic efficiencies to the aerobic sealed-vial efficiencies.

The work presented in this chapter was undertaken in collaboration with Dr. Gerald Watt of BYU and is based on a paper published in the journal *Renewable Energy* [10] in 2011. I generated the idea of using model compounds to test the enediol hypothesis, participated in testing those compounds, participated in analyzing the results, and, based on those results, helped generate the proposed mechanism for the oxidation. I was not involved in making or testing the viologen polymers as reported here. The data and conclusions based on the polymer data are included for the sake of completion.

4.2 Materials and methods

4.2.1 Methods

Oxygen-uptake measurements were conducted using a Microlab Pressure Sensor (Bozeman MT) or by the vial method as previously described in Chapter 3. Carbohydrate and viologen species were identified by MS (Agilent LC/MSD TOF) and by ^{13}C NMR (Inova 300). Microcoulometry was conducted as described in Chapter 3.

4.2.2 Materials

^{13}C labeled glucose, 99-atom % (Sigma-Aldrich, St. Louis, MO) and glyceraldehyde, 98-atom % (Micron Biochemicals, Indianapolis, IN) were used to identify reaction products. Formate (171 ppm), carbonate (168 ppm), carboxylic acids (~180 and ~20 ppm and $^{13}C_1$ of

glucose 96 and 98 ppm for C_1 carbon) were well-separated resonances used for identification as reported in Chapter 3. Reactions were conducted in 0.50 M phosphate buffer at pH 11 as in Chapter 3. Glycoaldehyde, acetoin, dihydroxy acetone (DHA), monohydroxy acetone (MHA), glyceraldehyde, glucose and methyl (MV) and ethyl (EV) viologens were purchased from Sigma. Polymer synthesis followed the procedures outlined in [9] and the text related to Table 4.1 outlines the polymers used.

4.3 Results

4.3.1 Viologen polymers

The results reported in Chapter 3 demonstrated that viologens can effectively catalyze the oxidation of various carbohydrates and that the coulombic efficiency (where $\eta_{coul} = n/n_{ideal}$, as described in Chapter 2) increases with increasing viologen/carbohydrate ratio to an efficiency of greater than 80%. 100% coulombic efficiency is defined as complete oxidation of a carbohydrate to CO_2 and H_2O. We initially proposed that high catalyst ratios favored carbohydrate oxidation by minimizing secondary reactions, which formed unreactive intermediates such as carbohydrate polymers, alcohols, simple aldehydes and carboxylic acids. By minimizing these secondary reactions, carbohydrate oxidation efficiency would be enhanced. To test this hypothesis, we synthesized the three polymers listed in Table 4.1 (two of those polymers were also tested after they were immobilized on graphite). The rationale was that polymers would create a high, localized concentration of reactive viologen catalyst, which would simulate the behavior at high ratios and enhance catalytic efficiency.

Table 4.1 Coulombic efficiency (%) of carbohydrate oxidation conducted by polymeric viologens and MV.

Carbohydrate	Polymer					
	1	2	3	2-immob.	3-immob.	MV monomer
glyceraldehyde	56.5	65.3	50.8	50.3	49.7	42.4
glucose	46.0	45.5		44.0	44.9	34.0
DHA	59.2	50.2		58.8		47.1

Polymer 1 is in-chain polymerized trimethylene viologen; polymer 2 is benzyl viologen appended to a polystyrene chain; polymer 3 is phenyl viologen appended to polystyrene chain, and are seen in Figure 4.1. Polymers 2 and 3 were tested as free polymers (columns 3 and 4) and were also tested after being immobilized on graphite (columns 5 and 6). Free polymer 3 had limited solubility and immobilized polymers 2 and 3 were bound to insoluble substrates and therefore all formed heterogeneous solutions.

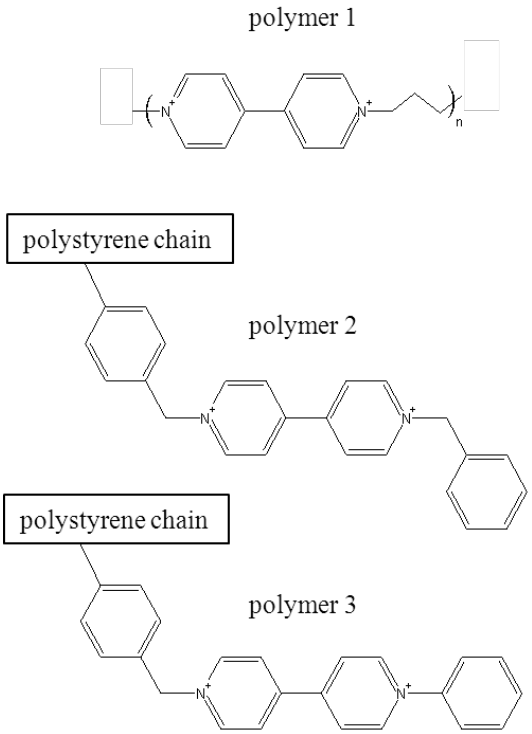

Figure 4.1 Viologen polymers.

Table 4.1 shows coulombic efficiencies (%) for the oxidation of the carbohydrates by the polymers, with the efficiencies for methyl viologen under the same conditions and effective monomer concentration shown for comparison. The reactions were conducted in 1.0 mL 0.50 M phosphate buffer pH 11.0 using the sealed-vial method. The monomer unit/carbohydrate ratio was 1.0 at a carbohydrate concentration of 0.02 M. Table 4.1 shows that the viologen polymers were effective in catalyzing oxidation of glyceraldehyde, glucose and DHA at pH 11.

Figure 4.2 shows a pressure-time curve at 45 ^{o}C for glyceraldehyde oxidation catalyzed by the soluble polymer 1 with formate and carbonate observed as major products along with smaller amounts of carboxylic acids. The higher temperature is required because the polymers react more slowly than the corresponding monomers. The reaction was conducted at 0.025 M glyceraldehyde with 10 mg of polymer 1 in 1.0 mL of 0.50 M phosphate buffer pH 11 with stirring.

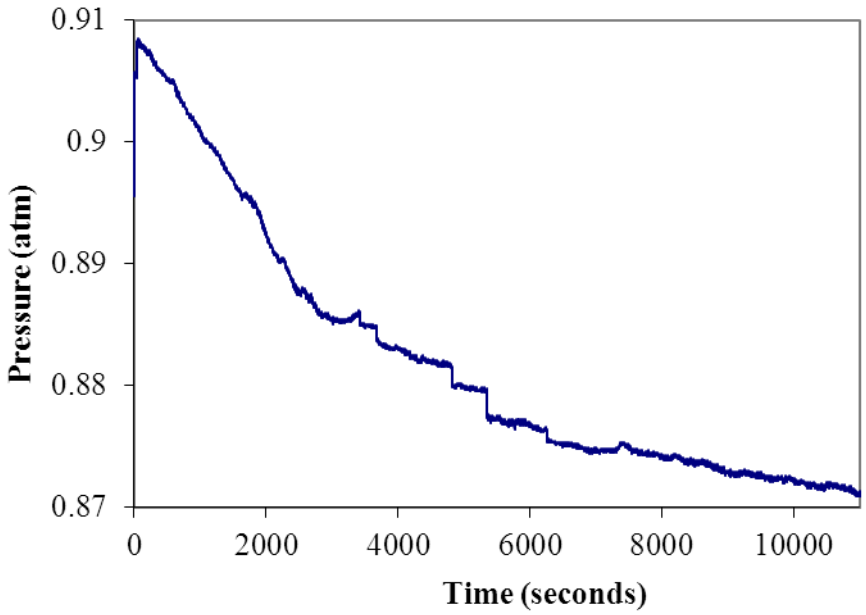

Figure 4.2 Glyceraldehyde oxidation by oxygen catalyzed by polymer 1.

For soluble polymers 1 and 2 at monomer unit/carbohydrate ratio of 1.0, the reactivity was generally about 25% higher than free MV monomers. Increasing the polymer/glyceraldehyde ratio to 5 increased carbohydrate oxidation efficiency, which is analogous to the results reported in Chapters 3 and 6. Thus, the anticipated improvement in carbohydrate oxidation efficiency was realized with polymer catalysis, but the increase was modest and the rates slower. We conclude that viologen polymers function as catalysts but are not well suited in their free form for carbohydrate oxidation or fuel cell use. The reason is that the free polymers react more slowly with electrodes, have poorer solubility that viologen monomers, require heating to greater than 40 ^{o}C, and seem to be more susceptible to degradation at higher pH than viologen monomers. However, the results are encouraging and suggest that stable, immobilized viologen polymer film electrodes or viologen conducting polymer electrodes would better serve as fuel cell catalysts.

As reported in Chapter 3, at MV/glucose ratio near 1, a glucose oxidation efficiency of approximately 30% was observed. The efficiency increased with increasing MV/glucose ratio. Similar enhanced efficiency was observed for glucose oxidation using polymers in Table 4.1. The polymer reactions required a pH of 11 and temperature of 45 ^{o}C. When polymers slowly break down under these conditions they consume O_2 and therefore give apparently higher glucose oxidation efficiencies than that from the catalyzed reaction. The results in Table 4.1 were corrected for this O_2-uptake from polymer degradation by simply subtracting the percentage of oxygen uptake found to have come from the polymer degradation using polymer-only control experiments.

4.3.2 Enhanced efficiency at high viologen/carbohydrate ratios

To explain enhanced efficiency with increasing catalyst ratio, we initially proposed that carbohydrates were inactivated by polymerization or by adduct formation at the anomeric carbon. Conducting reactions at intermediate levels of oxidation at various MV/glucose ratios, did not lead to the identification of dimers, trimers or higher multimers of glucose; nor did MS show any adducts of glucose formed by alteration of the anomeric carbon. These results indicate that polymerization and adduct formation are not major routes for glucose inactivation.

When examined by ^{13}C NMR, formate and carbonate were dominant ^{13}C-containing species, but using ^{13}C-enriched glucose at all carbon atoms, a number of smaller species were observed. The spectra were complicated because several related species were present, but carboxylic acid groups were easily identified (around 180 ppm). Instead of higher adducts or multimers causing decreased glucose oxidation efficiency at low ratios, the formation of smaller species (carboxylic acids), that are not reactive toward viologen-catalyzed oxidation cause the low efficiency at low ratios. Simple aldehydes, carboxylic acids or α-hydroxy carboxylic acids are not reactive under the same conditions as viologen-catalyzed carbohydrate oxidation.

The catalytic oxidation of glucose is slower than that of glyceraldehyde and other carbohydrates, possibly due to ring opening, which allowed monitoring of product formation by ^{13}C NMR during glucose oxidation at a 1:1 ratio. Figure 4.3 shows the product distribution of formate, carbonate and carboxylic acids as a function of time. The reaction conditions were of 0.015 M $^{13}C_1$-labeled glucose, 0.015 M MV in 1.0 mL of 0.50 M phosphate buffer pH 11.0.

Glucose decreases to near zero in approximately 3 hours but the other three products continue to increase up to approximately 12 hours, after which they remain constant. This is consistent with glucose being sequentially oxidized to shorter chain carbohydrates (pentose,

tetrose, etc.), which in turn undergo oxidation forming formate, carbonate and small amounts of carboxylic acids until carbohydrate oxidation is complete. The trend for carboxylic acids is only approximate because different carboxylic acids are formed at different times during the reaction and mixtures are always present. At MV/glucose ratios greater than 1.0, formate and carbonate increase and carboxylic acids decrease in concentration giving an overall increase in efficiency of glucose oxidation as observed.

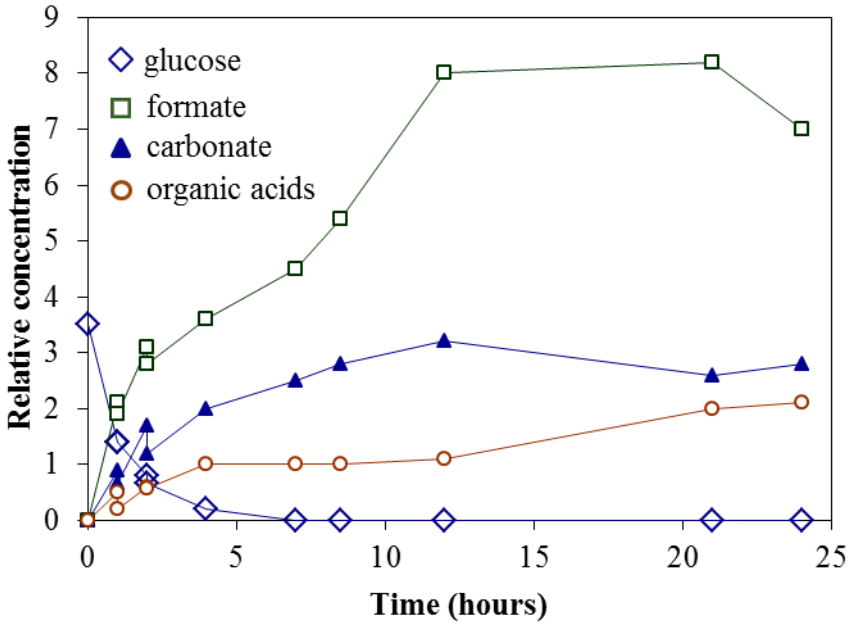

Figure 4.3 Species distribution from the MV-catalyzed oxidation of ^{13}C-labeled glucose determined by ^{13}C NMR. Each point is the average from two independent reactions. Line are a guide to the eye.

4.3.3 Model compounds

pH profiles for catalytic O_2-oxidation of both glyceraldehyde (pK = 9.5) and glucose (pK = 10.5) suggested that proton ionization preceded catalytic oxidation. Such ionization would produce a negatively charged enediol from carbohydrates containing terminal aldehydes. We hypothesized that the enediol is the reactive form of the carbohydrate that interacts with the

MV^{2+}, which then initiates catalytic oxidation of the carbohydrate. To test this hypothesis, we examined simpler molecules that only form a single enediol instead of the more complex carbohydrates of glyceraldehyde and glucose.

Glycoaldehyde reactivity: Glycoaldehyde (CH_2OH-CHO) is the simplest structure that can form an enediol. Complete oxidation of glycoaldehyde by oxygen is given by Equation 4.1, which shows that two O_2 are required to form carbon dioxide with transfer of 8 electrons to O_2. Equation 4.2 shows that two formic acids form by partial oxidation with transfer to O_2 of only 4 electrons. At pH 11, where the reactions were conducted, carbon dioxide forms carbonate and formic acid forms formate but this does not affect the electron count.

$$C_2H_4O_2 + 2\ O_2 = 2\ CO_2 + 2\ H_2O,\ 8\ e^- \quad (4.1)$$

$$C_2H_4O_2 + O_2 = 2\ HCO_2H,\ 4\ e^- \quad (4.2)$$

Based on the oxygen uptake seen in Figure 4.4, is was estimated that the oxidation of glycoaldehyde at room temperature using EV (same result with MV) as catalyst at a 1:1 ratio only goes to approximately 50-60% completion. The reaction consisted of adding 0.025 M glycoaldehyde to 0.025 M EV in 1.0 mL of 0.50 M phosphate buffer pH 11.0. The change in pressure corresponds to a 55% (4.4 electrons) efficiency of glycoaldehyde oxidation. Formate was the dominant ^{13}C-containing product. The slowness of the reaction is due to transport of O_2 into the aqueous solution because the reaction between glycoaldehyde and MV is nearly instantaneous. The reaction products were formate and only small amounts of carbonate.

When the reaction was carried out at a 15:1 catalyst ratio, there was no enhancement in the extent of reaction, contrary to previous results for glyceraldehyde and glucose. This result

indicates that the catalytic efficiency for glycoaldehyde was at a maximum at a 1:1 ratio, forming formate as product. A control reaction in the absence of MV or EV gave less than 5% oxidation under identical conditions. These results demonstrate that EV or MV dramatically increases the rate of glycoaldehyde oxidation to form formate.

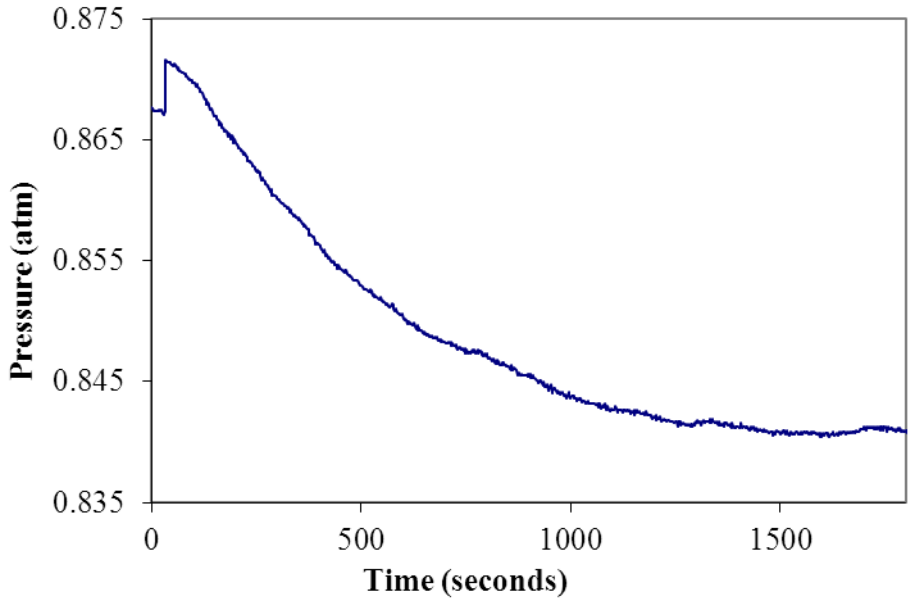

Figure 4.4 The change of pressure for the EV-catalyzed oxidation of glycoaldehyde.

An approximately 50-60% utilization of O_2 by glycoaldehyde corresponds to the transfer of 4.0-4.8 electrons to O_2 with formation of formate and smaller amounts of carbonate as shown in Equation 4.2. In the absence of additional constituents on glycoaldehyde, the reaction terminates with formation of formate and is independent of MV/glycoaldehyde ratio. Glycol, acetal, acetate or α-hydroxy acetate did not undergo MV-catalyzed oxidation under the same conditions, demonstrating that a carbonyl group and an adjacent hydroxy group are required for MV-catalyzed oxidation.

3-hydroxy-2-butanone (acetoin): Acetoin is similar to glycoaldehyde but has two methyl groups flanking the glycoaldehyde structure but should still form a simple enediol like glycoaldehyde. At room temperature, acetoin undergoes MV-catalyzed oxidation by O_2 about 10 times slower than glycoaldehyde, so the reaction was conducted at 45 ^oC to accelerate the rate. Equation 4.3 represents complete oxidation of acetoin to CO_2 and Equation 4.4 represents partial oxidation.

$$C_4H_8O_2 + 5\ O_2 = 4\ CO_2 + 4\ H_2O,\ 20\ e^- \quad (4.3)$$

$$C_4H_8O_2 + 2\ O_2 = CH_3COOH + CO_2 + HCOOH,\ 8\ e^- \quad (4.4)$$

Complete oxidation of acetoin requires 5 O_2 and liberates a total of 20 electrons. However, when catalyzed by MV only 40% oxidation of the acetoin is achieved, which is like glycoaldehyde but unlike glyceraldehyde and glucose. The major oxidation products were formate and acetate and small amounts of carbonate. From the products formed and the O_2-uptake, we conclude that Equation 4.4 represents the MV-catalyzed O_2-oxidation of acetoin. However, this reaction appears to be more complex because at its conclusion, the solution is a light red brown color, whereas the reaction with glycoaldehyde and other carbohydrates is colorless to pale yellow. The color intensifies with increasing ratio, suggesting possible modification of the catalyst during reaction. However, this effect must be minimal because the MV catalyst responds to subsequent additions of acetoin and NMR and MS do not show modified MV.

DHA and MHA: DHA and MHA are related to glyceraldehyde, except DHA has two hydroxy groups flanking a ketone group and MHA has one. DHA and MHA gave efficiencies

approximately 50% and 40% at a 1:1 ratio, respectively. The reactivity of DHA is greater than glyceraldehyde which is greater than MHA, but all gave similar ^{13}C product distributions, consisting mainly of formate and carbonate with small amounts of α-hydroxy acetate. The efficiency of DHA and MHA oxidation increases as a function of increasing MV ratio, indicating high oxidation efficiency also can be achieved at high MV/DHA, MHA ratios. In this respect, they differ from glycoaldehyde and acetoin, whose oxidation efficiencies are unresponsive to the catalyst ratio. The additional hydroxy group(s) on DHA and MHA changes their reactivity and allows them to undergo more extensive oxidation.

From O_2-uptake, the product distribution, and an examination of Equation 4.5-4.7, we conclude that Equations 4.6 most closely represents the major reaction (66.6% predicted efficiency vs. approximately 50% observed) with smaller contributions from Equation 4.7. Equation 4.5 gives the expected result for complete oxidation of glyceraldehyde or DHA by O_2 for 100% efficiency. Equations 4.6 and 4.7 describe partial oxidation reactions and show the corresponding number of electrons transferred to O_2.

$$C_3H_6O_3 + 3O_2 = 3CO_2 + 3H_2O,\ 12e \quad (4.5)$$

$$C_3H_6O_3 + 2O_2 = CO_2 + 2HCOOH + H_2O,\ 8e \quad (4.6)$$

$$C_3H_6O_3 + 3/2O_2 = CO_2 + C_2H_3O_2 + H_2O,\ 6e \quad (4.7)$$

4.3.4 Anaerobic vs. aerobic reactions

Results reported in Chapter 3, and those reported here, measured O_2-uptake during viologen-catalyzed carbohydrate oxidation by atmospheric O_2. To rule out nonspecific O_2-oxidation of possible O_2-sensitive oxidized carbohydrate intermediates, reactions were conducted anaerobically using controlled potential coulometry to oxidize reduced viologen at electrodes

instead of by O_2. This reactivity would parallel the conditions occurring in a fuel cell because the anodic compartment where carbohydrates are oxidized is anaerobic. This coulometry experiment is more fully explained in Chapter 3.

Figure 4.5 shows the results for electrochemical oxidation of DHA, glyceraldehyde and glycoaldehyde. The coulometric cell contained 2.0 mL of 0.50 M phosphate buffer pH 11.0 with 1.0 mM MV and was set at a controlled potential of -400 mV vs. the SCE until the current stabilized near 0.0 mA. DHA (1.00 mmol), glyceraldehyde (0.85 mmol) and glycoaldehyde (1.00 mmol) were then added separately and the current-time curves for each were integrated to determine the charge transferred to the electrode during carbohydrate oxidation.

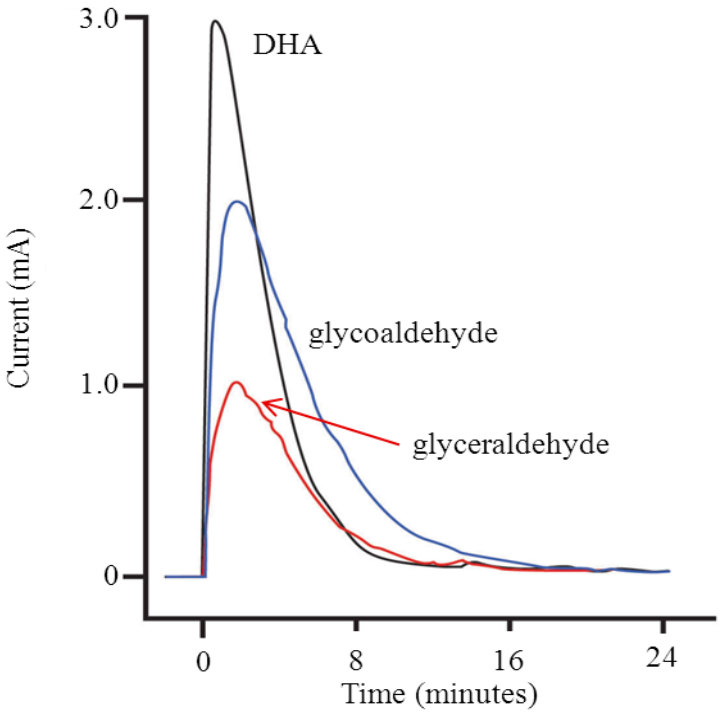

Figure 4.5 MV-catalyzed, controlled potential oxidation of DHA, glyceraldehyde and glycoaldehyde.

The overall shapes of the curves represent the reactivities of these three carbohydrates toward the MV catalyst. The initial steepness of the curves is the rate of carbohydrate oxidation by viologen. However, the peak current represents the brief pseudo-steady-state rate for carbohydrate reduction of viologen balanced by the rate of electrode oxidation of reduced viologen. The peak currents in Figure 4.5 give the relative carbohydrate oxidation rates as: DHA (2.7), glycoaldehyde (1.7) and glyceraldehyde (1.0). The areas under the curves give the total coulombs for each reaction from which the number of electrons removed from each carbohydrate was calculated. DHA is oxidized by 6.0 (5.6), glycoaldehyde by 3.7 (4.0) and glyceraldehyde by 3.9 (4.8) electrons, where the value in parenthesis is the extent of oxidation in air at the 1/1 ratio used. Thus, the anaerobic electrochemical oxidation is comparable with O_2-oxidation for all carbohydrates but is smallest for glyceraldehyde, suggesting that in the presence of air some non-catalyzed oxidation of glyceraldehyde or its oxidation products is occurring. This is not a problem during fuel cell operation because the anodic compartment of the fuel cell is anaerobic. These results validate results of the more convenient O_2-uptake experiments that measure the reaction characteristics of viologen-catalyzed carbohydrate oxidations.

4.4 Discussion

Using ^{13}C labeled glyceraldehyde and glucose demonstrated the presence of smaller oxidation products formed from carbohydrates during MV-catalyzed oxidation that were previously unobserved because of their low natural abundant ^{13}C concentrations. ^{13}C NMR and MS analysis have combined to show that oligomerization and modification of carbohydrates at their anomeric carbon are not the cause of inefficient carbohydrate oxidation catalyzed by methyl viologen as suggested in Chapter 3. Instead, formation of oxidized intermediates that are either kinetically or thermodynamically unable to undergo MV-catalyzed oxidation cause low

efficiencies. Thus, a strategy to prevent formation of these unreactive intermediates would increase carbohydrate oxidation efficiency and drive the reaction to form carbonate and formate.

Results reported in Chapter 3 showed that the oxidation efficiency could be increased by increasing the catalyst/carbohydrate ratio to greater than 10. It is not desirable to have such a high ratio of catalyst present and alternate means for bypassing unreactive intermediates were sought. The approach reported here of using viologen polymers to effectively increase the localized concentration of reactive viologen units and thereby decrease formation of unreactive, oxidized carbohydrate intermediates is clearly a productive route by showing polymers enhanced oxidation efficiency by approximately 25%. Viologen films on metallic electrodes or viologen-conducting polymeric electrodes offer greater promise than polymeric suspensions or soluble polymer catalysts. This is because inherent problems of polymer diffusion to and from electrodes and polymer-electrode contact of homogeneous polymeric catalysts all pose difficult and limiting problems.

4.4.1 Mechanistic considerations

The results reported here allow us to suggest a series of mechanistic steps outlining how MV and other viologens facilitate carbohydrate oxidation. First we note that simple aldehydes, carboxylic acids, alcohols or α-hydroxy carboxylic acids do not undergo MV-catalyzed O_2-oxidation at appreciable rates under conditions where carbohydrates readily react. Carbohydrates with constituents on the anomeric carbon (hemiacetals) are also unreactive, supporting the view that oxidation begins at the carbohydrate anomeric carbon. The slower reactivity of the hexose and pentose forms could be because these two species exist mainly as cyclic structures, which must revert to their linear forms before reaction can occur. Tetroses and trioses do not form the ring structure and so react directly and more rapidly as the linear form.

pH values of 10 or greater are required before carbohydrates undergo oxidation, suggesting that carbohydrates must undergo proton ionization before MV-catalyzed oxidation. Such ionization would occur at the anomeric carbon, forming an enediol between carbons 1 and 2.

The following mechanism is diagrammed is Figure 4.6. We propose that MV^{2+} reacts at the enediol and initiates oxidation sufficient to convert carbon 1 to formate or carbonate with formation of a pentose from a hexose. The pentose, in enediol form, undergoes another oxidation step similar to that of the hexose and forms formate or carbonate and a tetrose. This step-wise process continues until the triose finally undergoes oxidation to form glycoaldehyde. This stepwise process can also be halted at any step due to the formation of a carboxylate, as described below and illustrated in Figure 4.6 by the formation of a carboxylate group at the pentose stage. Oxidation cannot continue to form another hydroxy aldehyde and the reaction sequence changes. Glycoaldehyde forms an enediol, which provide a reaction site for oxidation by MV, but formation of another hydroxy aldehyde by oxidation cannot occur and the MV-catalyzed oxidation of glycoaldehyde terminates with formation of formaldehyde (Equation 4.2).

For glyceraldehyde, DHA and MHA, the presence of additional hydroxy groups allows the reaction to proceed to glycoaldehyde, which is oxidized to formate. The oxidation of the pentose and tetrose intermediates would also culminate in glycoaldehyde with oxidation to formate. For this idealized reaction scheme, formate is always produced as an end product of viologen-catalyzed carbohydrate oxidation via glycoaldehyde.

Under actual reaction conditions alternate pathways to the proposed stepwise mechanism could be taken, which would change carbohydrate oxidation behavior. Using glucose as an example, if oxidation of the anomeric carbon were incomplete and formed gluconic acid, the

reaction would stop. However, if oxidation released formate or carbonate and formed a pentose, the pentose could continue to undergo reaction resulting in a tetrose and this reactivity could continue down the carbohydrate chain without interruption. However, formation of unreactive intermediates at any point breaks the reaction sequence and terminates carbohydrate oxidation.

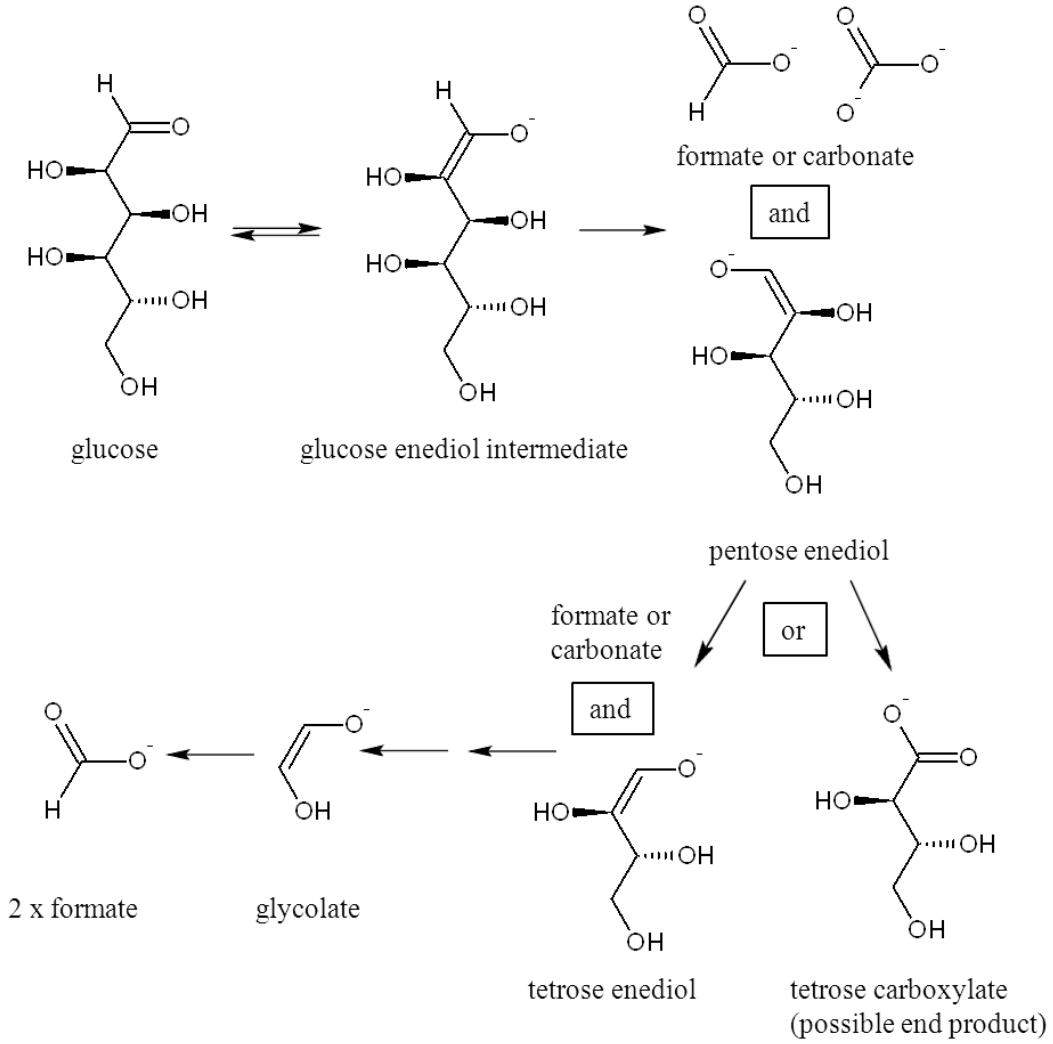

Figure 4.6 Schematic of the proposed mechanism for the oxidation of glucose catalyzed by viologen.

At a given MV/carbohydrate ratio, the variability in oxidation efficiency can be attributable to uncontrolled alternate reaction pathways forming unreactive intermediates. This view explains previous results for glucose and other carbohydrates that show that increasing the viologen/carbohydrate ratio increases carbohydrate oxidation efficiency. It is also consistent with previous results showing that $^{13}C_6$ labeled glucose forms ^{13}C labeled formate and some carbonate. Oxidation at C_6 of glucose only occurs as a last step in the sequence outlined above and requires that glucose be completely oxidized to ^{13}C formate and lesser amounts of carbonate.

The above interpretation suggests that if MV^{2+} is always present in excess in order to accept electrons, the reaction can proceed smoothly from hexose to pentose through to glycolate and then formate. If MV is limiting, reactive intermediates cannot transfer electrons rapidly enough to MV and will decay or rearrange to unreactive intermediates, which terminates the reaction sequence. Thus, efficient O_2-reoxidation of reduced MV during MV-catalyzed carbohydrate oxidation by air or fuel cell electrodes, during fuel cell operation, is required to maintain an excess of oxidized MV and prevent formation of inactive intermediates, which lower carbohydrate oxidation efficiency.

The use of polymeric viologens to mimic high, localized concentrations of viologen monomers is a viable approach to creating viologen catalysts for enhanced carbohydrate oxidation efficiency at lower catalyst/carbohydrate ratios. The enhanced efficiency of polymers is explained by formation of high, localized concentrations of viologen species that rapidly oxidize carbohydrates before unreactive intermediates can form. The use of polymeric catalysts should improve fuel cell function but must be in a form other than free-polymers suspension to minimize diffusion problems and ineffective polymer-electrode contact. Viologen polymers

bonded directly to metallic or carbon electrodes should be most effective for future fuel cell designs.

4.5 Conclusions

Viologen-catalyzed oxidation of carbohydrates occurs by a step-wise, single-carbon oxidation mechanism beginning at the anomeric carbon and continuing down the carbohydrate chain to glycoaldehyde. Glycoaldehyde is oxidized exclusively to formate terminating carbohydrate oxidation. High carbohydrate oxidation efficiency requires excess catalyst to avoid formation of unreactive carboxylic acid intermediates. Polymeric viologens or polymeric films can be used to increase carbohydrate oxidation efficiency.

5 CYCLIC VOLTAMMETRY INVESTIGATION OF VIOLOGENS, INDIGO CARMINE, AND METHYLENE BLUE FOR USE AS CATALYSTS IN DIRECT CARBOHYDRATE FUEL CELLS

5.1 Introduction

As seen in Chapters 2 and 3, viologens can be categorized in two types: disubstituted and monosubstituted. Disubstituted viologens have been extensively studied [64-74], while monosubstituted viologens have received relatively little attention. As reported in Chapter 3, monosubstituted viologens are more stable in strong base, and they appeared to have a more favorable redox potential compared to their analogous disubstituted viologens. Based on the results presented in Chapter 3 that show that monosubstituted viologens appear to have similar catalytic activity towards carbohydrates as disubstituted viologens, and based on the superior qualities of monosubstituted viologens mentioned above, we were led to investigate the monosubstituted viologens for a better understanding of their suitability for fuel cell use. In addition, researchers have looked at two redox dyes, indigo carmine (IC) and methylene blue (MB), for use in DCFCs [12, 75]. These two dyes were also examined with cyclic voltammetry and a comparison between all the investigated catalysts is made.

This investigation mainly focused on an electrochemical comparison, through cyclic voltammetry (CV), of the monosubstituted viologens, their analogous disubstituted viologens, and IC and MB. Cyclic voltammetry was chosen primarily for two reasons. One is that the method is commonly used to determine half-wave redox potentials ($E_{1/2}$) [9], which means we can compare our results to those in the literature. The other reason is that CV can be used to

quantify electrochemical processes that are limited by finite rates of electron transfer [123], given by the heterogeneous electron-transfer rate constant (k_{et}).

In a DCFC catalyzed by viologen or another redox dye, the redox value of the catalyst species plays an important role in the voltage efficiency ($\eta_{volt} = \Delta E/\Delta E_{ideal}$, as discussed in Chapter 2). Some of the chemical potential of the electrons in the carbohydrate fuel is used to reduce the catalyst species (the amount of which is the difference in redox potential between the carbohydrate fuel and the catalyst species). Therefore, the redox potential of the catalyst, and not of the carbohydrate being oxidized, determines the open circuit voltage (ΔE_{OCV}) of the cell. The open circuit voltage represents the maximum chemical potential of the electrons obtained by the cell. In a viologen catalyzed cell, once the viologen is reduced, the ΔE, and thus η_{volt}, obtained by the cell during operation, depends in part on the behavior of the viologen-controlled anode as current is drawn, which is part of the subject matter covered in Chapter 6.

It is likely that, to make a practical DCFC, the water-soluble catalysts investigated here must be immobilized on a surface. Our ongoing immobilization efforts involve attaching the viologen to a carbon substrate by alkyl chains. To inform such immobilization efforts, a series of four monoalkyl viologens was investigated, as were two aminoalkyl viologens. For the monoalkyl viologens, we assessed the variation in the redox potential as the length of the alkyl chain changed. The aminoalkyl viologens were investigated because they can potentially be immobilized at a surface via their amino end.

The mechanism for the reduction of disubstituted viologens is understood to follow two successive steps, as seen in Equations 5.1 and 5.2, with ethyl viologen (EV) being used for a generic disubstituted viologen.

$$EV^{2+} + e^- = EV^{1+} \quad (5.1)$$

$$EV^{1+} + e^- = EV^{o} \quad (5.2)$$

The initial one-electron reduction (Eq. 5.1) represents the reversible reduction of the EV^{2+} dication to the EV^{1+} radical cation (for EV this redox step is identified as EV-1 in this paper). A one-electron reduction of the EV^{1+} radical cation (Eq. 5.2) results in the formation of the EV^{o} neutral species (identified as EV-2). Relative to EV-1, the EV-2 step always occurs at a more negative redox potential.

Monosubstituted viologens only undergo one reversible reduction. With monoethyl viologen (MEV) as a generic monosubstituted viologen, the reduction reaction is presented in Equation 5.3. It is apparent that the cation/neutral redox step for the disubstituted viologens (Eq. 5.2) is analogous to the one reversible redox step seen for monosubstituted viologens, which is also a redox step between cation and neutral forms.

$$MEV^{1+} + e^- = MEV^{o} \quad (5.3)$$

5.2 Experimental methods

5.2.1 Materials

Methyl viologen, ethyl viologen, KOH, KCl, tetrabutylammonium hexafluorophosphate ($TBAPF_6$), tetrabutylammonium chloride (TBACl), 4,4'-bipyridine, methyl iodide, and bromopropylamine + HBr were obtained from Sigma and used without purification. Indigo carmine and methylene blue were the certified biological stains as supplied by Fisher Scientific. The monosubstituted viologens and aminoviologens tested were synthesized in house as

described in the section below. Acetonitrile (ACN) and dimethyl sulfoxide (DMSO) were obtained from Sigma and used without purification. All aqueous solutions were made with 18.2 MΩ Milli-Q water.

5.2.2 Synthesis of mono- and aminoviologens

The monoalkyl viologens were synthesized as described in Chapter 3. After the monoalkyl viologen was cleaned, a small amount of the remaining substance, approximately 0.75%, was dialkyl viologen. The dialkyl viologen does not appear to affect the cyclic voltammetry results seen for the monoalkyl viologen. No dialkyl peaks are seen, and in any case, the dialkyl and monoalkyl peaks do not overlap.

N-methyl-N'-(3-aminopropyl)-4,4'-bipyridinium (methylaminopropyl viologen, MAV) was prepared in two steps, in a modification of the method of Katz [130]. First, 1-methyl-4-(4'-pyridyl)-pyridinium iodide (monomethyl viologen, MMV) was obtained by reaction of 1.92 g (12 mmol) of 4,4'-bipyridine with 1.76 mL (28 mmol) of methyl iodide in acetone. The 4,4'-bipyridine was first dissolved in acetone in a turtle-neck flask. Then, methyl iodide was added dropwise while the solution was stirred. The reaction mixture was stirred for 8 hours under nitrogen at 60 ^{o}C. The light-orange precipitate was filtered and washed with acetone twice to remove unreacted 4,4'-bipyridine. The product was 3.35 g (40%) of MMV with a melting point above 300 ^{o}C. In the second step, 3.35 g (11 mmol) of MMV and 4.26 g (19 mmol) of bromopropylamine + HBr were placed in 25 mL of dry methanol and the mixture was stirred at 60 ^{o}C for 48 hours [130]. The precipitate was filtered and washed with pure ethanol and yielded 1 g (12%) of product. We did not carry out the recrystallization step of the product from water, and this may have caused the much lower yield compared with the 70% yield reported by Katz et.al. The final product was pure MAV.

N-(3-aminopropyl)-4,4'-bipyridinium (aminopropylviologen, APV) was obtained by reacting 0.219 g (1 mmol) of bromopropylamine + HBr with 0.468 g (3 mmol) of 4,4'-bipyridine in dry acetonitrile at 75 ^{o}C for two days with stirring. The white product species precipitated from the solution mixture. The mixture was filtered and washed with dry acetonitrile to remove any unreacted 4,4'-bipyridine. The product was 0.293 g with essentially 100% yield. The monosubstituted viologen produced by this process was nearly pure APV, with no detectable trace of the disubstituted viologen. The purity of the synthesized viologens was verified using NMR spectroscopy.

5.2.3 Apparatuses and procedures

Overview of cyclic voltammetry: Cyclic voltammetry (CV) is an electrochemical analysis technique. CV can be used to estimate redox potential(s), to estimate heterogeneous electron-transfer rate constants, and to estimate diffusion coefficients of the test species. CV is done with the three-electrode setup, as described in Chapter 2. The test species may be in solution or attached to the working electrode.

The chemical potential of the electrons in the working electrode is controlled by the potentiostat relative to the reference electrode. This potential is scanned in time in the form of a triangle wave, back and forth from more negative to more positive values. The more negative the relative potential, the higher the relative energy state of the electrons in the working electrode, and vice versa. Electrons are more likely to be found at lower energy states, so when the chemical potential of the electrons is higher in the working electrode than it would be in the test species, the electrons will reduce the test species, causing current to flow. This current is detected by the potentiostat. The values at which the electrons flow from the working electrode

into the test species and from the test species to the working electrode are used to determine the redox potential(s) of the species.

Cyclic voltammetry parameters: The cyclic voltammetry measurements were performed with a Gamry PC4/750 Potentiostat, and the software used in the analysis of the CV data was the Gamry Echem Analyst version 1.10. The instrument has a precision range of the range of ±5 mV. The data presented here were recorded at scan rates of 0.05, 0.08, 0.2, and 0.4 V s^{-1}.

The platinum working electrode (1.6 mm diameter) used in the CV tests was cleaned by rinsing it with 2 N nitric acid, followed by multiple rinses with Milli-Q water, between runs to remove any contamination. For the CV tests in ACN or DMSO, the electrode was dried and then rinsed twice with ACN. After rinsing, the electrode was dried and polished on qualitative-grade filter paper [131]. The counter electrode was high-surface-area platinum gauze.

The AgCl reference electrode used in the CV tests was made by anodizing a silver wire in 1 M KCl at 2 V for 10 minutes [122]. The reference electrode solutions used were 3 M KCl for aqueous tests, 0.1 M TBACl in ACN for the ACN tests, and 0.1 M TBACl in DMSO for the DMSO tests. All reference electrode solutions were saturated with AgCl. The solution in the reference-electrode compartment was changed daily and the reference electrode wire was refreshed (anodized) regularly to ensure stability.

For our tests, 10 mL of test solution was placed in a 30 mL glass jar. The lid to the jar had fitted holes for insertion of the electrodes and for the nitrogen to be bubbled through the solution, or for a nitrogen blanket to be maintained. The test solution was further isolated from atmospheric oxygen by placing the jar in a resealable plastic bag. Through the small holes intrinsic to the setup, the nitrogen was able to escape, but the positive pressure in both the jar and the bag kept the oxygen concentration to a minimum. The test solutions were purged of oxygen

by bubbling solvent-saturated nitrogen into the cell for 30 minutes, and a solvent-saturated nitrogen blanket was maintained over the test solution during tests. The flow rate of nitrogen was adjusted until no change was seen in the resulting voltammograms with increasing nitrogen flow rate. Reduced viologens are extremely sensitive to the presence of oxygen and a fairly vigorous flow of nitrogen was require for our setup to ensure no oxygen was present and correct results were obtained.

5.2.4 Test Solutions

The electrolytes used in the aqueous test solutions (whether of viologen, IC, or MB) depended on the species being tested and are detailed individually below, though the electrolyte anion was always 0.1 M Cl^-. All cyclic voltammetry tests done in ACN and DMSO were run with 0.1 M $TBAPF_6$ as the electrolyte. ACN and DMSO were used as solvents in addition to water, in part, because they are electrochemically stable at the potentials used in the tests and because one or both solvate all the test species.

Viologen solutions: To assist the reader and reduce confusion, Table 5.1 contains a list of abbreviations that are used for the tested viologen species. Table 5.1 also provides their level of substitution (mono- or di-), and the anion or anions of the respective viologens. Corresponding representative structures can be found in Figure 5.1.

Water is the solvent of choice for the intended fuel cell application of viologens, but the redox potentials of the monoalkyl viologens were found to be near the redox potential of water at pH 7. The reduction of water at the working electrode that occurred during testing at pH 7 caused interference with the CVs. The reduction potential of water is pH dependent, so to obtain clearer cyclic voltammograms the monoalkyl viologens were run in 1 M KOH with 0.1 M KCl,

and in the organic solvents ACN and DMSO. The monoalkyl viologens are stable, at least on the order of days, in 1 M KOH.

Table 5.1 Abbreviations for the viologens referred to in this report, their common name as used in the report, their level of substitution, and the anion or anions of the viologen.

Abbreviation	Viologen	Substitution	Anion(s)
MV	methyl	di	Cl^-
MMV	monomethyl	mono	I^-
MEV	monoethyl	mono	I^-
MPV	monopropyl	mono	I^-
MBV	monobutyl	mono	I^-
EV	ethyl	di	Br^-
APV	animopropyl	mono	Br^-
MAV	methylanimopropyl	di	I^- and Br^-

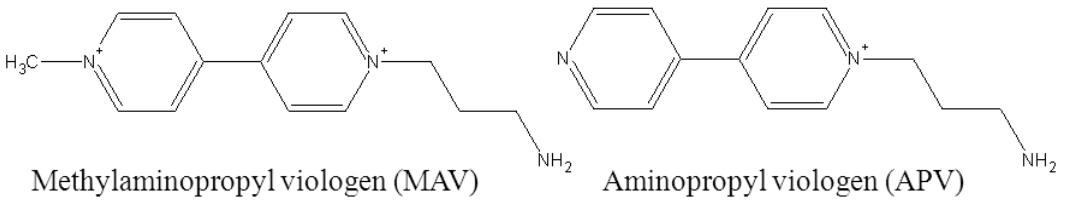

Methylaminopropyl viologen (MAV) Aminopropyl viologen (APV)

Figure 5.1 Images of representative viologens discussed in this document.

In 1 M KOH with 0.1 M KCl, CVs were generated for the monoalkyl viologens MMV, MEV, MPV, and MBV. The concentration of all the monoalkyl viologens was approximately 3 mM. As will be discussed in greater detail below, the identity and concentration of the anion of the electrolyte may affect the redox potential of the viologen, which is why 0.1 M KCl was included in the 1 M KOH solution.

In ACN, CVs were generated for the following monoalkyl viologens: MMV, MEV, MPV, and MBV. The concentration of all the monosubstituted viologens in ACN was

approximately 1 mM. In DMSO, CVs were generated for the following viologens: MMV, APV, and MAV. The concentration of all viologens in DMSO was approximately 1 mM. DMSO was used for the aminoviologens because the aminoviologens were found to not be soluble to the desired 1 mM in ACN.

To compare the mono- and aminoviologens with well-characterized dialkyl viologens, CVs of EV were run in ACN, DMSO, and aqueous 0.1 M KCl. CVs of MV were also run in aqueous 0.1 M KCl to help validate our experimental setup. The concentration of the two dialkyl viologens was approximately 1 mM in all solvents.

IC and MB solutions: CVs were generated for IC and MB in aqueous solution and in DMSO. Values for the redox potentials, heterogeneous electron-transfer rate constants, and the diffusion coefficients for IC and MB in water were found in the literature, and aqueous test solutions for these compounds were run to further validate our experimental setup. IC and MB were also run in DMSO so that they may be more accurately compared to the monosubstituted viologens (for which accurate values could not be obtained in aqueous solution).

The concentration of IC was approximately 2 mM in DMSO and approximately 0.3 mM in aqueous solution. The aqueous IC tests were done in 0.1 M TBACl because IC was not adequately soluble in 0.1 M KCl (the presence KCl was found to reduce the solubility of IC in water and at 0.1 M KCl, IC would not dissolve to the desired concentration). DMSO was used for IC and MB because IC was found to be insoluble in ACN. MB was approximately 1 mM in DMSO and 0.5 mM in aqueous solution. The aqueous MB tests were in 0.1 M KCl.

To compare the mono- and aminoviologens with well-characterized dialkyl viologens, CVs of EV were run in ACN, DMSO, and aqueous 0.1 M KCl. CVs of MV were also run in

aqueous 0.1 M KCl to help validate our experimental setup. The concentration of the two dialkyl viologens was approximately 1 mM in all solvents.

CVs were generated for indigo carmine (IC) and methylene blue (MB) in aqueous solution and in DMSO. IC was approximately 2 mM in DMSO and approximately 0.3 mM in aqueous solution. The aqueous IC tests were done in 0.1 M TBACl because IC was not adequately soluble in 0.1 M KCl. DMSO was used for IC and MB because IC is not soluble in ACN. MB was approximately 1 mM in DMSO and 0.5 mM in aqueous solution. The aqueous MB tests were in 0.1 M KCl.

5.3 Results and discussion

Voltammograms were used to obtain half-wave potentials ($E_{1/2}$), diffusion coefficients (D) and heterogeneous electron-transfer rate constants (k_{et}) [122, 123, 131].

5.3.1 Half-wave potentials

Table 5.2 shows the $E_{1/2}$ values of all the tested species, with literature values reported where available. The $E_{1/2}$ values were calculated as $E_{1/2} = (E_{pc} - E_{pa})/2$, where E_{pc} is the potential at the cathodic peak and E_{pa} is the potential at the anodic peak. The potentials for ACN come from Figure 5.2, for DMSO from Figures 5.3 and 5.4, and for aqueous solution in part from Figure 5.5. The standard deviation for the values seen in Table 5.2 was on the order of 1 to 2 mV, which is within the precision of the analysis software (±5 mV).

The data missing from Table 5.2, and in subsequent tables, is due to the test species not being run in a particular solvent, or values not being found in the literature. Reasons for not running a test species in a particular solvent include lack of solubility, as discussed above, or

redundancy. Running all the monoalkyl viologens in DMSO was considered redundant since they were found to be so similar in ACN and H_2O. Therefore, only MMV was run in DMSO.

Table 5.2 $E_{1/2}$ values. ACN and DMSO values vs. AgCl (0.1 M Cl^-) in ACN and DMSO respectively, and aqueous values vs. AgCl (3 M Cl^-). Values in parentheses are approximate, as discussed in text.

	$E_{1/2}$ (V)		
Species	ACN	DMSO	H_2O
MV-1			-0.65
			-0.654[a]
MMV	-0.77	-0.88	(-1.02)
MEV	-0.77		(-1.02)
MPV	-0.77		(-1.02)
MBV	-0.77		(-1.02)
EV-1 (Eq. 5.1)	-0.23	-0.39	-0.64
			-0.657[a]
EV-2 (Eq. 5.2)	-0.648	-0.76	(-0.94)
APV		-0.83	
MAV-1		-0.36	
MAV-2		-0.72	
IC		-0.610	-0.32
MB		-0.23	-0.24

a) Ref. [9]

The monosubstituted viologens all have similar redox potentials. The redox potentials for the cation/neutral redox step of the monosubstituted viologens (represented by Eq. 5.3) are approximately 0.1 V more negative than the cation/neutral redox step of their analogous dialkyl compounds (represented by Eq. 5.2). This is seen to be the case whether the solvent was water, ACN, or DMSO and whether the viologens were alkyl or aminoalkyl.

As seen in the ACN and H_2O columns of Table 5.2, it was found that the length of the alkyl chain had little effect on the $E_{1/2}$ values of the monoalkyl viologens. This lack of effect on

the $E_{1/2}$ value indicates that if viologen were to be immobilized on a graphite surface by an alkyl chain, so that it is functionally similar to a mono- or dialkyl viologen, we could expect the redox potential of the immobilized viologen to be similar to that of the homogeneous viologen.

The dialkyl viologen EV was run in 0.1 M KCl, rather than 1 M KOH as were the monoalkyl viologens. EV was run in 0.1 M KCl because dialkyl viologens begin to hydrolyze at the quaternary nitrogens as soon as they dissolve in 1 M KOH [9]. The cation/neutral species redox step (Eq. 5.2, reported as EV-2 in Table 5.2) of EV occurs at a potential where less interference is seen from the reduction of water at the working electrode compared to the interference seen with the monosubstituted viologens (Eq. 5.3). Therefore, the EV-2 peaks can be seen, and $E_{1/2}$ value estimated, without the need of putting the dialkyl viologen in 1 M KOH. The concentration of the electrolyte and the identity of the electrolyte anion are known to affect the redox potential of the viologens [9], which is why all the aqueous viologen solutions were at 0.1 M Cl^-, regardless of pH. However, the redox potentials of viologens are independent of pH [9]. So though the dialkyl and monoalkyl viologens were run at different pHs, the estimated $E_{1/2}$ values for both EV-2 and the monoalkyl viologens seen in Table 5.2 are thought to be accurate for all pH conditions and are therefore comparable.

Performing the aqueous monoalkyl viologen tests in 1 M KOH led to clearer peaks on the CVs, but water was still reduced at our platinum working electrode at around the same potential as the viologens, so we were unable to obtain precise redox data. We also cannot say with certainty whether or not the reduction of the monoalkyl viologens is reversible in aqueous solution from the voltammograms alone, though oxidation peaks are seen on the voltammograms, so it can be stated that the reduction is at least quasi-reversible. Due to the

interference from the reduction of water at the platinum working electrode the $E_{1/2}$ values for the monosubstituted viologens in aqueous solution in Table 5.2 are approximate.

In aqueous solution both IC and MB are seen to have potentials that are over 300 mV more positive than the dication/cation $E_{1/2}$ values (Eq. 5.1) of the dialkyl viologens, and nearly 700 mV more positive than the $E_{1/2}$ values of the monosubstituted viologens. These more-positive redox potentials will negatively influence the amount of power produced by a DCFC catalyzed by either IC or MB.

5.3.2 Diffusion coefficients

All the catalysts examined here are soluble in water. In a DCFC where the catalyst is homogeneous, the diffusion coefficient (D) can potentially be useful. Values for D can be found with cyclic voltammetry by using the Randles-Sevcik equation [9, 131, 132]:

$$i_p = 0.4463nR(anF/RT)^{1/2}AD^{1/2}c\nu^{1/2} \tag{5.4}$$

Where i_p is the peak current, n is the number of electrons exchanged during an oxidation or reduction step, R is the ideal gas constant, a is the charge-transfer coefficient (a = 0.5 in this case), F is the Faraday constant, T is the absolute temperature, A is the surface area of the working electrode, D is the diffusion coefficient, c is the bulk concentration of the diffusing species, and ν is the scan rate.

Other than the diffusion coefficient, all the other variables from Equation 5.4 are known. To limit the probability that any particular scan rate may give an erroneous value for D, a plot of the peak current (i_p) vs. the square root of the scan rate ($\nu^{1/2}$) can be made. This plot gives a

straight line that passes through the origin. The slope of this line is proportional to $D^{1/2}$. Table 5.3 contains values of D generated this way, with values available in the literature for some of the species tested here included for comparison. The D values, as expected, are larger in the low viscosity solvents ACN and H2O, and smaller in the higher viscosity DMSO.

Table 5.3 Diffusion coefficients (D) in ACN, DMSO, and H_2O solvents.

	10^6 D/cm^{2}s^{-1}		
Species	ACN	DMSO	H_2O
MV			8.4
	12.2[a,b]	2.5[a,b]	8.6[a]
MMV	11.2	2.96	
MEV	12.0		
MPV	14.6		
MBV	18.5		
EV	7.13	1.2	
APV		0.81	
MAV		0.80	
IC		0.99	9.4
			8.6[c]
MB		1.9	13.0[c]

a) Ref. [9].
b) anion is ClO_4^-.
c) Ref. [133].

In water, our preferred solvent for the DCFC, all the compounds tested appear to have similar diffusion coefficients, though MB has a D that is at about 50% larger than the other tested species. Due to the reduction of water at the working electrode, it was not possible to determine D for the monoalkyl viologens. However, as would be expected based on size and charge effects, in ACN and DMSO the Ds for the monoalkyl viologens were similar to, but a little larger than, those of the dialkyl viologens. It is thought that this trend continues in water.

The aminoviologens have the smallest observed D values. APV is MPV with an amine group attached to the terminal carbon, and it is thought that the amine group is the cause of the decrease in D, and other observed differences between the MPV and APV. If, in a homogeneous cell, D is an important consideration, then the aminoviologens are not a good choice as catalyst. However, it is unlikely that viologens of any sort will be used homogeneously in a commercial DCFC.

Due to the unusual shape of the CVs of MB in aqueous 0.1 M KCl, we were not able to calculate a D value for MB in H_2O. The value listed for MB in Table 5.3 is that from Ref. [133], and was determined with spectroelectrochemical techniques, rather than with cyclic voltammetry. Below, D is used in the calculation of k_{et}. The D used to calculate k_{et} for MB in H_2O is the value from Ref. [133], while the other values used in the k_{et} calculation for MB came from our CVs.

5.3.3 Heterogeneous electron-transfer rate constants

Information obtained from the CVs can also be used to determine the heterogeneous electron-transfer rate constant (k_{et}). These k_{et} values are important in determining the usefulness of the test species as catalysts in a fuel cell. The higher the value of k_{et}, the quicker the turnover of electrons and the more efficiently the cell will produce electricity and oxidize the carbohydrate fuel (the mechanism by which this occurs is discussed in Chapter 4). The k_{et} values can be determined by applying the electrochemical absolute rate equation proposed by Nicholson [134] and represented by the following equations:

$$\Psi = \gamma^{\alpha} k_{et} / (\pi a D_O)^{1/2} \quad (5.5)$$

$$\gamma = (D_O/D_R)^{1/2} \quad (5.6)$$

$$a = n F \nu / R T \quad (5.7)$$

where Ψ is a kinetic parameter from the Nicholson paper, k_{et} is the heterogeneous electron-transfer rate constant, D_O and D_R are the diffusion constants of the oxidized and the reduced species respectively, and the other variables and constants are as described after Equation 5.4 or how they are commonly understood.

The values of Ψ can be obtained from a table in the Nicholson paper [134] and are related to ΔE_p from the cyclic voltammograms. The ΔE_p value is the difference in potential between the anodic and cathodic peaks on the CV. A smaller ΔE_p (minimum 61 mV in the Nicholson paper) leads to a higher Ψ, and therefore a larger value for k_{et}.

The values for k_{et} determined from Equation 5.5, and the ΔE_p values taken from the CVs, are seen in Table 5.4. The k_{et} values were determined assuming that D for the oxidized and reduced forms of all test species were approximately equal, so that γ is equal to 1. The k_{et} values presented are the average of those calculated in the scan-rate range from 0.05 to 0.4 V s^{-1} [131]. Values available in the literature for some of the test species are included for comparison.

The value of k_{et} is directly related to the value of Ψ and the highest Ψ value from the Nicholson paper is about 20-fold greater than the values obtained for the di- and monosubstituted viologens tested here, meaning that the k_{et} values obtained for the tested viologens are not relatively fast. Along with seeking a more favorable redox potential, it would be useful to determine which viologens and other potential catalysts have the highest k_{et} values and what factors affect the k_{et} of all the catalysts, so that the k_{et} values could be improved.

As with the calculation of their D values, reduction of water at the working electrode made it impossible to determine k_{et} for the monoalkyl viologens in aqueous solution. The trend in ACN and DMSO is that the monoalkyl viologens have k_{et} values similar to the k_{et} values of the dialkyl viologens. This trend is likely to continue in aqueous solution.

Table 5.4 Heterogeneous electron-transfer rate constants (k_{et}) and ΔE_p values in ACN, DMSO, and H_2O.

	$10^2\ k_{et}$/cm s^{-1}			ΔE_p (mV)		
Species	ACN	DMSO	H2O	ACN	DMSO	H_2O
MV			1.7			80
			1.87[a]			
MMV	1.47	0.6		82	93	
MEV	1.52			88		
MPV	1.68			85		
MBV	1.89			84		
EV	1.67	0.47		79	85	
APV		0.13			133	
MAV		0.31			90	
IC		0.022	0.13		312	201
			0.054 to 0.17[b]			
			0.052[c]			
MB		0.45	3[d]		92	64
			0.33[e]			96
			0.24[c]			

a) value obtained by RDE, Ref. [9].
b) Ref. [135].
c) Ref. [133].
d) value with freshly cleaned working electrode.
e) value with MB adsorbed on the surface of the working electrode.

The literature values cited for IC and MB were found using spectroelectrochemical methods. Even so, there is good agreement between our values, found using CV, and the

literature values. The range in literature values for the second entry under IC, is due to a range of electrode potentials being used to determine the k_{et} values. As mentioned above, the literature D value for MB was used to calculate the first two values listed for k_{et} for MB in Table 5.4. The two CV values given for MB were due to the difference in the ΔE_p values obtained at a freshly cleaned working electrode vs. an electrode that had MB adsorbed on it. Further comparisons between the k_{et} values found in Table 5.4 can be found below in the "Comparison of the catalysts" subsection below.

The disubstituted viologen MV was used to compare the $E_{1/2}$, D, and k_{et} values generated in this work with the values available in the literature, so as to help validate our experimental setup. As can be seen from the values for MV in Tables 5.2, 5.3, and 5.4, similar values were found using our experimental setup as previous workers have found.

5.3.4 Examination of voltammograms

The concentration in solution of the test species that are shown in the voltammograms varied from approximately 0.3 mM to 2 mM. To correct for this difference in concentration in the plots of the CVs, the values used to plot the CVs were normalized to 1 mM. This normalization was done by dividing the plotted current (μA) values of the CVs by a unitless millimolarity value. For instance, if the solution was 2 mM, then the μA values were divided by 2. If the solution was 0.3 mM, then the μA values were divided by 0.3. This way, all CV curves are plotted as though they were run at precisely 1 mM.

Figure 5.2 shows cyclic voltammograms of EV, MMV, MEV, MPV, and MBV in ACN with 0.1 M $TBAPF_6$. Two oxidation and reduction waves are clearly seen for EV (a disubstituted viologen) and one oxidation and reduction wave is seen for each of the

monosubstituted viologens. The curves shown in Figure 5.2 were obtained at 0.2 V s^{-1}. As also seen in Table 5.2, the potential of the one monoalkyl viologen redox step (represented by Eq. 5.3) is similar to, and about 0.1 V more negative than, the cation/neutral species redox step of disubstituted EV (Eq. 5.2).

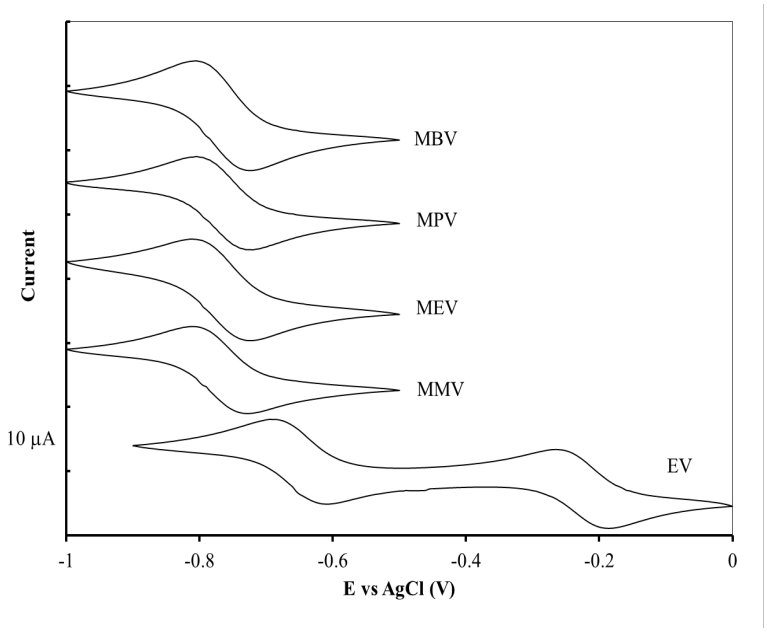

Figure 5.2 Cyclic voltammograms of EV, MMV, MEV, MPV, and MBV in ACN containing 0.1 M $TBAPF_6$ and vs AgCl (0.1 M Cl^-).

The ΔE_p for the viologens in ACN seen in Figure 5.2 varied within the range of precision of the Gamry software, ± 5 mV, for scan rates between 0.05 V s^{-1} and 0.4 V s^{-1}. The ΔE_p was on the order of 85 mV, as seen in Table 5.4. The peak-current ratio for the anodic and cathodic scans (i_{pa}/i_{pc}) was found to be near unity and independent of scan rate. Taken together, these facts indicate that the reduction of the monoalkyl viologens, as seen in Equation 5.3, is quasi-reversible in ACN (where a quasi-reversible process is characterized by a ΔE_p greater than ideal case of 59 mV per electron).

Figure 5.3 shows cyclic voltammograms of the EV, MMV, MAV and APV in DMSO with 0.1 M $TBAPF_6$, and were also obtained at 0.2 V s^{-1}. The behavior of the aminoviologens was different than that of the simpler alkyl viologens. The CV of APV, which is MPV with an amine group attached to the terminal carbon of the alkyl chain, is the most notably different. Whereas MMV has a clean scan with sharp peaks, APV has a small bump half way up the reduction peak and relatively flatter and smaller peaks. Additionally, APV has a ΔE_p of 133 mV in DMSO, whereas MMV, a monoalkyl viologen, has a ΔE_p of 93 mV in DMSO (see Table 5.4 for the ΔE_p values). This difference can be attributed to the amine group. In a commercial fuel cell, APV or MAV may be attached to the electrode surface at the amine group, so the influence of the amine group on ΔE_p may no longer appear once the viologens are immobilized.

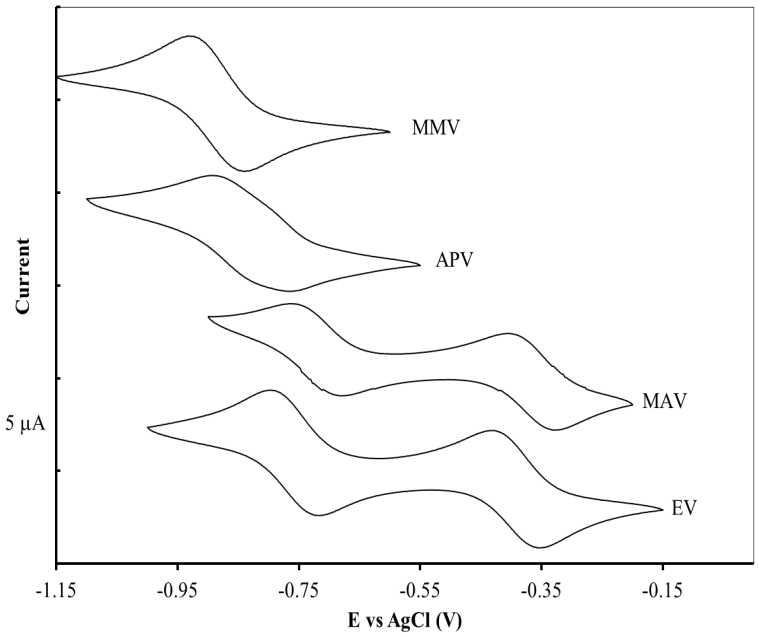

Figure 5.3 Cyclic voltammograms of EV, MMV, MAV, and APV in DMSO containing 0.1 M $TBAPF_6$ and vs AgCl (0.1 M Cl^-).

Figure 5.4 shows the voltammograms of IC and MB in DMSO. A plot separate from the aminoviologen DMSO plot was used for IC and MB, because despite the fact that the concentration of IC in DMSO was 2 mM, as opposed to 1 mM for the viologens, the IC peaks were too small to discern details if put on the same scale as the aminoviologens.

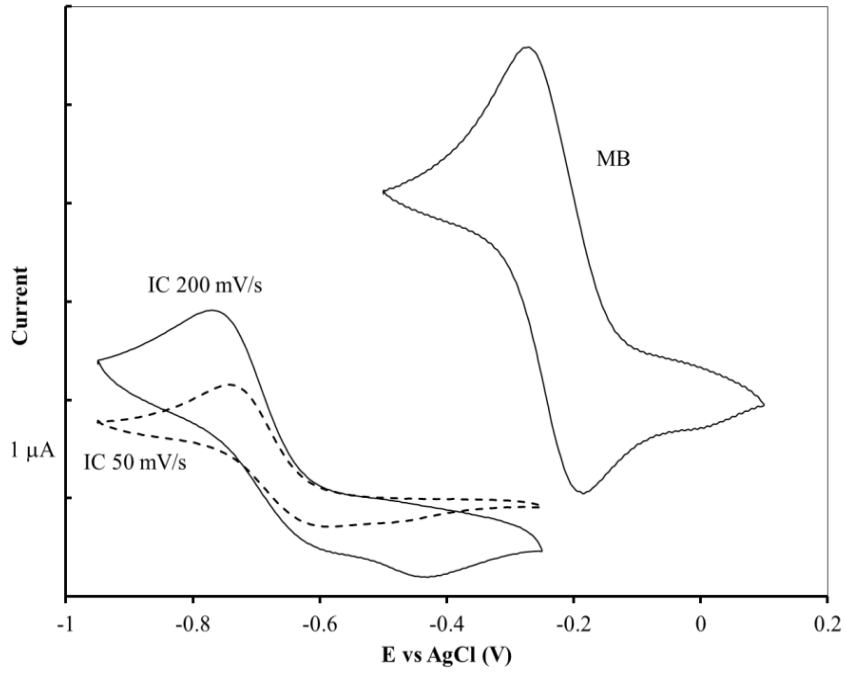

Figure 5.4 Cyclic voltammograms of IC and MB in DMSO containing 0.1 M $TBAPF_6$ and vs. AgCl (0.1 M Cl^-).

As can be seen in from the k_{et} and ΔE_p values for IC in Table 5.4, IC has slow heterogeneous electron-transfer kinetics. While all other tested catalysts showed no change in the form of the CV curve with change in scan rate, two CVs of IC in DMSO are shown because there is a change in the shape of the curve. At 50 mV s^{-1} the curve looks similar to a standard one-electron curve with fast kinetics, though the oxidation peak is less sharp and more flat, with some of the oxidation taking place at more positive potentials from the E_{pa} peak than with

kinetically faster species. At 200 mV s^{-1}, the E_{pa} peak value has clearly shifted from what is expected with faster kinetics. This peak-shifting phenomenon is also seen with IC in aqueous solution (Figure 5.5). If the shifted peak is used to generate ΔE_p values, then k_{et} values can be calculated which match the literature values, as seen in the Table 5.4. Whether or not the shift in peak value is due simply to slow kinetics or to some chemical complexation, the result is an electron-transfer rate constant that is more than an order of magnitude smaller than that of the viologens and MB.

In contrast to IC is the MB curve on Figure 5.4. Both the oxidation and reductions peaks of MB in DMSO are strong and sharp and no change in ΔE_p is seen as the scan rate increases. The ΔE_p of MB is similar to that of the viologens tested in DMSO.

Figure 5.5 shows voltammograms of MV, IC, and MB in aqueous solution. The CVs shown were recorded at 200 mV s^{-1}. As in Figure 5.4, the oxidation peak of IC is shown to be shifted considerably from where it would be under a faster kinetic regime. The more-positive oxidation peak on the MB curve is the adsorption of MB onto the working electrode. If multiple cycles are run during a scan, then this more-positive oxidation peak decreases in size until it is no longer visible. Initial scans after the working electrode is cleaned, show a much smaller ΔE_p than after MB has absorbed onto the surface. This difference in ΔE_p, and the resulting change in the calculated k_{et}, can be seen in Table 5.4. The curve of MV is included to show that even the dication/cation redox step of a dialkyl viologen is significantly more negative than those of IC and MB.

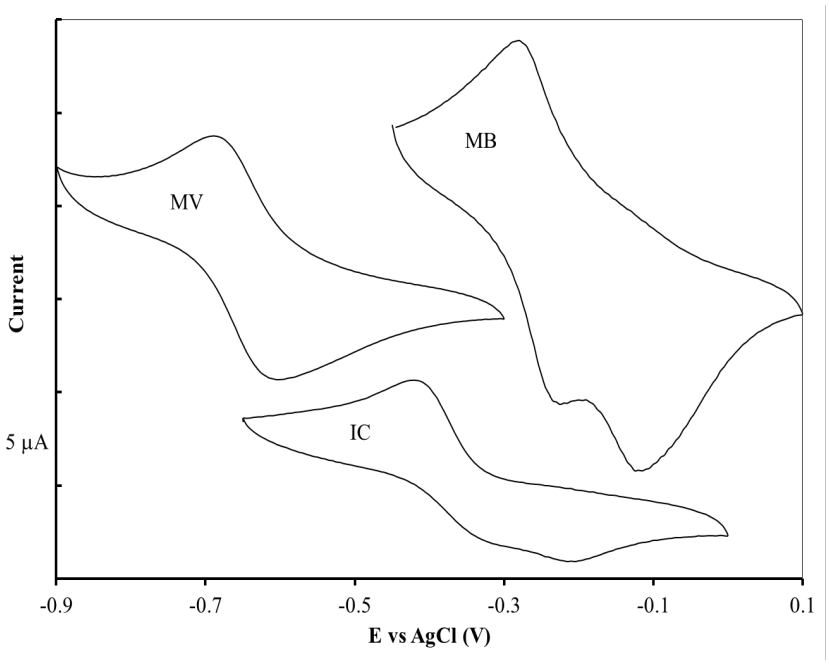

Figure 5.5 Cyclic voltammograms of MV, MB, and IC in H_2O containing 0.1 M NaCl, in the case of MB and MV, or 0.1 M TBACl, in the case of IC. CVs vs AgCl (3 M Cl^-).

5.3.5 Comparison of the catalysts

Five parameters for judging the fitness of these catalysts are examined in this work. These include three parameters from cyclic voltammetry: $E_{1/2}$, k_{et}, and D. In addition, we examined stability in alkaline solution and solubility in a semi-quantitative fashion. If the catalyst is immobilized on a surface, as in our intended application, both D and solubility may become less important.

$\underline{E_{1/2}}$: To better understand the operating conditions of a potential fuel cell, it is helpful to construct and examine a Pourbaix diagram for the system, as shown in Figure 5.6. The diagram shows results for a generic carbohydrate fuel (thermodynamic results do not differ appreciably from one fuel species to the next). The potential difference between the reduced catalyst at the anode and the O_2 at the cathode is the open-circuit voltage (ΔE_{OCV}) for the cell, and represents

the electric potential available to the cell. Similarly, the difference in potential between the fuel and the catalyst is the driving force for the oxidation of the fuel by the catalyst.

The values for MV and MMV seen in Figure 5.6 were taken from this work, while the values for MB, IC, and formate were taken from the literature [136, 137]. Under alkaline conditions, the reduction of MB and IC involves 2 electrons for every proton, so the slope of those lines is half that of the O_2 line. The carbohydrate fuel line was calculated using the ΔG of combustion for glucose and using the equation $\Delta G = -n\ F\ \Delta E$ [14]. Under alkaline conditions, where the carbohydrate reaction produces bicarbonate and carbonate rather than CO_2, the slope of the fuel curve reflects the reaction of 1.5 protons for every electron.

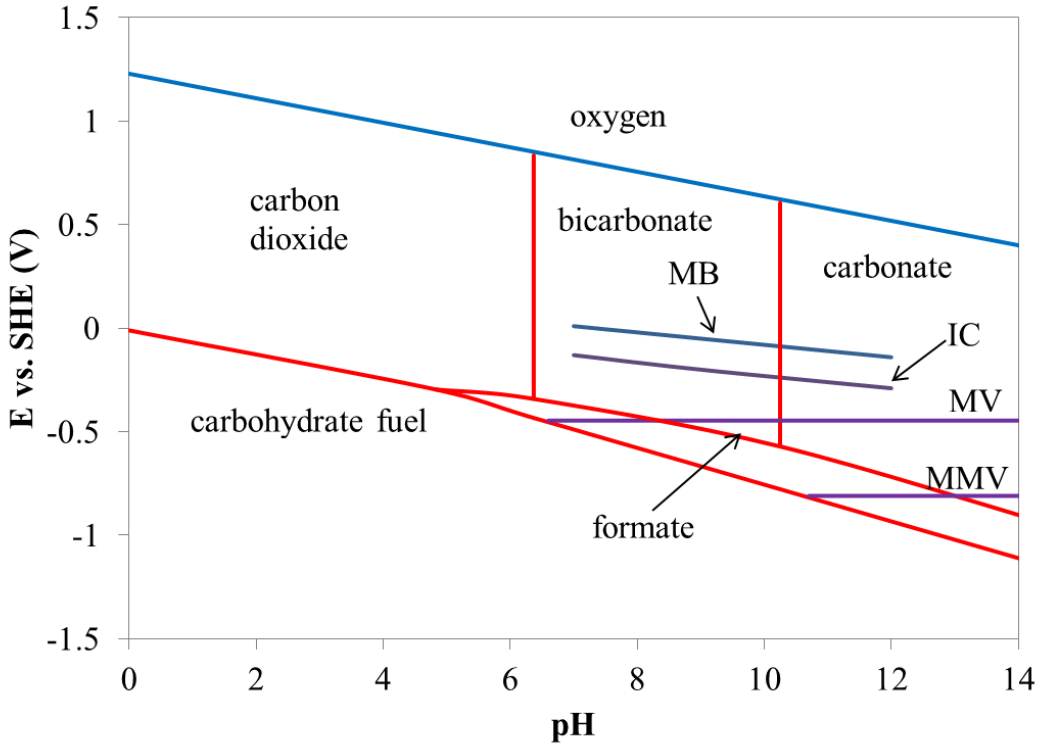

Figure 5.6 Pourbaix diagram for carbohydrate redox system, potentials given are vs. SHE. Included are the redox potentials of four of the catalysts examined in this chapter.

Because the redox potentials of IC, MB, the fuel, and oxygen depend on the pH we chose a single value, pH 12, as a reference to enable comparisons, as shown in Table 5.5. The data in Table 5.5 show that, if the carbohydrate fuel could be oxidized directly by the O_2 at pH 12, then we could access a ΔE_{OCV} of 1.45 V. Because kinetic overpotential in that case would be prohibitive, we use a catalyst to speed up the oxidation of the fuel; however that entails some loss of the available energy. At pH 12, over 90% of the energy in the carbohydrate fuel is retained if we use MMV as the catalyst, about 66% of the energy is retained if we use MV, and only about half the energy is retained if we use either IC or MB. If the ΔE_{OCV} available to the cell were the only consideration about which catalyst to use, then MMV, or viologen immobilized so that it is functionally similar to a monosubstituted viologen, would be the superior catalyst.

Table 5.5 Redox potentials vs. SHE in hypothetical DCFCs at pH 12. Also included are calculations of the ΔE_{OCV} between the reduced catalyst and the oxygen at the air cathode in a fuel cell, the ΔE between the fuel and the catalyst, and the percentage of energy retained from the fuel in the reduced catalyst molecule

Species	Redox potential (V)	ΔE_{OCV} (V)	ΔE vs. carb. (V)	Energy retained (%)
O_2	0.519		-1.451	
fuel	-0.932	1.451	0	100
MV	-0.444	0.963	-0.488	66
MMV	-0.81	1.329	-0.122	92
IC	-0.29	0.809	-0.642	56
MB	-0.08	0.599	-0.852	41

Another design consideration is the driving force for the oxidation of the fuel by the catalyst, which is represented by the "ΔE vs. carb." column of Table 5.5. If the redox potentials of the catalyst and the fuel are too close, the kinetics of the reaction may be too slow to be useful

in a fuel cell. From the tests reported in this paper we were unable to determine what effect the ΔE has on the rate of reaction, but a forthcoming paper by our group will examine homogeneous rate constants (not included in this dissertation).

Figure 5.6 illustrates a balance that must be struck in any potential DCFC. For the viologens, an alkaline pH is required so that there is a ΔE to drive the oxidation of the fuel by the catalyst. However, as the pH increases, less energy is retained by the viologen from the oxidation of the fuel and therefore less is available to power an external circuit.

Factors affecting the redox potentials of viologens: From Table 5.2 we can see that changing the length of the alkyl chain has little effect on the $E_{1/2}$ of viologens. There are other factors, however, that are known [9] to have a substantial effect on the $E_{1/2}$ values, and these factors can potentially be used to optimize the redox potentials of viologens for use in a DCFC. These factors include the anion of the supporting electrolyte, the concentration of supporting electrolyte, and the substituents at the nitrogens of the viologens.

Due to interest in its use in electrochromic displays, heptyl viologen (HV), is the viologen with which the electrolyte concentration and anion effects have been the most heavily studied. As seen in Ref. [9], on a gold working electrode the $E_{1/2}$ value for the HV dication/cation redox step, HV-1, is -0.698 V vs. SCE when the anion of the electrolyte is bromide (0.3 M) and -0.848 V vs. SCE when the anion is formate (0.4 M), a difference of 150 mV. The major source of anions in a working viologen DCFC will necessarily be hydroxide ions, which have been shown to have little effect [9] on the viologen redox potentials. It is possible, however, that an additional species of anion can be added to the reaction solution if necessary to optimize the redox potential in the operating cell.

The effect of anion concentration on the $E_{1/2}$ values of HV has also been studied [9]. It is shown that, as electrolyte concentration increases, the value of $E_{1/2}$ for HV-1 becomes more positive and the value of HV-2 becomes more negative. For a concentration range covering four orders of magnitude, the $E_{1/2}$ values for HV-1 and HV-2 both change by over 100 mV. As with the anion type, it is likely that in an optimized DCFC the anion concentration will be dictated more by the need to tune the hydroxide concentration to produce the best current, than to affect the $E_{1/2}$.

The substituents on symmetrical viologens are also known to affect the $E_{1/2}$ values. Again from Ref. [9], reported values of the dication/cation redox step vary from -0.710 vs. SCE for *n*-hexyl viologen with bromide anion, to -0.315 vs. SCE for CH(CN)Ph viologen with unknown anion, a difference of nearly 400 mV. Given the large difference in redox potential based on the identity of the substituent attached to the quaternary nitrogens, it is likely that the $E_{1/2}$ values of immobilized viologens can be optimized by changing the substituents.

$\underline{k_{et}}$: The amount of power produced by a cell depends on the current the cell can produce. The current produced by the cell depends, in part, on the kinetics at the anode, which are described by the heterogeneous electron-transfer rate constant, k_{et}.

The k_{et} values we are interested in are seen in Table 5.4. The DMSO column in Table 5.4 gives a complete set of information which allows us to compare representatives of all the types of catalysts tested. In DMSO, the species with the highest k_{et} is MMV, followed closely by EV and MB. Lower still are the aminoviologens, and the species with by far the lowest k_{et}, more than an order of magnitude lower than the k_{et} for MMV, is IC. Looking at the ACN column shows us that viologens, whether they be di- or monosubstituted have roughly similar k_{et} values.

The H_2O column shows us a pattern similar to that in the DMSO column. IC has a k_{et} that is more than an order or magnitude smaller than that of MV. Also of interest in the H_2O column is the k_{et} values for MB. The top value listed for MB is that seen when a pristine working electrode is initially used in the aqueous MB solution. In the initial CV of MB in H_2O, the ΔE_p is, at 64 mV, near the value of an ideal reversible redox reaction, indicating fast heterogeneous electron-transfer kinetics. After adsorption of MB at the surface the ΔE_p value increases significantly, as is seen in the second value listed for MB in H_2O. It is unknown if this same fouling effect would take place at a current collector of a DCFC. If no such fouling of the surface takes place, then the greater k_{et} of MB would recommend it for use in a DCFC. However, as seen in the $E_{1/2}$ section just above, MB retains the least amount of energy, only half of what the monosubstituted viologens retain, during oxidation of the carbohydrate fuel. The viologens, in general, have the next highest k_{et} values, and no fouling is observed at the working electrode.

D: It is likely that, in any commercial DCFC, the catalysts will necessarily need to be immobilized in the cell. However, if the catalyst is not immobilized on the surface, then the diffusion coefficient is potentially important. As can be seen in Table 5.3, there is not a great deal of difference in the diffusion coefficients of any of the catalysts tested. For these reasons there is little to differentiate the catalysts on the basis of diffusion.

Stability at high pH: In order to semi-quantitatively assess stability, solutions of 1 mM concentration of MV, IC, and MB were all made in pH 12 aqueous KOH. The solutions were allowed to sit at room temperature and were examined over time visually, by CV, and by NMR.

Visually, the MV solution showed no change in color over the course of a week, while the MB solution took on a purple hue and the IC solution changed from indigo to light yellow

within 60 hours. After 60 hours the solutions underwent CV testing, and the peaks produced by the MV and MB solutions showed little or no degradation. IC showed no peaks within the scan range when tested after 60 hours and appears to have become electrochemically inert. The solutions were also examined with H^1 NMR at 60 hours and after 40 days. MV and MB showed trace amounts of degradation products after 40 days. The NMR of IC was highly altered from the control after 60 hours. Compared to IC, MV and MB appear to be far more stable in alkaline solution.

Solubility: In a cell where the catalyst is immobilized, the solubility may be less important. However, the solubility of the homogeneous species can still inform us how the immobilized species will interact with the solvent. Immobilization will probably take place by tethering the catalyst to the surface with an alkyl chain. If solubility is high, then the immobilized catalyst will prefer in interact with the solvent, and the fuel in the solvent, rather than with the electrode surface.

We are unaware of previous solubility data for MV and MMV, so tests where done where the viologens were slowly added in known quantities to water until the viologens no longer dissolved. The final volume of the solutions was then assessed and molar solubility estimated. MV was soluble to approximately 3.3 M and MMV was soluble to approximately 3.1 M at 25 ^{o}C. IC is soluble to 10 g/L in water at 25 ^{o}C (approximately 20 mM) and MB is soluble to 40 g/L in water at 25 ^{o}C (approximately 120 mM) [138]. The viologens are more than an order of magnitude more soluble than IC or MB and are therefore more likely to interact with the fuel in the solvent when immobilized.

Comparison summary: The relative merits of the each of the types of catalysts were investigated above. Due to the superior energy retention produced by monosubstituted

viologens, we judge them to be the most viable candidate for a future DCFC. The k_{et} values for monosubstituted viologens were also some of the highest tested, and these compounds have relatively good stability in alkaline solution. Disubstituted viologens are a good second choice, since they have been shown to be stable at pH 12 for up to 40 days and have high k_{et} values, but they have lower energy retention when compared to the monosubstituted viologens. Methylene blue potentially has the largest k_{et} value, and is stable at pH 12, but MB retains less than half of the energy of the fuel molecule when it oxidizes the fuel. From the parameters examined here, indigo carmine is the least desirable catalyst due to its low energy retention, low k_{et}, low stability in alkaline solution, and low solubility in solution.

Immobilization of the viologens: Our group is investigating methods for the immobilization of viologen on carbon surfaces. Carbon is being considered because it is likely to be the substrate of choice in a functioning DCFC due to its relative low cost and high surface area. The two aminoviologens examined in this text, MAV and APV, are candidates for immobilization, being immobilized at the amino end. When immobilized, MAV will function like a dialkyl viologen and APV will function like a monoalkyl viologen. Other immobilization schemes are also being considered. The motivation for the immobilization of viologen on the electrode surface is that viologens are toxic, costly, and soluble in water. Considerations may be different for an MB or IC catalyzed cell, since both of those dyes are cheaper and less toxic than viologen, though it is still hard to envision an economical cell with homogeneous catalyst.

5.4 Conclusions

Monosubstituted viologens were investigated electrochemically because they have been found, like their disubstituted viologen analogs, to catalytically oxidize carbohydrates and carbohydrate-like molecules, and they are more stable than their disubstituted viologen analogs

under the high pH conditions where that catalysis occurs. The potential of the single reversible redox step of the monosubstituted viologens has been found to be similar to, but somewhat more negative than, the potential of the cation/neutral redox step of their analogous disubstituted viologens. This trend in redox potential is seen between EV and MEV in water and ACN solvents and is seen between MAV and APV in DMSO solvent, so it appears to be consistent between both species and solvent. Additionally, the larger potential difference between a reduced monosubstituted viologen and oxygen than between a reduced disubstituted viologen and oxygen, for a given pH, means higher harvestable energy per electron.

Tests on the series of monoalkyl viologens in ACN and water show that the length of the alkyl chain has little apparent effect on the redox potential and k_{et} value of the viologens. This lack of effect has implications in the immobilization of the viologen, meaning that the length of the chain is unlikely to affect the redox potential of the immobilized viologen.

A higher k_{et} value means faster electron turnover, a higher concentration of viologen in the oxidized state, and increased cell current. It would be useful to investigate if other viologens have higher k_{et} values, and what factors affect the k_{et} value of viologens.

Methylene blue and indigo carmine were also analyzed and found to be deficient compared to viologens due to relatively low energy retention for carbohydrate oxidation and low solubility levels. IC also has low k_{et} values and low stability in aqueous solution.

6 COULOMBIC EFFICIENCY AND ANODE OVERPOTENTIAL FOR THE OXIDATION OF CARBOHYDRATES BY METHYL VIOLOGEN

6.1 Introduction

When oxidized to CO_2 and H_2O, glucose has a ΔG = -4420 Wh/kg, which can be compared to the complete oxidation of two other fuels proposed for other types of fuel cells, methanol (-5530 Wh/kg) and ethanol (-7450 Wh/kg). As described in Chapter 2, the percentage of the energy of a fuel that is obtained by a fuel cell is the product of the coulombic efficiency ($\eta_{coul} = n/n_{ideal}$) and the efficiency with which the chemical potential of the electrons in the fuel is utilized (voltage efficiency, $\eta_{volt} = \Delta E/\Delta E_{ideal}$). A custom-made fuel cell-like device was used to obtain both coulombic efficiency and voltage efficiency data for a homogeneous-viologen-catalyzed DCFC.

Coulombic efficiency: From Equation 2.3 we see that if glucose is oxidized all the way to carbonate, 24 electrons are liberated. If the liberation of all 24 electrons is taken to be a coulombic efficiency of 100% (which is the definition used throughout this dissertation), then the coulombic efficiencies reported in the literature for MV-catalyzed oxidation of carbohydrates range from between 2.5% [12] up to 80% (Chapter 3). This is a wide variation. Accurate and controllable coulombic efficiencies are important because the energy density, and thus utility, of the carbohydrate fuel relies directly on the extent to which the fuel can be oxidized by the viologen catalyst.

A fuel cell-like device was used to obtain the 2.5% coulombic efficiency (0.6 of 24 electrons) reported in Ref. [12]. In a later report [75], this same group at the University of Hawaii, obtained approximately 11% efficiency (2.6 electrons). For these experimental setups, no attempt was made to make the cell anaerobic and the cell also had a relatively low ratio between the superficial surface area of the current collector and the volume of the compartment containing the fuel and catalyst, in which diffusion was the only mode of transport. Additionally, the cathode was, necessarily, open to the air, which allowed additional oxygen to diffuse into the fuel compartment. Any oxygen in the cell affects the coulombic efficiency because oxygen readily oxidizes MV^{1+} to MV^{2+}. Also, in the presence of hydroxide, oxygen directly oxidizes carbohydrates and renders them inactive towards the viologen, as is shown below. Electrons that are used to reduce oxygen in this way are not detected by the potentiostat, and are therefore not counted. The low ratio between the volume of the fuel solution and the current collector may also cause undercounting of electrons because only a relatively small current may be produced for the given amount of fuel and, even without oxygen in the cell, hydroxide is known to degrade carbohydrates [129]. At low relative current, the fuel may therefore be degraded in the highly alkaline environment before it has a chance to be oxidized by the viologen catalyst.

The coulombic efficiencies reported in Chapter 3 were obtained by measuring oxygen uptake after a reaction when the viologen, carbohydrate, and an alkaline buffer solution had been placed in a sealed vial and allowed to react to completion. This indirect method is perhaps not as accurate in measuring the coulombic efficiency as counting the amount of charge passed by a cell, and the conditions present in the vial are not the same as those in a fuel cell.

Other methods for oxidizing carbohydrates have produced different apparent coulombic efficiencies: precious-metal catalyzed cells produce only about 2 of the available 24 electrons [139], microbial cells are kinetically slow, but can liberate all the available electrons [140], and cells that use enzymes as catalysts can usually only liberate 2 electrons [39].

Voltage efficiency: In a viologen-catalyzed DCFC, some of the chemical potential of the electrons in the carbohydrate fuel is used to reduce the viologen (the amount of which is one of the subjects covered in Chapter 5). Once the viologen is reduced, the difference in potential energy between the anode (MV^{1+}) and the cathode (oxygen) of a functioning cell, ΔE, depends, in part, on the behavior of the viologen-controlled anode as current is drawn. The voltage efficiency (%) of a cell is the quotient of the ΔE during operation and the ΔE at zero current (open circuit). This can also be expressed in terms of overpotential. Overpotential is the difference between the potential of an electrode at equilibrium and when current is flowing. The overpotential represents the energy lost to force the electrode reaction to proceed at the desired current density.

Though some cell-polarization curves (that is, the behavior of ΔE as a function of current) have been reported in the literature [12, 75], the geometry of the cells used previously did not allow for the use of a reference electrode. Without the use of a reference electrode it is not possible to separate out the overpotential at the anode from that of the cathode, and thereby isolate the current-vs.-potential performance at each electrode. In other words, to understand the main sources of inefficiency in an electrochemical cell, it is important to separate the overpotential of the anode from that at the cathode using a reference electrode.

6.2 Experimental

6.2.1 Materials

Methyl viologen, KOH, fructose, glucose, dihydroxy acetone (DHA), and glyceraldehyde were obtained from Sigma and used without purification. The KCl was obtained from Mallinckrodt Chemicals. The chemicals were used with no purification. The water used for the solutions was 18.2 MΩ.

6.2.2 Fuel cell

A fuel cell-like device was used to collect coulombic-efficiency and anodic-polarization data to compare the viologen-carbohydrate reaction under various conditions. The fuel cell was a modified direct methanol fuel cell that is commercially available (fuelcellstore.com, SKU 1071041). The current collector was nickel foam (Marketech International, USA) and the cathode material was the E-4 air cathode (electric-fuel.com). A Teflon-coated stir bar was used to stir the homogeneous test solution of aqueous MV, carbohydrate, and KOH. The fuel-containing compartment at the anode was closed to mass flow. The cathode was open to the air. The tests were conducted at room temperature; 23 ^{o}C. The current was collected using a Gamry PC4/750 Potentiostat. To ensure repeatability, the air cathode material was soaked in 6 M KOH for at least 24 hours before being used in the cell. The air cathode was then rinsed in 18.2 MΩ water and patted dry before the cell was assembled.

To ameliorate concerns about the presence of oxygen in the cell, steps were taken to reduce the oxygen to the minimum amount possible. It was, however, not possible to make the anode compartment entirely anaerobic, due to the cathode being open to the air and the lack of using an oxygen-impermeable membrane that is stable at high pH. Some candidates for anion-

exchange membranes were obtained, but were found to have short useful lives under the conditions of our tests. Therefore, no ionomer membrane was used. The fuel cell (Figure 6.1) was assembled in a way that allowed a resealable plastic bag to be held between the bottom stainless steel plate and the bottom piece of acrylic. A fitted hole in the bag allows oxygen to reach the air cathode. The rest of the bag surrounded the anode compartment of the cell, which is otherwise open to the air to allow the easy insertion of a reference electrode, and was used to maintain a low oxygen environment around the fuel and viologen test solution. In this way, quasi-anaerobic conditions were maintained in the test solution.

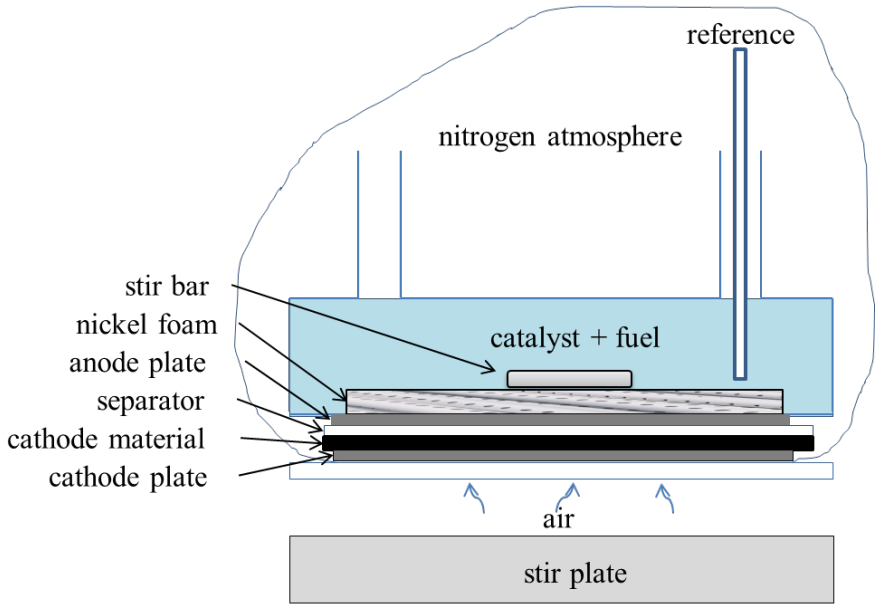

Figure 6.1 Schematic detailing the construction of the preliminary fuel cell.

The KOH solution used in the cell was purged with nitrogen for 10 minutes before being added to the anode compartment. Simultaneously, nitrogen was blown into the closed bag to create a low oxygen environment. For runs with higher carbohydrate concentrations (0.25 M to 0.5 M), solid carbohydrate was added to the deoxygenated KOH solution and allowed to dissolve

before the solution was added to the cell. For lower concentration runs, the carbohydrate was added to the cell as a 3.2 M solution after the KOH solution was added to the cell. After the anode compartment in the cell was filled with the deoxygenated KOH solution, and with the carbohydrate present, the viologen was added to the cell with a glass syringe as a saturated solution (approximately 3.2 M).

To address concern over a low current being generated for the volume of fuel solution, a relatively large current collector (9 cm^2 for 7.4 mL of test solution) was used and a stir bar was utilized to provide convection. Additionally, the coulombic-efficiency tests were run at a closed circuit potential. The closed circuit potential allowed for a fast discharge of the cell, which minimizes possible side reactions.

6.2.3 Reference electrode

A silver chloride (AgCl) reference electrode was used for the anode-overpotential tests. The wire for the reference electrode was made by anodizing a silver wire in 1 M KCl at 2 V for 10 minutes [122]. A two millimeter diameter plastic tube with fritted-glass junction (Microelectrodes, Inc. MI-402) was used for the housing. The reference electrode solution used was 3 M KCl saturated with AgCl (Microelectrodes, Inc.). The solution in the reference-electrode compartment was changed daily to ensure stability. No ohmic correction was made for the results presented, but any correction was expected to be small due to the high hydroxide concentration in the cell.

6.3 Results and discussion

Figure 6.2 shows representative structures for the carbohydrates, intermediates, and possible end products referred to below. Fructose, gluconic acid, DHA, and the intermediate enediol form of DHA are shown.

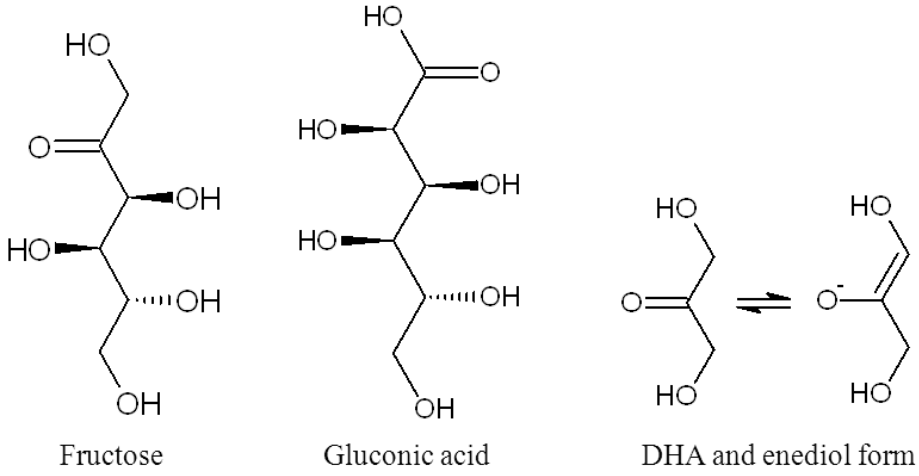

Figure 6.2 Representative structures for the carbohydrates, intermediates, and potential end products discussed in text.

6.3.1 Coulombic-efficiency control experiments

Control experiments were run (all in 1 and/or 3 M KOH) of MV only, fructose only, MV with gluconic acid, and DHA incubated in aerobic 1 M KOH for 12 hours. Carbohydrates are spontaneously oxidized in high pH solution [4], so a control of fructose in alkaline solution was run to separate out the catalytic ability of the viologen from the spontaneous oxidation. Because MV is auto-reduced in alkaline solution [9], a control with only MV in alkaline solution was run to separate out any charge passed due to auto-reduced MV. It has been suggested [12] that the two-electron oxidation product of glucose and fructose, gluconic acid, is the end product of the viologen catalysis, so a control of gluconic acid with MV was run. To test if dissolved oxygen

can directly oxidize carbohydrates in alkaline solution and make the carbohydrate inactive to viologen, a control was run in which DHA was incubated in aerobic 1 M KOH. The results and conditions of all control experiments are seen in Table 6.1.

Table 6.1 Control-test conditions and results.

Control-test species	MV	Fructose	Gluconic acid and MV	Incubated DHA and MV
Species conc (mM)	46	44	2000 and 28	115 and 9.2
KOH conc. (M)	1	1	3	<1
e^- passed per oxidized species	1	0.7	0.2	0
Coulombic efficiency	-	2.9%	0.09%	0

In a 24-hour fructose control test, only approximately 0.7 e^- per fructose had passed. The purpose of this control test was to determine if oxidation of fructose at the nickel current collector contributed significantly to the amount of charge passed by the cell. The maximum current produced was approximately 60 $\mu A\ cm^{-2}$, relatively a very low amount. Therefore, corrections were not made to take into account for oxidation of carbohydrates at the current collector. A plot of the fructose control can be seen in Figure 6.3 (seen below). Curves for both the fructose control and the MV control are seen at the bottom of the plot and nearly overlap.

For the fructose control test, the current was still approximately 55 $\mu A\ cm^{-2}$ when the test was stopped. Therefore, the coulombic efficiency reported in Table 6.1 for fructose does not reflect the actual coulombic efficiency that may be obtained if the cell would have been fully discharged. This is in contrast to the coulombic efficiencies reported in Table 6.2, where the tests were run until the current had fallen to between a 100^{th} and a 1000^{th} of the peak current, indicating that the fuel had been utilized to its practical limit. The addition of a small amount of

carbohydrate yielded an increase in current, indicating that the current produced by the cell was not limited by hydroxide concentration or catalyst degradation.

Viologens hydrolyze at the quaternary amine in high pH solution [9], which causes reduction of other, intact, viologen in the solution. In previous preliminary fuel cell experiments [12, 75] in which high pH solutions were used, no effort was made to account for this auto-reduction. In a 15 hour test, at the end of which the current had dropped to approximately 10% of its peak value, it was seen that, in 1 M KOH, nearly one e^- per viologen passed. Similar results are seen if 3 M KOH is used. The information on how many electrons are passed per viologen is important for interpreting experiments in which a high viologen-to-carbohydrate ratio is used to push the oxidation of the carbohydrate to its fullest extent. Both the MV and the fructose controls can be seen as producing a very low current relative to the MV-and-fructose tests.

Due to its stability, it was though that gluconic acid cannot act as a fuel in a viologen-catalyzed fuel cell, and a control with MV and gluconic acid was run to confirm this. The gluconic acid and MV control was run to show that gluconic acid does not react with, or reacts at a very low rate with, MV, nor is the gluconic acid spontaneously oxidized in 3 M KOH. This non-reactivity of gluconic acid indicates that any coulombic efficiency above approximately 8% (for 2 out of the 24 available electrons in fructose that are obtained by oxidation to the carboxylic acid form) must be due to a reaction pathway that is alternative to this proposed two-electron pathway. It is seen that, despite having gluconic acid at a 2 M concentration, very little charge passed. The amount of charge that passed can mostly be accounted for by the viologen in the cell, strongly indicating that gluconic acid is an end product.

For the carbohydrate-incubation test, DHA was added to 1 M KOH and the solution was stirred in air for 12 hours. At the beginning of the incubation period, the solution quickly became the yellow color associated with the formation of the carbohydrate enediol [75]. At the end of the incubation period, the solution was nearly colorless; indicating that the enediol form was no longer present. After the 12 hours, the solution was tested for pH using pH paper, which indicated that the pH had dropped below pH 14, but was above pH 13. The solution was then added to the anode compartment and a closed circuit potential imposed. Within a minute, 20 μL of 3.2 M MV was added to the anode compartment. The solution remained almost colorless, as opposed to the intense purple of the reduced viologen normally observed at that concentration, and a very low, approximately 20 μA cm^{-2}, current was observed. The cell was given 10 minutes in which time there was no change. After the 10 minutes, 50 μL of fresh 3.2 M DHA was added and the current increased, within seconds, to approximately 16.7 mA cm^{-2}. This result strongly indicates that, in addition to rapidly oxidizing the MV^{1+} to MV^{2+}, oxygen in the cell also causes the carbohydrate to become inactive to the viologen.

6.3.2 Coulombic efficiency

The coulombic efficiency and some of the variables controlling that efficiency are important to the discussion of the use of carbohydrates as a fuel source in DCFCs; the practical energy density of the fuel depends on that coulombic efficiency.

Our quasi-anaerobic and stirred-anode tests run at closed circuit potential give us a better understanding of the upper limit on the coulombic efficiencies that are possible for carbohydrates. The closed circuit has little direct effect on the oxidation of the carbohydrate (see the fructose control) but it does affect the turnover of MV^{1+} to MV^{2+}. As is reported in Chapter

4, if the viologen/carbohydrate ratio is low, electron transfer from the carbohydrate to MV^{2+} becomes limiting and the carbohydrate undergoing oxidation rearranges into unreactive intermediates. At high ratios, and when the concentration of MV^{2+} is effectively increased from rapid turnover, the viologen more efficiently oxidizes the carbohydrate and minimizes formation of unreactive intermediates. For these reason the cell was run at a closed circuit potential.

Table 6.2 shows the coulombic efficiencies achieved with fructose and glucose under various reaction conditions, as well as literature values that are available. Also included in Table 6.2 are the ratio of viologen to carbohydrate, and whether the cell was under aerobic or quasi-anaerobic conditions. Table 6.2 confirms a trend seen in the sealed-vial experiments of Chapter 3, that higher MV concentration pushes oxidation of the carbohydrate further. Additionally, the sealed-vial reactions indicated that far more than two electrons per carbohydrate were liberated by the viologen. The fuel cell experiments indicate the same, but by precisely counting the amount of charge passed, rather than through estimation from the consumption of oxygen.

Table 6.2 Coulombic-efficiency results. Cases 7 and 8 are literature values. Parenthetical values come from the total number of electrons per carbohydrate passed; non-parenthetical values are corrected values that take into account electrons that may have come from auto-reduced viologen. The blank spot in case 8 is from the value not being explicit in the literature

Case	1	2	3	4	5	6	7[a]	8[b]
Carbohydrate	glucose	fructose	fructose	fructose	fructose	fructose	glucose	glucose
MV:carbohydrate	1:1	1:50	1:1	2:1	5:1	1:1	3:200	
Quasi-anaerobic	yes	yes	yes	yes	yes	no	no	no
e^- per oxidized carb.	4.5 (6.0)	4.1	5.2 (6.3)	6.0 (8.2)	7.7 (13.2)	2.5 (3.6)	0.6	2.6
Lower-bound efficiency	19%	17%	22%	25%	32%	10%	3%	11%

a) Ref. [12].
b) Ref. [75].

Case 1 in Table 6.2 shows that for glucose, approximately 19% of the available electrons are harvested by the viologen at a 1/1 MV to glucose ratio. The range seen in the 'e^- per oxidized carb.' row is due to the auto-reduction of viologen. If all the charge which passed came strictly from the glucose, then 6 electrons per glucose are seen passing, which is the number seen in parentheses. As discussed above, though, some of the charge may have come from the auto-reduction of viologen. If 1 e^- per viologen was passed, then only 4.5 e^- per glucose is seen passing, which is the number seen out of the parentheses. This 4.5 e^- per glucose number was used to generate the 19% coulombic-efficiency number, which is considered the lower bound for the efficiency at the given conditions. The number which takes into account possible electrons from the viologen is the number which is used to calculate the coulombic efficiency for all the different tests shown. Due to the unavoidable presence of oxygen in a cell with an air cathode, it is thought that the actual coulombic efficiency for the catalytic oxidation of glucose by viologen is certainly higher than the 19%, which should be viewed as a lower level estimate of the possible extent of reaction.

Cases 2 through 5 on Table 6.2 are results for MV and fructose at different concentration ratios. As per the theory expressed in Ref. [10], as the ratio of viologen to carbohydrate increases, which means the concentration of MV^{2+} increases, more of the carbohydrate is oxidized, even accounting for the auto-reduction of viologens. At a ratio of 1:50 approximately 17% of the electrons are seen passing, indicating that even at this relatively low concentrations of viologen in quasi-anaerobic conditions, more electrons are passed than the two that would be if the carbohydrate was oxidized only to the carboxylic acid form. At a ratio of 5:1, approximately 13.2 electrons per carbohydrate molecule are observed passing. After accounting for the large number of electrons that potentially come from such a high concentration of viologen, 7.7 of the

available 24 electrons in a fructose molecule must necessarily have come from the fructose. That 7.7 number is considered a lower bound as well, because some of the fructose must have been oxidized directly by the trace oxygen in the cell, as well as some of the MV^{1+} may have been oxidized by the same trace oxygen.

A comparison of the results from the glucose case, which was performed at a 1:1 ratio, with the fructose case at the same ratio is instructive. Higher currents are achieved with fructose as the fuel, because it more readily forms the enediol intermediate than glucose [75]. For the 1:1 ratio, the coulombic efficiencies for glucose and fructose are within a fraction of an electron per carbohydrate of each other. This indicates that though the current produced by glucose is less than that produced by fructose, the rate of formation of unreactive intermediates appears to be slower for glucose as well.

Case 6 of Table 6.2 has the results of fructose and MV at a 1:1 ratio in a cell that no precautions were taken to make the cell anaerobic. Nitrogen was not bubbled through the KOH solution before testing, and the anode compartment was not isolated in a nitrogen filled bag. It can be seen that the coulombic efficiency is less than half that seen in a 1:1 cell that is quasi-anaerobic.

Cases 7 and 8 of Table 6.2 contain the data of the Hawaii group. Case 7 contains earlier results, and case 8 shows more recent results. Though Ref. [75] is not clear on the precise concentrations used to achieve the given results, it states that when the cell was completely discharged, around 2.6 electrons per carbohydrate molecule were passed. It is notable how similar their results are with our aerobic results seen in case 6, despite the difference in our cell geometries.

6.3.3 Closed-circuit current curves

It is informative to not only look at the coulombic efficiency, but also at the current-vs.-time plots used to estimate that efficiency. The shape of the curves can inform us on what currents we can obtain as the amount of charge passed by the cell increases, though in a fuel cell with steady-state operation (flowing fuel) the current would be a weighted average of what is seen.

Figure 6.3 shows two representative curves at different MV/fructose ratios. At relatively low ratios (1:50), there are two distinct regimes to the catalysis. The first regime produces a much higher current than the second. The high-ratio test (5:1) shows only one regime, the shape of which is different than either the low-ratio test or the two control tests which are also shown on Figure 6.3. Both tests were conducted in quasi-anaerobic 1 M KOH. The low-ratio test was 4.6 mM MV and 220 mM fructose. The high-ratio test was 115 mM MV and 22 mM fructose. The difference in the concentrations explains the difference in the current produced by the cells. Once the KOH solution and carbohydrate were added to the cell, the cell was set at a closed circuit potential and recording for the test began. Within a minute, the MV in the oxidized state, MV^{2+}, was added to the cell, and the curves shown are the result. This slight delay explains why the current starts near zero and then increases to its maximum; the oxidation of the carbohydrate by MV^{2+} happens at a finite rate. This rate, and others, is the focus of an upcoming publication by our group. If the cell is allowed time to equilibrate with respect to viologen oxidation state, then the high current is produced once the test begins, but the overall shape of the resulting curves are similar to those shown.

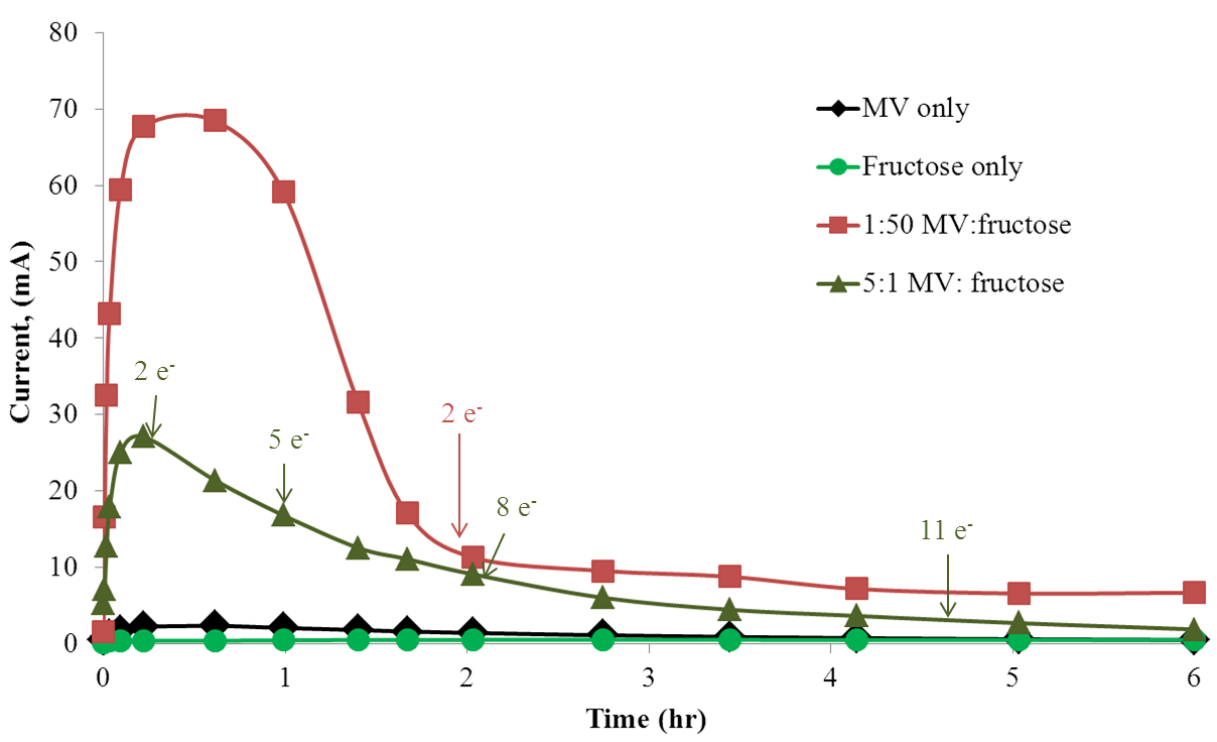

Figure 6.3 Plot of the current generated at a closed circuit potential for the control experiments of MV only and fructose only in 1 M KOH and by the oxidation of fructose at different ratios of MV to fructose in the anolyte. Cumulative electrons passed per fructose molecule for the test runs are indicated with arrows. Lines are a guide to the eye.

The number of electrons per fructose molecule passed during the initial, high-current regime of the low-ratio test correspond closely to the two electrons that are expected to come from the enediol form of the carbohydrate. This indicates that these two electrons are readily accessible to the viologen. The second, lower-current regime appears after the first two electrons have been passed, and continues at a nearly steady state for a much longer period than the initial regime. In the test that is shown, the cell was allowed to run for another 10 hours, for a total of 14 hours in the low-current regime, during which two more electrons passed. To pass that total of four electrons per fructose, each viologen must have been reduced and then oxidized

approximately 200 times. An anodic-polarization plot comparing both the high- and low-current regions of a similar test is seen below.

The behavior of the current at high MV/fructose ratios is significantly different than at a low ratio and more electrons, nearly 8, are harvested per fructose molecule in the former case. There are not two distinct regimes at the high catalyst ratio. A max current is reached within minutes, but unlike the low-ratio test, the current declines slowly and steadily. Nor does the current plateau, like the second regime of the low-ratio test, but instead continues to decline for the full 12 hours that the cell was run. Both the coulombic efficiencies reported here, and the plots of the runs themselves, are consistent with the unreactive-intermediate hypothesis as outlined in Chapter 4.

6.3.4 Cell polarization

Cell polarization tests were run to determine the performance of the cell with respect to pH variation and carbohydrate identity to allow for comparison with the anodic polarization tests discussed below. The curves for the cell are shown in Figure 6.4. Figure 6.4a shows the polarization curves for four different carbohydrates in 1 M KOH with 4.6 mM viologen, Figure 6.4b shows the curves for fructose with 4.6 mM MV at three different pH values, and Figure 6.4c shows the curves for DHA with 4.6 mM MV at the different pH values. The values shown were taken at a pseudo steady-state potential. This potential was usually reached within seconds after a given current was imposed and the potential did not significantly change for several minutes so that pseudo steady state was assured. Higher currents than those shown were imposed, but since pseudo steady state was not achieved for those currents, those data are not shown. This same procedure was used to generate the anode-polarization data discussed below.

From Figure 6.4a it appears that most of the tested carbohydrates perform similarly at pH 14. The exception is glucose, which is the carbohydrate that least readily forms the enediol intermediate.

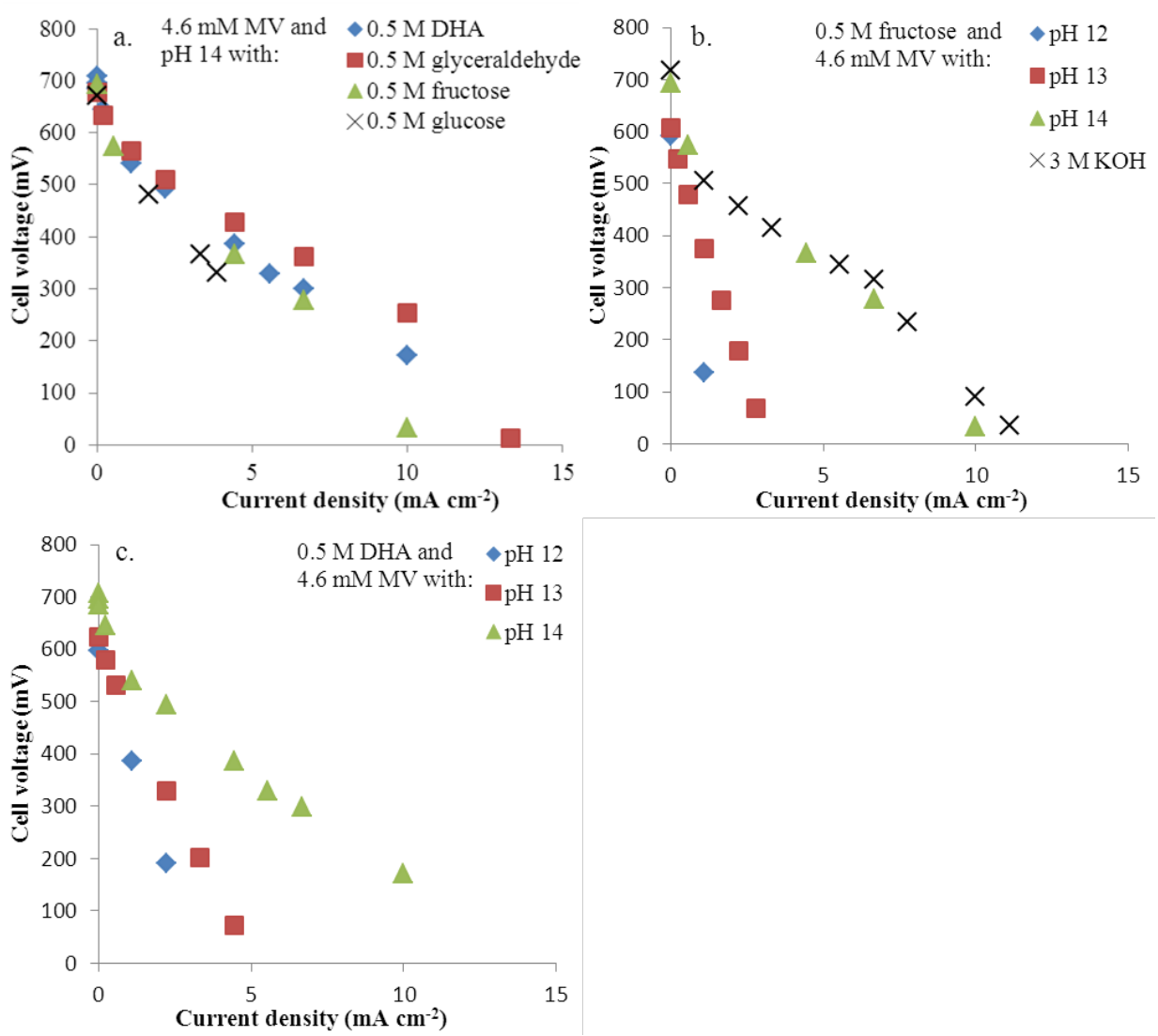

Figure 6.4 Pseudo-steady cell polarization curves for the MV-carbohydrate system under varying conditions.

Figures 6.4b and 6.4c show a common trend: that as the pH increases the performance of the cell improves. Both fructose and DHA have similar curves at pH 14. At a cell potential of

about 400 mV, both produce a current of 4.4 mA cm^{-2} for our cell. Fructose and DHA behave differently at lower pH, though. At a current density of 1.1 mA, cell potential for fructose is about 140 mV, while the cell potential is 390 mV at the same current for DHA. That difference is telling, because the cathode is functioning the same at pH 12, so the difference must be due to the behavior at the anode.

6.3.5 Anode polarization

Anode polarization plots (Figure 6.5) were obtained, with the use of a reference electrode, to separately identify the overpotential of the anode with respect to pH, carbohydrate and MV concentration, and carbohydrate identity. Unless otherwise noted, the data in Figure 6.5 were generated at the beginning of the oxidation of the carbohydrate (before 2 e^- per carbohydrate have passed), which means the performance shown corresponds to the high-current regime as seen in the 1:50 ratio curve in Figure 6.3. Once all the reactants had been added to the oxygen free cell, the cell was given 10 minutes to reach equilibrium with respect to viologen oxidation state, at which time current is passed and galvanostatic data collected.

The anode polarization curves share features common to electrode polarization curves of other fuel cell systems. At zero current, the equilibrium potential is seen. While current is flowing there is a deviation from the potential at equilibrium. This deviation is called overpotential. The constituents of the overpotential can be grouped into three categories; kinetic, Ohmic, and concentration. The three constituents of overpotential are additive and Figure 6.6a is a plot showing the combined shape of the potential as the current increases. For comparison, also included in Figure 6.6a is the plot of the experimental DHA points from Figure 6.5a. The "Combined overpotential" curve in Figure 6.6a is shown for purposes of illustration and is not meant to show a rigorous fit of the data from Figure 6.5a.

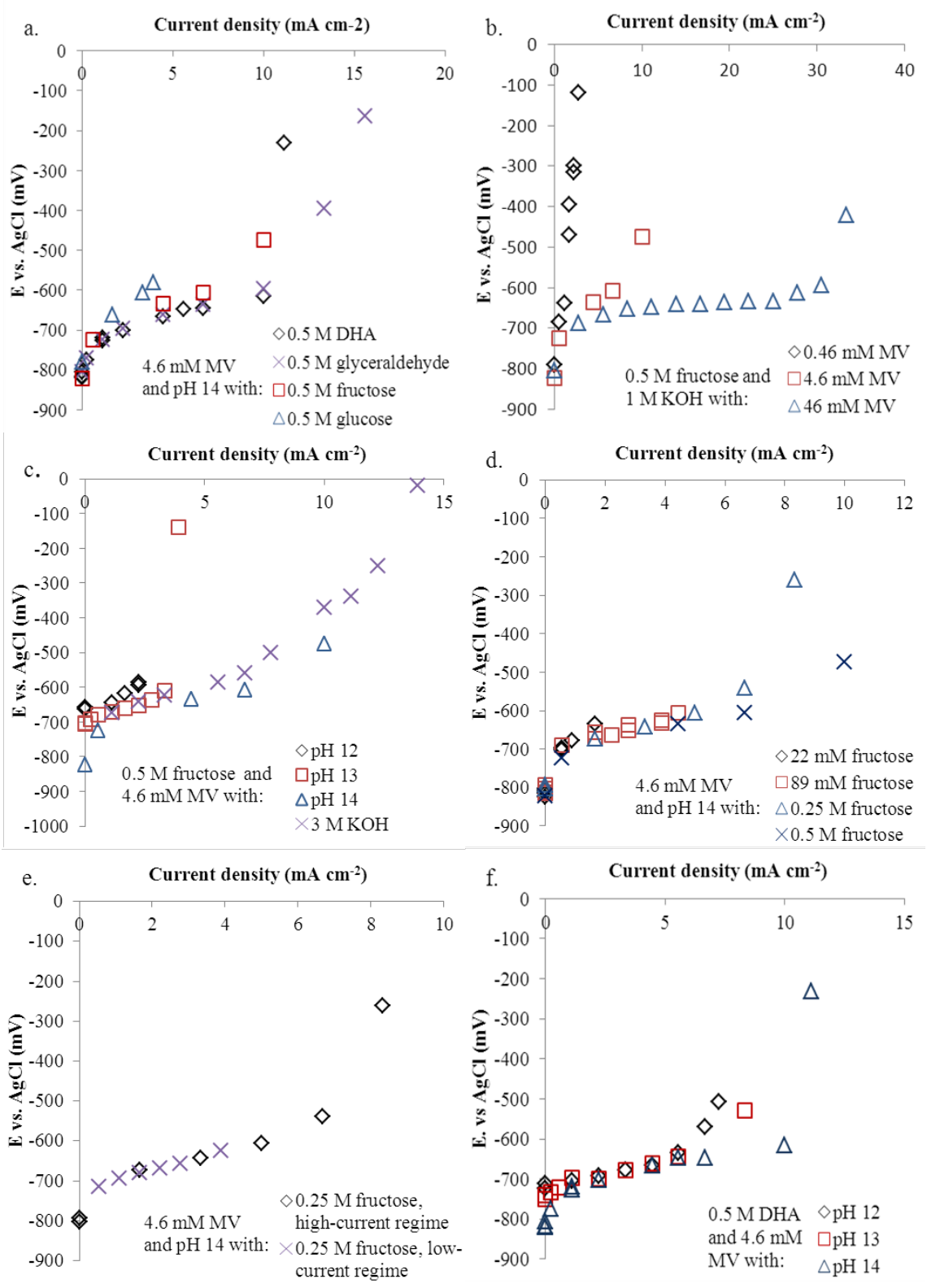

Figure 6.5 Pseudo-steady anodic polarization curves under varying conditions. For Figure 6.5e, high- and low-current regimes are as seen in Figure 6.3.

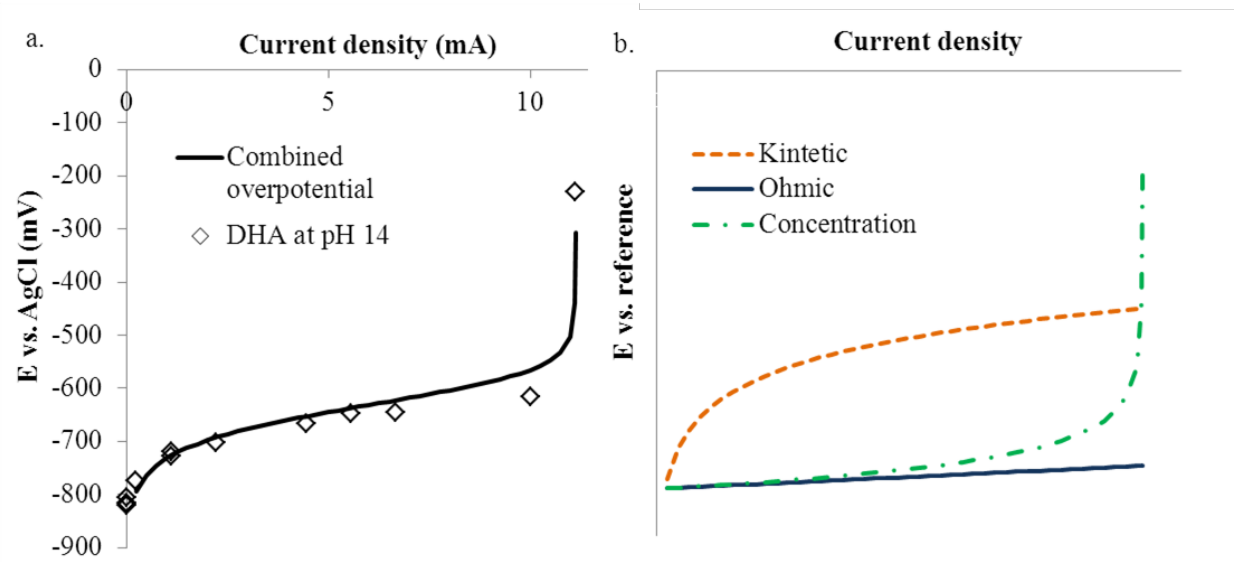

Figure 6.6 The constituents of overpotential plotted together and separately. The curves in Figure 6.6b are examples of typical overpotential curves.

Figure 6.6b illustrates the constituents of the overpotential as separate curves [14]. The kinetic overpotential depends logarithmically on the current density and the Ohmic overpotential depends linearly on the current density. The concentration overpotential is negligible at low currents, but becomes dominant as the concentration of charge carriers becomes depleted at the electrode surface. The concentration overpotential goes to infinite magnitude at the limiting current, which is the current at which reactants go to zero at the electrode interface due to mass transport limitations.

Figure 6.5a shows curves for the anode at 0.5 M carbohydrate for four different carbohydrates with 4.6 mM MV in 1 M KOH. These carbohydrates were chosen because they are either some of the most abundant on earth (glucose and fructose) or are readily derived from glycerol (DHA and glyceraldehyde) [141], which is a byproduct of biodiesel production, and are therefore the most promising fuel sources of a future commercial fuel cell. Figure 6.5a tells a similar story to Figure 6.4a. At a constant pH, if the carbohydrate produced a superior current

for a given potential on the cell polarization curve, then the current vs. potential was also superior on the anodic polarization curve. These findings are in agreement with those in the literature [75], in which the carbohydrates that most easily form the enediol intermediate produce the highest current.

Figures 6.5b-d show the effect of variation of the different participants in the catalytic reaction: the concentration of the catalyst, the carbohydrate, and hydroxide. All concentrations were varied over at least an order of magnitude, with the MV and hydroxide being varied over three orders.

Figure 6.5b shows curves for 0.5 M fructose with MV concentration variation in 1 M KOH. The MV concentrations were chosen to approximate the wide range of concentrations previously used by our group and the Hawaii group. (A similar rationale was used in selecting fructose concentrations for the tests shown in Figure 6.5d). Figure 6.5b shows that, when carbohydrate and hydroxide concentration are held constant, the current can be vastly increased by increases in the catalyst concentration. This is good news, because methyl viologen is soluble to approximately 3.2 M, which is nearly two orders of magnitude above the 46 mM that was the maximum used in these tests. Additionally, observed increases in the current indicate that under the given conditions the cell is not limited by the concentration of the enediol forms of the carbohydrate but rather the concentration of the viologen.

Figure 6.5c shows curves for 0.5 M fructose with 4.6 mM viologen with pH variation. The higher pH values were chosen because cathodic polarization is affected by pH, as is evident in a comparison of Figures 6.4c and 6.5f. The lower pH values were chosen because both viologen and the carbohydrate fuels are unstable, to varying degrees, at the higher pH values, so it is of value to know the performance of the anode at lower pH values. Figure 6.4b, and the

polarization curves in Ref. [4], show that as hydroxide concentration increases, so does the current produced by the cell for a given potential.

Perhaps counterintuitively, if we just look at the overpotential at the anode, as seen in Figure 6.5c, when fructose and MV concentrations are held constant and hydroxide concentration increases from 1 M OH^- to 3 M OH^-, the anode performs more poorly. This is consistent with unpublished data from our lab that show that greater ionic strength of the solution leads to a lower current at constant potential. (The unpublished data were tests of different strength phosphate buffers at the same pH). Thus, the increase in the current seen in the cell polarization curves (Figure 6.4b) is due to the improved performance of the cathode in 3 M OH^-. This suggests that an optimum pH can be reached, in which the positive and negative effects of increasing hydroxide concentration are balanced.

Figure 6.5d shows curves for fructose concentration variation with 4.6 mM MV in 1 M KOH. It shows that as MV and hydroxide concentrations are held constant, that increasing the carbohydrate concentration increases the limiting current at the anode, and hence delays mass-transport limitations, while having little effect on the overpotential at the anode below that region. The limiting current was difficult to exactly measure with this apparatus because under those conditions the cell frequently did not exhibit quasi-steady behavior. Nevertheless we can conclude from Figures 6.5b and 6.5d that limiting current depends on both MV and carbohydrate concentrations, with MV concentration dependence being the stronger effect. This suggests that boundary layers formed next to the current collector in which both MV and carbohydrate diffusive transport are important.

Figure 6.5e shows curves for 0.25 M fructose taken at the high- and low-current regimes (as seen in Figure 6.3), with 4.6 mM MV in 1 M KOH. Curves were obtained at the low- and

high-current regimes to determine what effect the change in kinetic regime has on the potential at the anode as a function of current. In the low-current regime the mass-transport control is reached at approximately 4 mA cm^{-2}, vs. after 7 mA cm^{-2} for the high current regime, but the overpotential at the anode for both curves is similar until that point. This is similar to what is seen Figure 6.5d, where the limiting current depends on the concentration of the carbohydrate. The kinetic overpotential doesn't seem to be strongly affected by concentration or by the regime of the oxidation, whereas the limiting current is affected by these variables.

Figure 6.5f shows curves for 0.5 M DHA with 4.6 mM MV with pH variation and can be compared to Figure 6.5c. Variation in pH was also done with DHA fuel to establish the effect that carbohydrate identity has on the performance at the anode as pH changes. Figure 6.5c shows that for fructose the potential at the anode in severely compromised at lower pH values, whereas in Figure 6.5f there is relatively little sensitivity in the behavior at the anode for the different pH values. Again, we see a pH dependence on the mass-transport-controlling regime at high currents, particularly for pH less than 13. This result is especially important because DHA, and glyceraldehyde, can easily be made by mildly oxidizing glycerol [141]. In biodiesel production, the glycerol emerges from the process at pH 13. After the glycerol is oxidized to DHA and glyceraldehyde under mild conditions, the carbohydrates can potentially be used directly by a viologen-catalyzed cell to produce electricity.

Some comparative and summary statements can be made from Figures 6.4 and 6.5. Figures 6.4b and 6.4c show relatively poor performance for the entire cell at pH 12 and 13. Figure 6.5f shows the anode polarization curves for the cell polarization curves seen in Figure 6.4c. As can be seen, for the anode, there is relatively little change in overpotential between the pH values, so the most significant portion of the overpotential is at the cathode. The cathode

performs very poorly at pH 12 and 13, and limits the current produced by the cell at a given potential.

Taken together, Figures 6.4a, 6.5b, and 6.5f indicate strongly that one of the main limiting factors in the production of electrons from the cell is the formation of the enediol intermediate. DHA, a ketose incapable of forming an enediol-inhibiting ring structure, forms the enediol readily whether the cell is in pH 12, 13, or 14. Fructose, also a ketose, forms the enediol more readily than glucose, an aldose, and thus higher current density is generated. Glucose readily forms a stable six-membered ring, and is known to be one of the most stable carbohydrates.

Figures 6.5b, 6.5d, and 6.5f taken together indicate that one of the major limitations in current production from the cell is the concentration of the catalyst. When the equilibrium concentration of the enediol intermediate is quickly reached regardless of pH, as in 6.5f, the current does not increase as rapidly with an increase in pH. Relatively large increases in current, however, are achieved when the concentration of catalyst is increased on the same order of magnitude.

6.3.6 Anode polarization: comparison between MV and monomethyl viologen

In order to compare the catalytic ability of MMV to MV, anode polarization curves were taken (Figure 6.7). After the cleaning procedure described below, it was found, through quantitative NMR analysis, that approximately 0.75% of the resulting powder was MV, with the rest being the MMV. The curves show tests with 0.46 mM MV and 46 mM MMV in 3 M KOH with 0.5 M fructose. The 46 mM MMV, which is approximately 0.75% MV, yields an MV concentration of approximately 0.35 mM. The similarity between the curves may indicate that MMV has a lower catalytic ability than is indicated by the results reported in Chapter 3.

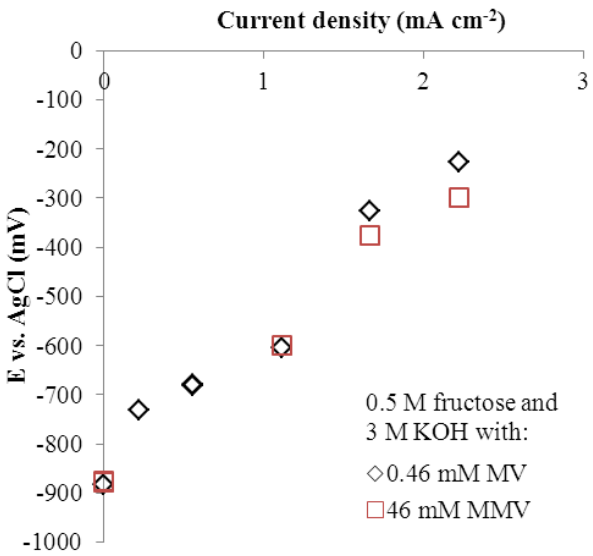

Figure 6.7 Anode polarization curves for 46 mM MMV (with 0.75% MV) and 0.46 MV.

The monomethyl viologen (MMV) used for this test was prepared as described in Chapter 3. When the MMV is prepared, some MV is also made and must be separated to obtain higher purity MMV. The following steps were taken to clean the MMV of MV: 1) dry pyridine added to the MMV/MV mixture, 2) liquid removed to a separate container, 3) one part acetone and three to four parts hexanes added to the one part pyridine, 4) solution placed in freezer for 3 hours, 5) precipitate filtered. The pyridine dissolves MMV, but relatively little MV, and the dissolved MMV precipitates out in the freezer. Therefore, the precipitate from step 5 is higher purity MMV.

6.4 Conclusion

Coulombic efficiencies for the catalytic oxidation of carbohydrates by viologen were presented. Under the various conditions tested, coulombic efficiencies between 17% and 33% were observed, and are compared with values found in the literature ranging from 2.5% to 80%.

Fuel cell results confirm a similar trend seen with the sealed-vial experiments in Chapter 3, where the higher the concentration of the viologen, the higher the coulombic efficiency that was achieved. This higher coulombic efficiency is partly due to minimizing the formation of unreactive intermediates.

The tests reported here were conducted at room temperature, 23 ^{o}C in this case. The previous 80% coulombic efficiency data were obtained from tests at lower pH levels than used here, typically pH 11, and at elevated temperatures, typically between 40 ^{o}C and 50 ^{o}C. Both variables may have affected the coulombic efficiency achieved.

The reported coulombic efficiencies show what is possible given ideal conditions at room temperature. In 1 M KOH a large fraction, up to 33%, of the electrons are made available by the viologen. However, closed-circuit-potential tests at both low and high MV/fructose ratio show a decrease in the current as the catalysis proceeds. At the low catalyst ratio, the first two electrons are harvested relatively quickly, after which the current produced by the cell decreases dramatically. At a high ratio, there is no sudden decrease in current, but rather a slow decline. Either way, a tradeoff needs to be made between the number of electrons harvested and the size of the fuel cell.

A reference electrode was used to separate the overpotential at the anode from that at the cathode for a viologen DCFC. The more easily the carbohydrate formed the enediol intermediate, the lower the overpotential at the anode, for a given current. Higher concentrations of viologen lead to dramatically improved performance at the anode. The hydroxide concentration had multiple effects, which also depended on the identity of the carbohydrate tested. Fructose performed poorly at the lower pH values tested, and as the hydroxide concentration increased from 1 M to 3 M, the performance at the anode decreased, which is

likely due to ionic-strength effects. The hydroxide concentration had a relatively small effect on the anode of the cell with DHA as the fuel. This is likely due to the fact that DHA more readily forms the enediol intermediate. It was also found that, especially at the lower pH values tested, there was significant overpotential in the cell due to the cathode.

7 SUMMARY AND RECOMMENDATIONS FOR FUTURE WORK

7.1 Summary

The primary goal of this work was to answer questions about the effectiveness and utility of viologen as a catalyst for use in direct carbohydrate fuel cells (DCFCs). This work has answered questions starting from the most basic (are viologens catalytically active in the oxidation of carbohydrates?) to the determination of heterogeneous kinetic values and the generation of a proposed mechanism by which that catalysis proceeds.

Chapter 3 established that all tested viologens are indeed catalytically active towards carbohydrates. By examining which molecules were active towards the viologen and what the products of the reactions were, we obtained evidence that was used to generate a hypothesis for the mechanism, as discussed in Chapter 4. Chapter 3 also established that high coulombic efficiencies, perhaps up to 80%, are achievable under the proper conditions.

Chapter 4 provides information on the mechanism by which viologen catalyzes the oxidation of carbohydrates. It was confirmed that viologens react with the enediol form of the carbohydrate, and that viologens oxidize all tested molecules that are capable of forming the enediol, not just carbohydrates. That fact, together with NMR evidence that shows formate and carbonate as major products provides evidence that the carbohydrates are oxidized in a stepwise fashion, with another enediol intermediate forming after the previous carbon-carbon bond is broken.

Chapter 5 established that, of the organic dyes that have been suggested as catalysts for DCFCs, viologens perform the best, based on the parameters examined in that chapter. Compared to the other dyes, viologens have superior or equivalent redox potentials, heterogeneous electron-transfer rates, and stability. It was also found that substituent length does not significantly affect redox potential, so procedures to immobilize viologen by an alkyl chain need not take into account the redox potential when chain length is determined, and other parameters can be used.

Chapter 6 showed that a large number of the electrons contained in the tested carbohydrates are also liberated by the viologens catalyst under fuel cell conditions. Knowledge of coulombic efficiencies is very important because it provides information about the usable energy density of the fuel. The behavior of a viologen-controlled anode under various conditions was elucidated, showing the important result that for the carbohydrates DHA and glyceraldehyde the performance at the anode is hardly affected by the pH, down to at least pH 12. This means that dialkyl viologens are potentially good catalysts for those fuels because the dialkyl viologens are stable on the order of months at pH 12. Also, current densities that are superior to the other techniques for obtaining electricity from carbohydrate were demonstrated, with a current density of 30 mA cm^{-2} achieved before the transport limit at the anode was reached for certain conditions. Current densities given for other cells, as described in Chapter 2, are typically on the order of 1 mA cm^{-2} or less, sometimes far less.

Figure 6.5b shows that the anode of a viologen-catalyzed cell can produce a current density of at least 30 mA cm^{-2} before the limiting current is reached. If a cathode can be obtained that performs well at pH 14, the pH of the tests in Figure 6.5b, then it is conceivable that a ΔE of 0.5 V for the cell could be maintained at a current density of 30 mA cm^{-2}, producing

a power output of 15 mW cm^{-2}. At this level of power output, a cell around 0.7 m^2 in superficial electrode area could power a 100 W light bulb.

7.2 Future work

Now that we have a good idea about the capabilities and limitations of homogeneous viologens, it is appropriate to begin synthesis and testing of immobilized viologens.

Therefore, the main future work in this BYU project is to immobilize viologen and test it for catalytic activity. Chapter 2 lists a large number of immobilization techniques. These techniques should be examined closely and evaluated for suitability. Criteria could include whether or not the immobilized viologen has been tested for stability in alkaline conditions, surface coverage, known electroactivity, and redox potential. Once the immobilized viologen has been made, the redox potential and electroactivity should be tested using CV.

The ability of the immobilized viologen to catalytically oxidize carbohydrates should then be tested. The catalytic ability should first be tested using a rotating disk electrode, where the carbohydrate in solution will be oxidized at the viologen-coated electrode, generating a current. Once catalytic ability has been established, testing can move to a fuel cell setting.

The best prospects for the fuel for a commercial viologen-catalyzed DCFC are the three-carbon carbohydrates glyceraldehyde and DHA. These potential fuel sources work with the catalyst at relatively low pH values (pH 12 and below), meaning that the catalyst will be stable for a longer period of time compared to the higher pH values used for larger carbohydrates. Challenges at the low pH values include the performance of the cathode, which does not perform well at pH values where the dialkyl viologens are more stable.

A project related to the fuel cell would be to quantify the effect that ionic strength has on the current produced by the cell, and determine the source of that effect. As seen in the Chapter

6, as the concentration of the hydroxide increases from 1 M to 3 M, the current produced by the cell improves, but this improvement is only at the cathode. The anode actually performs more poorly as the hydroxide concentration increases from 1 M to 3 M. Little quantitative information on the ionic strength effect was obtained and that information would be useful.

Spectrophotometry-based experiments are already underway by our group to obtain kinetic data for the homogeneous reaction between viologen and carbohydrates. The participants of the reaction; the carbohydrate, the hydroxide, and the viologen have been shown to be first order. The carbohydrate actually participates in the enediol form, and the carbohydrates that form the enediol more easily, like DHA, have much higher rate constants and lower activation energies, than carbohydrates that do not form the enediol as easily, like glucose.

Because the actual catalytic activity of the monoalkyl viologens is unknown, due to variable contamination form dialkyl viologen (discussed in the methods section of Chapter 3), more work needs to be done to separate the monoalkyl catalytic activity from that of the dialkyl viologen. The monoalkyl viologens are of interest because they are more stable at higher pH values, so determining their precise level of catalytic ability of also of interest. Due to the difficulty in obtaining pure monosubstituted viologen, perhaps a good way to separate out the catalytic activity of the monosubstituted viologen is to immobilize functionally monosubstituted viologen on an electrode surface and test the surface for catalytic activity. This task is already underway by our group.

Determination of the products of the oxidation could provide additional insight into the course of the reaction at different catalyst ratios. This detection can be undertaken using a gas chromatograph-mass spectrometry (GC-MS) instrument. Challenges include the presence of high concentrations of salts ($K^+ + OH^-$) required for the reaction to take place, which negatively

affect the instrument. This issue can be overcome with the use of a simple device, the ion exchange device (IED). The IED, described more fully in Appendix A, makes use of Nafion, allowing the K^+ ion in the reaction solution to diffuse into an HCl solution while H^+ ions diffuse into the test solution and combine with the OH^- there, making water. In this way, the pH of the solution can be neutralized while greatly reducing the presence of salt in the test solution. The solution can then be diluted with methanol, a solvent that is better suited for use in a GC-MS, and then run through the instrument.

The enediol form of the carbohydrate is produced as the carbohydrate is incubated in alkaline solution. Having a higher enediol concentration when the carbohydrate meets the viologen would cause a larger current than with fresh carbohydrate. It would be interesting to study the effect of incubation time on the current. Also, it would be interesting to determine the effect incubation on coulombic efficiency.

As can be seen in Equation 2.8, the oxidation of carbohydrates in alkaline conditions leads to the productions of carbonate and the consumption of OH^-. Carbonates potentially have low solubility, and the formation of a precipitate within the cell could affect the long-term performance of the cell. The main cation in the fuel solution is the counter ion to the hydroxide. Thus, care should be taken in the selection of this counter ion. Approximately 8 moles of potassium carbonate dissolve into 1 L of water, meaning that if potassium is used as the counter ion it is unlikely that a potassium precipitate would form in the cell.

The high consumption of the OH^- could also be a problem for a practical cell if carbonate is the product. However, upon mild heating, carbonate dissociates into OH^- and CO_2. The CO_2 would simply bubble off and the OH^- could then be recycled. If a commercial cell were attached

to a biodiesel refinery (discussed in section 2.4) then the waste heat from the facility may be used for to heat the used-fuel stream and liberate the OH^-.

The performance at the viologen-catalyzed anode was the focus of Chapter 6. Commercially available cathode material was used to gather that data. As discussed in Chapter 6, the cathode material performed relatively poorly at the lower pH values tested (i.e. pH 12 and 13). The viologen catalyst, however, is most stable at those lower pH values. The cathode material that was used is typically used for zinc-air batteries that operate at high pH. If the cathode catalyst material was altered so that the catalyst particles have a higher surface area, such as by increasing the surface-area-to-volume ratio by reducing the size of the particle, then the material may have improved performance at the lower pH values.

BIBLIOGRAPHY

[1] H.S. Stoker, General, Organic, and Biological Chemistry 3rd ed., Houghton Miflin, Boston, New York, 2004.

[2] J. McGinley, F.N. McHale, P. Hughes, C.N. Reid, A.P. McHale, Biotechnology Letters, 26 (2004) 1771-1776.

[3] S.K. Chaudhuri, D.R. Lovely, Nature Biotechnol., 21 (2003) 1229–1232.

[4] S.B. Aoun, G.S. Bang, T. Koga, Y. Nonaka, T. Sotomura, I. Taniguchi, Electrochem. Comm., 5 (2003) 317-320.

[5] H.-F. Cui, J.-S. Ye, X. Liu, W.-D. Zhang, F.-S. Sheu, Nanotechnology, 17 (2006) 2334-2339.

[6] S. Kerzenmacher, J. Ducree, R. Zengerle, F.v. Stetten, Journal of Power Sources, 182 (2008) 1-17.

[7] L. Yu, M.J. Wolin, J. Bacteriol, 98 (1969) 51-55.

[8] D.R. Wheeler, J. Nichols, D. Hansen, M. Andrus, S. Choi, G.D. Watt, Journal of the Electrochemical Society, 156 (2009) B1201-B1207. Reproduced by permission of ECS - The Electrochemical Society.

[9] P.M.S. Monk, The Viologens Physicochemical Properties, Synthesis and Applications of the Salts of 4,4' Bipyridine, John Wiley & Sons, Chichester, 1998.

[10] G.D. Watt, D. Hansen, D. Dodson, M. Andrus, D. Wheeler, Renewable Energy, 36 (2011) 1523-1528.

[11] D. Hansen, Y. Pan, J. Stockton, W. Pitt, D. Wheeler, Journal of the Electrochemical Society, (2012) Accepted for publication. Reproduced by permission of ECS - The Electrochemical Society.

[12] D. Scott, B.Y. Liaw, Energy & Environmental Science, 2 (2009) 965-969.

[13] D. Hansen, G. Watt, D. Wheeler, Journal of the Electrochemical Society, (2012) Sumbitted. Reproduced by permission of ECS - The Electrochemical Society.

[14] J. Newman, K.E. Thomas-Alyea, Electrochemical Systems Third Edition, John Wiley & Sons, Inc, Hoboken, NJ, 2004.

[15] J. Larminie, A. Dicks, Fuel Cell Systems Explained, John Wiley & Sons, Ltd, Chichester, 2000.

[16] S.C. Thomas, X. Ren, S. Gottesfeld, P. Zelenay, Electrochimica Acta, 47 (2002) 3741-3748.

[17] E. Fuel, in, 2009.

[18] R. O'Hayre, S.-W. Cha, W. Colella, F.B. Prinz, Fuel Cell Fundamentals, John Wiley & Sons, Inc., Hoboken, New Jersey, 2006.

[19] J. Liu, H. Wang, S. Cheng, K.-Y. Chan, Journal of Membrane Science, 246 (2005) 95-101.

[20] S.H. Seo, C.S. Lee, Applied Energy, 87 (2010) 2597-2604.

[21] B.S. Pivovar, Polymer, 47 (2006) 4194-4202.

[22] P. Berg, K. Promislow, J.S. Pierre, J. Stumper, B. Wetton, Journal of the Electrochemical Society, 151 (2004) A341-A353.

[23] Z. Qi, A. Kaufman, Journal of Power Sources, 109 (2002) 38-46.

[24] O. Savadogo, Journal of New Materials for Electrochemical Systems, 1 (1998) 047-066.

[25] X. Li, Principles of Fuel Cells, Taylor & Francis Group, LLC, New York, 2006.

[26] K.A. Mauritz, R.B. Moore, Chemical Reviews, 104 (2004) 4535-4585.

[27] S. Slade, S.A. Campbell, T.R. Ralph, F.C. Walsh, Journal of the Electrochemical Society, 149 (2002) A1556-A1564.

[28] M. Unlu, J. Zhou, P.A. Kohl, Angewandte Chemie Int. Ed., 49 (2010) 1299-1301.

[29] E.H. Yu, K. Scott, R.W. Reeve, Journal of Applied Electrochemistry, 36 (2006) 25-32.

[30] H.L.S. Salerno, F.L. Beyer, Y.A. Elabd, Polymer Physics, 50 (2012) 552-562.

[31] H. Zarrin, J. Wu, M. Fowler, Z. Chen, Journal of Membrane Science, 394-395 (2012) 193-201.

[32] M.R. Hibbs, M.A. Hickner, T.M. Alam, S.K. McIntyre, C.H. Fujimoto, C.J. Cornelius, Chemistry of Materials, 20 (2008) 2566-2573.

[33] M. Faraj, E. Elia, M. Boccia, A. Filpi, A. Pucci, F. Ciardelli, Polymer Chemsitry, 49 (2011) 3437-3447.

[34] J. Qiao, J. Fu, L. Liu, Y. Liu, J. Sheng, International Journal of Hydrogen Energy, 37 (2012) 4580-4589.

[35] J. Zhao, M. Unlu, I. Anestis-Richard, P.A. Kohl, Journal of Membrane Science, 350 (2010) 286-292.

[36] J.-J. Kang, W.-Y. Li, Y. Lin, X.-P. Li, X.-R. Xiao, S.-B. Fang, Polymers for Advanced Technologies, 15 (2004) 61-64.

[37] S. Lu, J. Pan, A. Huang, L. Zhuang, J. Lu, PNAS, 105 (2008) 20611-20614.

[38] J. Wang, J. Wang, S. Li, S. Zhang, Journal of Membrane Science, 368 (2011) 246-253.

[39] F. Davis, S.P.J. Higson, Biosensors and Bioelectronics, 22 (2007) 1224-1235.

[40] R.A. Bullen, T.C. Arnot, J.B. Lakeman, F.C. Walsh, Biosensors and Bioelectronics, 21 (2006) 2015-2045.

[41] A.T. Yahiro, S.M. Lee, D.O. Kimble, Biochimica et Biophysica Acta, 88 (1964) 375-383.

[42] A. Heller, Physical Chemistry Chemical Physics, 6 (2004) 209-215.

[43] L. Mor, E. Bubis, K. Hemmes, P. Schechner, IEEE, (2004) 278-281.

[44] R. Larsson, B. Folkesson, P.M. Spaziante, W. Veerasai, R.H.B. Exe, Renewable Energy, 31 (2006) 549-552.

[45] S. Kerzenmacher, J. Ducree, R. Zengerle, F.v. Stetten, Journal of Power Sources, 182 (2008) 66-75.

[46] D.H. Park, S.K. Kim, I.H. Shin, Y.J. Jeong, Biotechnology Letters, 22 (2000) 1301.

[47] D.H. Park, J.G. Zeikus, Appl Microbiol Biotechnol, 59 (2002) 58-61.

[48] A. Pizzariello, M. Stred'ansky, S. Miertus, Bioelectrochemistry, 56 (2002) 99-105.

[49] E. Katz, O. Lioubashevski, I. Willner, J. Am. Chem. Soc., 127 (2005) 3979-3988.

[50] V. Soukharev, N. Mano, A. Heller, Journal of the American Chemical Society, 126 (2004) 8368-8369.

[51] P. Kavanagh, S. Boland, P. Jenkins, D. Leech, Fuel Cells, 9 (2009) 79-84.

[52] P. Beltrame, M. Comotti, C.D. Pina, M. Rossi, Applied Catalysis A: General, 297 (2006) 1.

[53] P. Schechner, E. Kroll, E. Bubis, S. Chervinsky, E. Zussman, Journal of The Electrochemical Society, 154 (2007) B942-B948.

[54] C. Jin, I. Taniguchi, Materials Letters, 61 (2007) 2365-2367.

[55] C. Zhao, C. Shao, M. Li, K. Jiao, Talanta, 71 (2007) 1769-1773.

[56] E. Bubis, L. Mor, N. Sabag, Z. Rubin, U. Vaysban, K. Hemmes, P. Schechmer, in: Proceedings of FUEL CELL 2006, Fourth International Conference on Fuel Cell Science, Engineering and Technology, ASME, Irvine, California, 2006, pp. 1007-1014.

[57] C.K. Jin, T.V. Dang, Y. Ikee, T. Yamada, S. Sano, M. Shiro, Y. Nagao, ChemInform, 38 (2007) no-no.

[58] D. Basu, S. Basu, International Journal of Hydrogen Energy, 37 (2012) 4678-4684.

[59] M.R. Stetten, D.W. Stetten, Journal of Biological Chemistry, 187 (1950) 241-252.

[60] A. Kloke, B. Biller, U. Kraling, S. Kerzenmacher, R. Zengerle, F.v. Stetten, Fuel Cells, 11 (2011) 316-326.

[61] H. Lerner, J. Giner, J.S. Soeldner, C.K. Colton, Journal of the Electrochemical Society, 126 (1979) 237-242.

[62] P. Schechner, E. Bubis, L. Mor, in: Proceedings of FUEL CELL 2005, Third International Conference on Fuel Cell Science, Engineering, and Technology, AMSE, Ypsilanti, MI, United States, 2005, pp. 661-665.

[63] L. Michaelis, Chem. Rev., 16 (1935) 243-290.

[64] C.L. Bird, A.T. Kuhn, Chemical Society Reviews, 10 (1981) 49 - 82.

[65] E. Pia, R. Toba, M. Chas, C. Peinador, J.M. Quintela, Tetrahedron Letters, 47 (2006) 1953-1956.

[66] C. Lee, Y.W. Sung, J.W. Park, Journal of Electroanalytical Chemistry, 431 (1997) 133-139.

[67] Y.N. Forostyan, A.P. Oleinik, V.M. Artemova, Soviet Electrochemistry, 7 (1971) 691-692.

[68] O. Poizat, C. Sourisseau, J. Corset, Journal of Molecular Structure, 143 (1986) 203-206.

[69] K.P. Butin, A.A. Moiseeva, S.P. Gromov, A.I. Vedernikov, A.A. Botsmanova, E.N. Ushakov, M.V. Alfimov, Journal of Electroanalytical Chemistry, 547 (2003) 93-102.

[70] G. Tayhas, R. Palmore, H. Bertschy, S.H. Bergens, G.M. Whitesides, Journal of Electroanalytical Chemistry, 443 (1998) 155-161.

[71] L. Pospisil, J. Kuta, J. Volke, Electroanalytical Chemistry and Interfacial Electrochemistry, 58 (1975) 217-227.

[72] P.M.S. Monk, N.M. Hodgkinson, Electrochimica Acta, 43 (1998) 245-255.

[73] A. Nakahara, J.H. Wang, J. Phys. Chem., 67 (1963) 496-498.

[74] J.A. Farrington, A. Ledwith, M.F. Stam, Journal of the Chemical Society D: Chemical Communications, (1969) 259-260.

[75] D.M. Scott, T.H. Tsang, L. Chetty, S. Aloi, B.Y. Liaw, Journal of Power Sources, 196 (2011) 10556-10562.

[76] K. Arihara, F. Kitamura, Journal of Electroanalytical Chemistry, 550-551 (2003) 149-159.

[77] A. Fernandez, M. Innocenti, R. Guidelli, Journal of Electroanalytical Chemistry, 532 (2002) 237-246.

[78] B. Barroso-Fernandez, M.T. Lee-Alvarez, C.J. Selisker, W.R. Heineman, Analytica Chimica Acta, 370 (1998) 221-230.

[79] J. Litong, J. Ping, Y. Jiannong, F. Yuzhi, Talanta, 39 (1992) 145-147.

[80] M.E. Ghica, C.M.A. Brett, Analytica Chimica Acta, 532 (2005) 145-151.

[81] D. Quan, D.G. Min, G.S. Cha, H. Nam, Bioelectrochemistry, 69 (2006) 267-275.

[82] R. Maalouf, H. Chebib, Y. Saikali, O. Vittori, M. Sigaud, N. Jaffrezic-Renault, Biosensors and Bioelectronics, 22 (2007) 2682-2688.

[83] T. Komura, K. Kijima, T. Yamaguchi, K. Takahashi, Journal of Electroanalytical Chemistry, 486 (2000) 166-174.

[84] T. Ohsaka, H. Yamamoto, M. Kaneko, A. Yamada, M. Nakamura, S. Nakamura, N. Oyama, Bull. Chem Soc. Jpn., 57 (1984) 1844-1849.

[85] A. Walcarius, L. Lamberts, E.G. Derouane, Electrochimica Acta, 38 (1993) 2257-2266.

[86] L.L. A. Walcarius, E. G. Derouane, Electrochimica Acta, 38 (1993) 2267-2276.

[87] J.-H. Ryu, J.-H. Lee, S.-J. Han, K.-D. Suh, Colloids and Surfaces A: Physicochemical and Engineering Aspects, 315 (2008) 31-37.

[88] N. Vlachopoulos, J. Nissfolk, M. Möller, A. Briançon, D. Corr, C. Grave, N. Leyland, R. Mesmer, F. Pichot, M. Ryan, G. Boschloo, A. Hagfeldt, Electrochimica Acta, 53 (2008) 4065-4071.

[89] Z. Sharrett, S. Gamsey, P. Levine, D. Cunningham-Bryant, B. Vilozny, A. Schiller, R.A. Wessling, B. Singaram, Tetrahedron Letters, 49 (2008) 300-304.

[90] T. Yamaguchi, K. Takahashi, T. Komura, Electrochimica Acta, 46 (2001) 2527-2535.

[91] A.K.M. Kafi, D.-Y. Lee, S.-H. Park, Y.-S. Kwon, Microchemical Journal, 85 (2007) 308-313.

[92] J. Li, G. Cheng, S. Dong, Electroanalysis, 9 (1997) 834-837.

[93] J. Li, J. Yan, Q. Deng, G. Cheng, S. Dong, Electrochimica Acta, 42 (1997) 961-967.

[94] N.-S. Lee, H.-K. Shin, D.-J. Qian, Y.-S. Kwon, Thin Solid Films, 515 (2007) 5163-5166.

[95] J.-Y. Ock, H.-K. Shin, Y.-S. Kwon, J. Miyake, Colloids and Surfaces A: Physicochemical and Engineering Aspects, 257-258 (2005) 351-355.

[96] T. Sagara, H. Tsuruta, N. Nakashima, Journal of Electroanalytical Chemistry, 500 (2001) 255-263.

[97] S. Dong, J. Li, Bioelectrochemistry and Bioenergetics, 42 (1997) 7-13.

[98] H.C.D. Long, D.A. Buttry, Lanmuir, 8 (1992) 2491-2496.

[99] A. Factor, G.E. Heinsohn, Journal of Polymer Science. Part B, Polymer Letters, 9 (1971) 289.

[100] L. Futian, Y. Xianda, F. Liangbo, L. Shuben, European Polymer Journal, 31 (1995) 819-824.

[101] H. Sato, T. Tamamura, Journal of Applied Polymer Science, 24 (1979) 2075-2085.

[102] M.S. Simon, P.T. Moore, Journal of Polymer Science: Polymer Chemistry Edition, 13 (1975) 1-16.

[103] K. Ageishi, T. Endo, M. Okawara, Macromolecules, 16 (1983) 884-887.

[104] X. Liu, K.G. Neoh, E.T. Kang, Marcomolecules, 36 (2003) 8361-8367.

[105] M. Okawara, Journal of Polymer Science: Polymer Chemistry Edition, 17 (1979) 927-930.

[106] T. Ohsaka, M. Nakanishi, O. Hatozaki, N. Oyama, Electrochimica Acta, 35 (1989) 63-64.

[107] P. Bauerle, K.U. Gaudl, Synthetic Metals, 43 (1991) 3037-3042.

[108] M. Pravda, in, 2000.

[109] D.R. Rosseinsky, P.M.S. Monk, R.A. Hann, Electrochimica Acta, 35 (1990) 1113-1123.

[110] C.-Y. Hsu, C.-H. Liao, K.-C. Ho, Solar Energy Materials and Solar Cells, 92 (2008) 194-202.

[111] L. Coche, A. Deronzier, J.-C. Moutet, Journal of Electroanalytical Chemistry, 198 (1986) 187-193.

[112] T. Komura, T. Yamaguchi, K. Furuta, K. Sirono, Journal of Electroanalytical Chemistry, 534 (2002) 123-130.

[113] H.C. Ko, S.-a. Park, W.-k. Paik, H. Lee, Synthetic Metals, 132 (2002) 15-20.

[114] D.-J. Qian, C. Nakamura, J. Miyake, Thin Solid Films, 374 (2000) 125-133.

[115] Z. Shi, K.G. Neoh, E.T. Kang, Biomaterials, 26 (2005) 501-508.

[116] J. Zhang, T. Abe, M. Kaneko, Journal of Electroanalytical Chemistry, 438 (1997) 133-138.

[117] T. Sata, Journal of Membrane Science, 118 (1996) 121-126.

[118] Y. Ikeda, M. Ikeda, F. Ito, Solid State Ionics, 169 (2004) 35-40.

[119] C.J. Schoot, J.J. Ponjee, H.T.v. Dam, R.A.v. Doorn, P.T. Bolwijn, Appl. Phys. Lett. , 23 (1973) 64-65.

[120] J.C. Thompson, B.B. He, Applied Engineering in Agriculture, 22 (2006) 261-265.

[121] Y. Zheng, X. Chen, Y. Shen, Chemical Reviews, 108 (2008) 5253-5277.

[122] P.M.S. Monk, Fundamentals of Electroanalytical Chemistry, John Wiley & Sons Ltd., Chichester, 2001.

[123] D.T. Sawyer, A. Sobkowiak, J. Julian L. Roberts, Electrochemistry for Chemists, John Wiley & Sons, New York, 1995.

[124] V.S. Bagotsky, Fundamentals of Electrochemistry John Wiley & Sons, Inc. , Hoboken, New Jersey, 2006.

[125] A. Read, D. Hansen, S. Aloi, W.G. Pitt, D.R. Wheeler, G.D. Watt, Renewable Energy, 46 (2012) 218-223.

[126] G.D. Watt, Analytical Biochemistry, 99 (1979) 399-400.

[127] Y. Miao, J.Y. Chen, X. Jiang, Z. Huang, Applied Biochemistry and Biotechnology, 167 (2012) 358-366.

[128] W. Zhang, G. Wei, Energy Sources, Part A: Recovery, Utilization, and Environmental Effects, 34 (2012) 1178-1186.

[129] B.Y. Yang, R. Montgomery, Carbohydrate Research, 280 (1996) 27-45.

[130] E. Katz, A.L.d. Lacey, J.L.G. Fierro, J.M. Palacios, V.M. Fernandez, Journal of Electroanalytical Chemistry, 358 (1993) 247-259.

[131] N.G. Tsierkezos, Journal of Solution Chemistry, 36 (2007) 1301-1310.

[132] J.E.B. Randles, Transactions of the Faraday Society, 44 (1948) 327-338.

[133] T. Yinxuan, Y. Hangsheng, S. Baoen, Dianhuaxue (Electrochemistry), 3 (1997) 334-337.

[134] R.S. Nicholson, Analytical Chemistry, 37 (1965) 1351-1355.

[135] S. Bao-En, W. Gui-Liang, T. Yin-Xuan, Wuli Huaxue Xuebao (Acta Physico-Chimica Sinica), 8 (1992) 476-480.

[136] W.M. Clark, Oxidation-Reduction Potential of Organic Systems, The Williams & Wilkins Company, Baltimore, 1960.

[137] T. Reda, C.M. Plugge, N.J. Abram, J. Hirst, PNAS, 105 (2008) 10654-10658.

[138] S. Budavari, M.J. O'Neal, A. Smith, P.E. Heckelman, The Merck Index: An Encyclopedia of Chemicals, Drugs, and Biologicals Eleventh Edition, Eleventh ed., Merck & Co., Inc., Rahway, New Jersey, 1989.

[139] N. Fujiwara, S.-i. Yamazaki, Z. Siroma, T. Ioroi, H. Senoh, K. Yasuda, Electrochemisty Communications, 11 (2009) 390-392.

[140] H.P. Bennetto, G.M. Delaney, J.R. Mason, S.D. Roller, J.L. Stirling, Biotechnology Letters, 7 (1985) 699-704.

[141] M.A. Dasari, P.-P. Kiatsimkul, W.R. Sutterlin, G.J. Suppes, Applied Catalysis A: General, 281 (2005) 225-231.

APPENDIX A. ION EXCHANGE DEVICE FOR REMOVING INORGANIC SALTS FROM TEST SOLUTIONS

This appendix describes a method that can be used to remove some inorganic salts from alkaline solutions so that the solutions can be tested in a gas chromatography-mass spectrometry (GC-MS) instrument, or other mass spectrometry instruments.

GC-MS can be used to identify the presence of organic compounds. The GC-MS instruments work by evaporating the compounds of interest, and can therefore be sensitive to the presence of compounds that are difficult to volatize, such as inorganic salts. Additionally, the presence of salts in the solution can cause an effect called "ion suppression," where the peaks of some of the species are suppressed by the salt.

The viologen-catalyzed oxidation of carbohydrate requires the presence of hydroxide (OH^-) ions, which are typically supplied to the solution in the form of potassium hydroxide (KOH). Some of the salts formed by the K^+, such as KOH, or KCl if the reaction is quenched with HCl, can clog the instrument tips when the solvent that is carrying them is evaporated.

The following simple device, the ion-exchange device (IED), can be used to significantly reduce the presence of K^+ in the solution while simultaneously quenching the reaction, which is also useful if it is desired for the reaction to be followed by time series.

Figure A.1 shows a piece of Teflon, or other acid-resistant material, machined to make a well. In the well, place HCl (typically 1 to 3 M). On top of the well, place a piece of Nafion (for a description of Nafion, see Chapter 2). On top of the Nafion, place the reaction solution you

wish to quench. Nafion is highly conductive of cations like H^+ and K^+ and effectively blocks the passage of anions. The H^+ ions from the HCl will diffuse freely up through the Nafion. While the reaction solution is alkaline, the OH^- in the reaction solution will combine with the H^+ to make water, causing a net diffusion of H^+ into the reaction solution from the HCl solution. This process will stop when the solution in neutralized.

In order to balance the charge of the system, and because the Cl^- does not travel well through the Nafion, the H^+ ions counterdiffuse with the K^+ ions initially present in the reaction solution. It is possible that other species also travel though the membrane, but the oxidation products are typically negatively charged (formate, glyceric acid) and larger than K^+. Nafion is highly conductive of K^+, so it is unlikely that a significant amount of the larger oxidation products will travel through the Nafion while the reaction solution is being quenched.

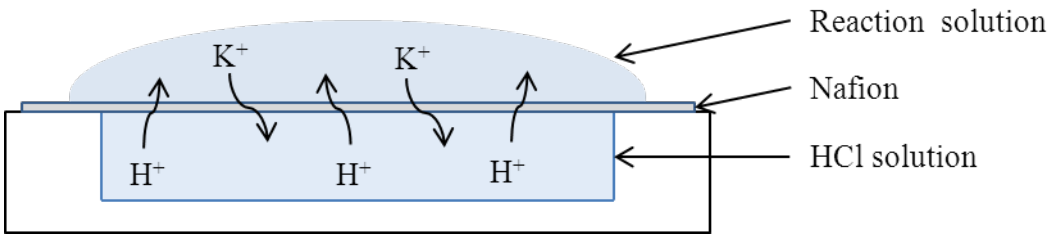

Figure A.1 Schematic of the ion-exchange device

Preliminary tests with the IED indicate that the device significantly reduces the presence of salt in the reaction solution within 15 of minutes. A test was run with 1 M KOH solution on the top of the Nafion and 1 M HCl on the bottom. When left overnight, and then evaporated, the solution on top of the Nafion had a retained a small fraction, perhaps less than 10%, of the salt, while the solution on the bottom had perhaps 90% of the salt.